WILLIAM & MARY
CHARTERED 1693

Dissertations, Theses, and Masters Projects   Theses, Dissertations, & Master Projects

2000

Carbon dynamics in a tidal freshwater marsh

Scott C. Neubauer
College of William and Mary - Virginia Institute of Marine Science

Follow this and additional works at: https://scholarworks.wm.edu/etd

Part of the Biogeochemistry Commons, and the Ecology and Evolutionary Biology Commons

INFORMATION TO USERS

∧.

This manuscript has been reproduced from the microfilm master. UMI films the text directly from the original or copy submitted. Thus, some thesis and dissertation copies are in typewriter face, while others may be from any type of computer printer.

The quality of this reproduction is dependent upon the quality of the copy submitted. Broken or indistinct print, colored or poor quality illustrations and photographs, print bleedthrough, substandard margins, and improper alignment can adversely affect reproduction.

In the unlikely event that the author did not send UMI a complete manuscript and there are missing pages, these will be noted. Also, if unauthorized copyright material had to be removed, a note will indicate the deletion.

Oversize materials (e.g., maps, drawings, charts) are reproduced by sectioning the original, beginning at the upper left-hand corner and continuing from left to right in equal sections with small overlaps.

Photographs included in the original manuscript have been reproduced xerographically in this copy. Higher quality 6" x 9" black and white photographic prints are available for any photographs or illustrations appearing in this copy for an additional charge. Contact UMI directly to order.

UMI®

Carbon Dynamics in a Tidal Freshwater Marsh

A Dissertation

Presented to

the Faculty of the School of Marine Science

of the College of William and Mary

in Partial Fulfillment

of the Requirements for the Degree of

Doctor of Philosophy

----

by

Scott Christopher Neubauer

2000

APPROVAL SHEET

This dissertation is submitted in partial fulfillment of the requirements for the degree of

Doctor of Philosophy
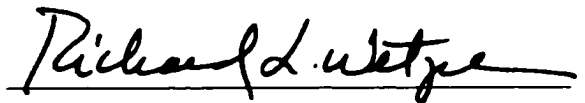
Scott Christopher Neubauer

Approved August 2000

Iris Cofman Anderson, Ph.D.
Committee Co-chair/Advisor

Richard L. Wetzel, Ph.D.
Committee Co-chair/Advisor

James E. Bauer, Ph.D.

Elizabeth A. Canuel, Ph.D.

Carolyn A. Currin, Ph.D.
NOAA National Ocean Service
Beaufort, NC

Stephen A. Macko, Ph.D.
University of Virginia
Charlottesville, VA

DEDICATION

To my beautiful daughter Isabella:

May you enjoy finding out how this world works...

iii

TABLE OF CONTENTS

v

vii

ACKNOWLEDGEMENTS

First, I would like to thank my co-advisors Iris Anderson and Richard Wetzel. Iris was a very active advisor and was involved in all stages of planning this research and analyzing the data - this project would not have been as successful without her guidance. Although Dick was more laid back in his advising style, he was always willing to discuss my research whenever I poked my head into his office. My other committee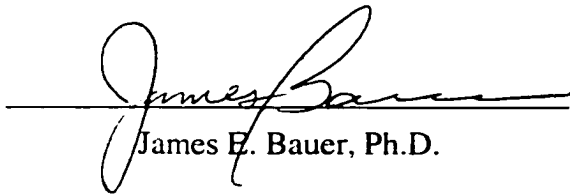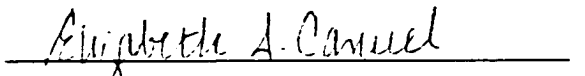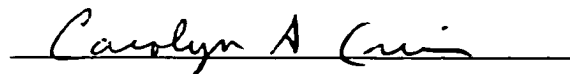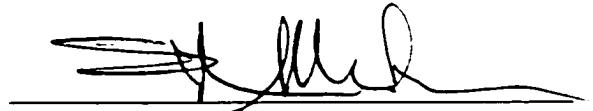 members - James Bauer, Elizabeth Canuel, Carolyn Currin, and Stephen Macko - also contributed to this project. Steve ran countless stable isotope samples and contributed a lot of time and energy to this project; my DOC samples were analyzed in Jim's lab; and everyone helped with comments and criticism throughout my research. Willy Reay, CB-NERRVA research coordinator, was very helpful when I requested NERRS equipment.

Of course, thank you to everyone who provided field and laboratory assistance including (in alphabetical order): Britt Anderson, Eva Bailey, Chris Buzzelli, Mike Campana, Matt Church, José Constantine, Dave Fugate, Beth Hinchey, Tami Lunsford, Dave Miller, Alan Moore, Betty Berry Neikirk, Michelle Neubauer, Yongsik Sin, Craig Tobias, Denise Wilson, and anyone else I may have forgotten. Of these, several people deserve special recognition: Dave (Miller) who was constantly helping in the field and lab during the early stages of this research; José whose excitement was inspirational at a time when I needed it (and he did lots of field and lab work too); and Beth and Michelle who each cheerfully (?) spent a night out in the cold/rainy/foggy marsh filtering water samples. Thanks also to Steven Kuehl and Linda Meneghini for help with the radioisotope dating; and Libby MacDonald and Krisa Arzayus for help with trouble-shooting the elemental analyzer when it decided not to work (which seemed to be whenever I wanted to use it). Finally, Michael Gaylor has run many of my samples through his freeze dryer - there always seems to be "just one more" experiment to do.

During the summer of 1999 I worked part-time at York River State Park. The staff there - Tom, Brad, J, Maurice, Audrey - helped me keep my sanity.

Thank you to my parents, Nancy and Russell, who have always been there for encouragement, support, and motivation. And finally, thank you to my wife Michelle and daughter Isabella who have been especially patient with me during the last couple months and make me happier than anyone else can.

LIST OF TABLES

LIST OF FIGURES

LIST OF APPENDICES

ABSTRACT

The sources and fates of carbon in a mid-Atlantic tidal freshwater marsh (Sweet Hall marsh: Pamunkey River, Virginia) were determined to understand the role that tidal freshwater marshes play with respect to estuarine carbon cycling. A carbon gas flux model. based on measured field fluxes of carbon dioxide and methane, was developed to calculate annual rates of macrophyte and microalgal photosynthesis and community and belowground respiration. Because gaseous carbon fluxes out of marsh sediments may underestimate true belowground respiration if sediment-produced gases are transported through plant tissues, gross nitrogen mineralization was used as a proxy for belowground carbon respiration. A mass-balance model of macrophyte-influenced carbon cycling indicated that translocation was critical in controlling seasonal biomass patterns. Annual community respiration exceeded gross photosynthesis, suggesting an allochthonous input of organic carbon to the marsh.

Sediment deposition during tidal flooding was measured as a potential exogenous carbon source. Short term deposition rates (biweekly to monthly) were spatially and temporally variable, with highest rates measured near a tidal creek during summer. Annual deposition on the marsh was sufficient to balance the effects of relative sea level rise and measured respiration. Sediment inventories of ^7Be indicated that spatial patterns of sedimentation were not due to sediment redistribution within the marsh. Accretion rates calculated from ^{137}Cs (decadal scale) and ^{14}C (centuries to millennia) were substantially less than annual deposition rates.

The concentration and isotopic composition ($\delta^{13}C$ and $\delta^{18}O$) of dissolved inorganic carbon (DIC) were measured in a marsh creek which drained the study site. Seasonal isotopic variations in DIC were explained by marsh porewater drainage and decomposition of marsh-derived carbon. A model linking DIC concentrations and water transport showed that DIC inputs from the marsh occurred throughout the tidal cycle and, when exported from the marsh, could explain a significant portion of excess DIC production in the York River estuary.

Similarly, the role of the marsh as a source or sink for dissolved and particulate organic carbon (DOC and POC) was assessed. Isotopic mass mixing models indicated seasonal variability in the importance of phytoplankton as a source of dissolved and particulate carbon to a marsh tidal creek. However, due to an overlap in concentration and $\delta^{13}C$ values for marsh and riverine DOC and POC, there was no evidence for a flux of these materials between the marsh and estuary. On an annual basis, the marsh carbon budget was closely balanced, with carbon sources exceeding sinks by approximately 5 percent. This similarity suggests that those processes which were not quantified (DOC and POC export, losses due to consumption by riverine and marsh fauna) were quantitatively unimportant with respect to the entire marsh carbon budget. When integrated over thousands of years, a slight imbalance between sources and sinks can result in significant carbon sequestration under the marsh.

PROJECT OVERVIEW

Carbon Dynamics in a Tidal Freshwater Marsh

.

BACKGROUND AND JUSTIFICATION

Intertidal marshes are fundamentally open systems which potentially exchange large amounts of both material and energy with estuarine, riverine, and upland systems. Previous measurements of high rates of phytoplankton production and community respiration in waters adjacent to marsh-dominated estuaries suggested an export ("outwelling") of inorganic nutrients and labile organic matter from the marshes (e.g. Odum 1968; Gosselink et al. 1973; Hopkinson 1985). Furthermore, statistical correlations between estuarine fisheries yields and total marsh area have indicated a significant link between tidal marsh primary production and estuarine secondary production (e.g. Turner 1977; Turner and Boesch 1988). This idea that marshes could influence estuarine production was initially presented as a hypothesis (Kalber 1959; "A hypothesis on the role of tide-marshes in estuarine productivity"). However, as outlined by Nixon (1980), this "hypothesis" quickly became a "conclusion" before there were sufficient data available to evaluate it. Based on over 40 years of measurements since Kalber's hypothesis, the current consensus is that marsh-estuary exchanges are highly variable in terms of the direction and magnitude of carbon and nutrient (nitrogen and phosphorus) fluxes (see reviews by Nixon 1980; Childers 1994; Dame 1994).

Tidal freshwater marshes are located along the estuarine gradient between tidal salt marshes and non-tidal freshwater wetlands. Along the Atlantic coast of North America, tidal freshwater marshes cover approximately 164,000 hectares (Odum *et al.*, 1984). Within Chesapeake Bay, these marshes account for 21% (26,345 ha) of the total tidal

2

marsh area (124,122 ha; Stevenson et al. 1988). Because of their location at the heads of estuaries where the ratio of marsh area to open water is large, tidal freshwater marshes have a significant potential to interact with, and potentially modify riverine and estuarine productivity dynamics and water quality. For example, Sismour (1994) observed that larval fishes in freshwater marsh habitats showed significantly higher rates of growth than those from riverine areas. These enhanced growth rates were attributed to higher plankton production and greater prey availability in tidal creeks and related to organic matter and nutrient cycling within tidal freshwater marsh–creek systems. Similarly, McIvor et al. (1989) observed that most fish collected on a tidal freshwater marsh during high tide were juveniles or small adults and hypothesized that the marsh surface acted as a refuge from predation and a source of food to these fishes. Additionally, higher bacterial growth rates in the tidal freshwater reaches of the York River estuary (Virginia) suggested a labile dissolved organic carbon (DOC) source from tidal freshwater marshes (Schultz 1999) while greater rates of CO_2 evasion and supersaturation implied riverine catabolism of terrestrial and marsh-derived organic carbon and/or the direct export of dissolved inorganic carbon (DIC) produced within the marshes (Raymond et al. in press).

On time scales of years or longer, tidal freshwater (and salt) marshes must grow vertically (by accreting autochthonous production and/or mineral sediments) at a rate similar to relative sea level rise or risk conversion to a different habitat type (e.g. intertidal mudflat or open water). The balance between these accretion mechanisms depends on suspended sediment supply, the frequency of marsh inundation, and rates of marsh primary production. Frequently, tidal freshwater marshes are located within or

3

near the estuarine turbidity maximum where water column suspended sediment concentrations are high. As the marshes are flooded, a decrease in water column turbulent energy can lead to high rates of sediment deposition on the marsh surface (Leonard and Luther 1995; Leonard et al. 1995). Therefore, tidal marshes have the potential to sequester large quantities of sediments and associated nutrients and pollutants.

There is a conspicuous lack of data on nutrient exchanges (e.g. carbon, nitrogen and phosphorus) in pristine tidal freshwater marsh systems. Except for studies conducted in the tidal fresh regions of the Chickahominy and Pamunkey Rivers (Virginia), most tidal freshwater marsh nutrient flux studies have been conducted in eutrophic or hypereutrophic marshes impacted by sewage effluent or urban runoff (Table 1). While there is considerable spatial and temporal variability in nutrient flux rates, it appears that tidal freshwater marshes are seasonal sinks for phosphorus and inorganic nitrogen (as nitrate and ammonium; Grant and Patrick 1970; Simpson et al. 1978; Bowden et al. 1991; Campana 1998; Anderson et al. 1998). However, ammonium and phosphate may also be released to the water column during late summer as marsh vegetation decomposes and subsequently stimulate phytoplankton production.

With the exception of Anderson et al. (1998), none of these studies have simultaneously considered tidal freshwater marsh carbon cycling in more than cursory detail. Due to the interactions between the carbon and nitrogen cycles, nutrient loading may affect the overall marsh carbon balance. For example, nitrate reduction requires an

4

Table 1: Tidal freshwater marsh nutrient concentrations (NH_4^+ and NO_3^-) for systems along the Atlantic coast of North America. Data are roughly arranged from most oligotrophic to most eutrophic. All data are from marsh tidal waters except for Cerco (1988) who studied a shallow embayment fringed by tidal marshes.

Site	NH_4^+ (µM)	NO_3^- (µM)	Citation
Sweet Hall marsh (Pamunkey River, VA)	2.9 (0.3 to 31.0)[a] (2.2 to 3.5) (1.7 to 7.0)	6.0 (0.0 to 16.0) (2.3 to 15.0)[b] (1.4 to 56.1)	Anderson et al. 1998 Campana 1998 Reay 1989
Eagle Bottom marsh (Chickahominy River, VA)	(4 to 12)	no data	Chambers 1992
(North Inlet, MA)	11.7 (0.0 to 151.5)	25.9 (0.0 to 83.1)	Bowden et al. 1991
Herring Creek marsh (James River, VA)	(32 to 34)	(35 to 114)[b]	Adams 1978; Lunz et al. 1978
Hamilton Marshes (Delaware River, NJ)	(<5 to >100)[c]	(<5 to >120)[c]	Simpson et al. 1978
Gunston Cove (Potomac River, VA)	43.6 (4.3 to 211.4)	91.4 (7.1 to 192.1)	Cerco 1988
Tinicum marsh (Delaware River, PA)	208.3 (7.1 to 830.7)	37.7 (3.6 to 105.7)	Grant and Patrick 1970

[a] Mean concentration with observed range in parentheses.

[b] Nitrate plus nitrite.

[c] Approximate range estimated from figures.

organic carbon substrate so nitrate loading in groundwater or terrestrial runoff may result in increased inorganic carbon losses from the marsh (e.g. Paludan and Blicher-Mathiesen 1996). Additionally, exogenous nutrient additions can accelerate rates of decomposition of nitrogen poor substrates (e.g. macrophyte litter; Valiela et al. 1985; Jordan et al. 1989; Gale et al. 1992).

PROJECT OBJECTIVES

In this project, the exchanges of carbon between a mid-Atlantic tidal freshwater marsh, the atmosphere, and adjacent tidal river were considered. This research was guided by the following questions which were addressed in four sections as outlined below:

1) What are the sources of carbon to a pristine mid-Atlantic tidal freshwater marsh?

2) What are the ultimate fates of this carbon?

Section I: *Carbon cycling in a tidal freshwater marsh ecosystem: A carbon gas flux study.* In order to predict the net balance of carbon within an ecosystem, accurate estimates of autotrophic production and community respiration must be obtained. In this section, a process-based carbon gas flux model was developed to calculate rates of total macrophyte and sediment microalgal photosynthesis, and community and belowground respiration for a tidal freshwater marsh. The gas flux results were combined with biomass harvest and literature data to create a conceptual mass balance model of

6

macrophyte-influenced carbon cycling. These data represent a first step in developing a process-based carbon mass balance for a mid-Atlantic tidal freshwater marsh.

Section II: *Sedimentation in a mid-Atlantic tidal freshwater marsh.* In order to understand the factors controlling marsh elevation, sediment deposition and accretion rates were measured over a range of time scales (biweekly to centuries). Biweekly to monthly measurements of deposition onto sediment collection tiles were used to estimate annual sedimentation rates for a mid-Atlantic tidal freshwater marsh. Depth profiles of ^{137}Cs were used to calculate decadal rates, while long term (centuries to millennia) rates were estimated using ^{14}C dating. Sediment inventories of the radioisotope ^{7}Be were used to assess the role of erosion in marsh sediment dynamics, and seasonal measurements of sediment respiration examined the importance of biological utilization of sediment-associated carbon in controlling deposition and accretion rates.

Section III: *Tidal freshwater marsh dissolved inorganic carbon dynamics: concentration, isotopic composition, and evidence for export:* Several recent studies have suggested a significant tidal marsh source of DIC to estuarine waters in order to balance measured levels of CO_2 supersaturation (Cai and Wang 1998; Cai et al. 1999; Raymond et al. in press). In this section, hourly measurements of DIC concentration were made in a tidal creek draining a tidal freshwater marsh and at the mouth of this creek over diurnal cycles to determine if the marsh was a source of DIC to the creek and if any added DIC was ultimately exported to the river. Marsh porewater DIC concentrations were combined with stable isotopic measurements of water column and

7

porewater DIC ($\delta^{13}C$ and $\delta^{18}O$) to identify the source(s) of DIC within the marsh–creek system. The observed tidal and seasonal changes in DIC concentration were combined with estimates of water transport through marsh tidal creeks to quantify the annual export of DIC from the marsh.

Section IV: *Pathways of carbon and nitrogen cycling in a tidal freshwater marsh deduced from stable carbon and nitrogen isotopes:* The stable isotope ratios of carbon and nitrogen within a marsh will reflect, and can therefore be used to infer pathways of biogeochemical cycling within the marsh. In this section, the stable isotope ratios ($\delta^{13}C$ and $\delta^{15}N$) of dissolved and suspended particulate matter were used to deduce dominant carbon and nitrogen sources in a tidal freshwater marsh. Samples were collected in a tidal freshwater marsh tidal creek, at the mouth of the creek over complete diurnal cycles, and from shallow marsh porewater at low tide in the early and late summer (June and August) and at the end of the growing season (November). The ^{13}C and ^{15}N signatures of marsh primary producers (macrophytes and benthic microalgae) were measured as possible organic matter sources from the marsh itself. Isotopic mass balance models were used to estimate the relative contributions of phytoplankton versus marsh-derived dissolved and particulate organic matter to the water column.

8

LITERATURE CITED

Adams DD 1978. *Habitat development field investigations: Windmill Point marsh development site, James River, Virginia; Appendix F: Environmental impacts of marsh development with dredged material: Sediment and water quality, vol II: Substrate and chemical flux characteristics of a dredged material marsh*. US Army Waterways Exp. Station Tech. Rep. D-77-23, Vicksburg MS.

Anderson IC, Neubauer SC, Neikirk BB, Wetzel RL 1998. *Exchanges of carbon and nitrogen between tidal freshwater wetlands and adjacent tributaries*. Final report submitted to the Virginia Coastal Resources Management Program, Virginia Department of Environmental Quality.

Bowden WB, Vörösmarty CJ, Morris JT, Peterson BJ, Hobbie JE, Steudler PA, Moore III B 1991. Transport and processing of nitrogen in a tidal freshwater wetland. *Water Resour Res* 27(3):389-408.

Cai W-J, Wang Y 1998. The chemistry, fluxes, and sources of carbon dioxide in the estuarine waters of the Satilla and Althamaha Rivers, Georgia. *Limnol. Oceanogr.* 43(4): 657-668.

Cai W-J, Pomeroy LR, Moran MA, Wang Y 1999. Oxygen and carbon dioxide mass balance for the estuarine-intertidal marsh complex of five rivers in the southeastern U.S. *Limnol. Oceanogr.* 44(3): 639-649.

Campana ML 1998 *The effect of* Phragmites australis *invasion on community processes in a tidal freshwater marsh* M.S. Thesis, College of William and Mary, Virginia Institute of Marine Science, Gloucester Point.

Cerco CF 1988. Sediment Nutrient Fluxes in a Tidal Freshwater Embayment. *Water Resour. Bull.* 24(2): 255-260.

Chambers RM 1992. A fluctuating water-level chamber for biogeochemical experiments in tidal marshes. *Estuaries*. 15: 53-58.

Childers DL 1994. Fifteen years of marsh flumes: A review of marsh-water column interactions in southeastern USA estuaries. in Mitsch WJ (ed). *Global wetlands: Old World and New*. Elsevier: New York. pp. 277-293.

9

Dame RF 1994. The net flux of materials between marsh-estuarine systems and the sea: The Atlantic coast of the United States. in Mitsch WJ (ed). *Global wetlands: Old World and New*. Elsevier: New York. pp. 277-293.

Gale PM, Reddy KR, Gratz DA 1992. Mineralization of sediment organic matter under anoxic conditions. *J. Env. Qual.* 21: 394-400.

Gosselink JG, Odum EP, Pope RM 1973. *The value of the tidal marsh*. Work paper No. 3. Center for Wetland Resources, Louisiana State University, Baton Rouge.

Grant Jr RR, Patrick R 1970. Tinicum marsh as a water purifier. In: *Two studies of Tinicum marsh*. The Conservation Foundation, Washington D.C. 105-123.

Hopkinson CS 1985. Shallow-water benthic and pelagic metabolism: evidence of heterotrophy in the nearshore Georgia Bight. *Mar. Biol.* 87: 19-32.

Jordan TE, Whigham DF, Correll DL 1989. The role of litter in nutrient cycling in a brackish tidal marsh. *Ecology.* 70: 1906-1915.

Kalber Jr FA 1959. A hypothesis on the role of tide-marshes in estuarine productivity. *Est. Bull.* 4(1):3.

Leonard LA, Luther ME 1995 Flow hydrodynamics in tidal marsh canopies *Limnol. Oceanogr.* 40: 1474-1484.

Leonard LA, Hine AC, Luther ME 1995 Surficial sediment transport and deposition processes in a *Juncus roemerianus* marsh, west-central Florida *J. Coast. Res.* 11: 322-336.

Lunz JD, Zweigler TW, Huffman RT, Diaz, RJ, Clairain EJ, Hunt LJ 1978. *Habitat development field investigations: Windmill Point marsh development site, James River, Virginia; summary report*. US Army Waterways Exp. Station Tech. Rep. D-79-23, Vicksburg MS.

McIvor CC, Rozas LP, Odum WE 1989. Use of the Marsh Surface by Fishes in Tidal Freshwater Wetlands. In: Sharitz RR, Gibbons JW (eds). *Freshwater Wetlands and Wildlife* USDOE Office of Scientific and Technical Information DOE Symposium Series No. 61: 541-552.

Neubauer SC, Miller WD, Anderson IC 2000. Carbon cycling in a tidal freshwater marsh ecosystem: A carbon gas flux study. *Mar. Ecol. Prog. Ser.* 199:13-30.

Nixon SW 1980. "Between Coastal Marshes and Coastal Waters - A Review of Twenty Years of Speculation and Research in the Role of Salt Marshes in Estuarine Productivity and Water Chemistry." in Hamilton P, McDonald KB (eds). *Estuarine and Wetland Processes with Emphasis on Modelling*. Plenum Press: New York. pp. 437-525.

Odum WE, Smith III TJ, Hoover JK, McIvor CC 1984. *The ecology of tidal freshwater marshes of the United States east coast: a community profile*. US Department of the Interior, Fish and Wildlife Service, FWS/OBS-83/17.

Odum EP 1968. "A Research Challenge: Evaluating the Productivity of Coastal and Estuarine Water." in *Proceedings of the Second Sea Grant Conference*. University of Rhode Island. pp. 63-64.

Paludan C, Blicher-Mathiesen G 1996. Losses of inorganic carbon and nitrous oxide from a temperate freshwater wetland in relation to nitrate loading. *Biogeochem*. 35: 306-326.

Raymond PA, Bauer JE, and Cole JJ in press. Atmospheric CO_2 evasion, dissolved inorganic carbon production, and net heterotrophy in the York River estuary. *Limnol. Oceanogr*.

Reay, W. G. *A geohydrologic approach to subsurface hydrodynamics and nutrient exchange within an extensive tidal freshwater wetland*. MS thesis, College of William and Mary, Virginia Institute of Marine Science, Gloucester Point

Schultz GE 1999. *Bacterial dynamics and community structure in the York River estuary*. Ph.D. Dissertation. College of William and Mary, Virginia Institute of Marine Science, Gloucester Point

Simpson RL, Whigham DF, Walker R 1978. Seasonal patterns of nutrient movement in a freshwater tidal marsh. In: Good RE, Whigham DF, Simpson RL (eds) *Freshwater wetlands: ecological processes and management potential*. Academic Press, New York, p 89-98.

Sin Y, Wetzel RL, Anderson IC 1999. Spatial and temporal characteristics of nutrient and phytoplankton dynamics in the York River estuary, Virginia: Analyses of long-term data. *Estuaries*. 22(2A): 260-275.

11

Sismour EN 1994. *Contributions to the Early Life Histories of Alewife and Blueback Herring: Rearing, Identification, Ageing, and Ecology*. Ph.D. Dissertation, College of William and Mary, Virginia Institute of Marine Science, Gloucester Point

Stevenson JC, Ward LG, Kearney MS 1988. Sediment Transport and Trapping in Marsh Systems: Implications of Tidal Flux Studies. *Mar. Geol.* 80: 37-59.

Turner RE 1977. "Intertidal Vegetation and Commercial Yields of Penaeid Shrimp." *Trans. Amer. Fish. Soc.* 106: 411-416.

Turner RE, Boesch DF 1988. "Aquatic Animal Production and Wetland Relationships." in *Ecology and Management of Wetlands*. Timber Press: Portland, OR. 25-39.

Valiela I, Wilson J, Buchsbaum R, Rietsma C, Bryant D, Foreman K, Teal J 1985. Importance of chemical composition of salt marsh litter on decay rates and feeding by detrivores. *Bull. Mar. Sci.* 35(3): 261-269.

SECTION I

Carbon Cycling in a Tidal Freshwater Marsh Ecosystem: A Carbon Gas Flux Study[†]

ABSTRACT

A process-based carbon gas flux model was developed to calculate total macrophyte and microalgal production, and community and belowground respiration for a *Peltandra virginica* dominated tidal freshwater marsh in Virginia. The model was based on measured field fluxes of CO_2 and CH_4, scaled to monthly and annual rates using empirically derived photosynthesis vs. irradiance and respiration vs. temperature relationships. Because the gas exchange technique measures whole system gas fluxes and therefore includes turnover and seasonal translocation, estimates of total macrophyte production will be more accurate than those calculated from biomass harvests. One limitation of the gas flux method is that gaseous carbon fluxes out of the sediment may underestimate true belowground respiration if sediment-produced gases are transported through plant tissues to the atmosphere. Therefore we measured gross nitrogen mineralization (converted to carbon units using sediment C/N ratios and estimates of bacterial growth efficiency) as a proxy for belowground carbon respiration. We estimated a total net macrophyte production of 536 to 715 $g\ C\ m^{-2}\ yr^{-1}$, with an additional 59 $g\ C\ m^{-2}\ yr^{-1}$ fixed by sediment microalgae. Belowground respiration calculated from nitrogen mineralization was estimated to range from 516 to 723 $g\ C\ m^{-2}\ yr^{-1}$ versus 75 $g\ C\ m^{-2}\ yr^{-1}$ measured directly with sediment chambers. Methane flux (72 $g\ C\ m^{-2}\ yr^{-1}$) accounted for 11 to 13% of total belowground respiration. Gas flux results were combined with biomass harvest and literature data to create a conceptual mass balance model of macrophyte-influenced carbon cycling. Spring and autumn translocation and re-translocation are critical in controlling observed seasonal patterns of above and

14

belowground biomass accumulation. Annually, a total of 270 to 477 g C m^{-2} of macrophyte tissue is available for deposition on the marsh surface as detritus or export from the marsh as particulate or dissolved carbon.

15

INTRODUCTION

Tidal freshwater marshes are located at the head of the estuarine gradient where a suitable combination of freshwater supply and tidal range permits their development. On the eastern coastal plain of North America, the most expansive tidal freshwater marshes are located between New Jersey and Virginia and in South Carolina and Georgia (Odum *et al.*, 1984). In contrast with east coast salt marshes, which are dominated by one (generally *Spartina alterniflora*) or several (i.e. *S. patens* and *Distichlis spicata*) macrophyte species, it is not unusual to find 50 to 60 plant species in a freshwater marsh (Pickett. 1984; Perry, 1991). Dominant vegetation changes seasonally and can include fleshy broadleaf plants such as *Peltandra virginica, Pontederia cordata*, and *Sagittaria latifolia* and grass-like species such as *Leersia oryzoides, Phragmites australis, Typha latifolia*, and *Zizania aquatica*.

Intertidal salt and freshwater marshes have long been considered highly productive ecosystems. Salt marshes dominated by monospecific stands of *Spartina alterniflora* have been well studied, with aboveground plus belowground net macrophyte production ranging from 1000 to 8000 gdw m^{-2} yr^{-1} (Schubauer and Hopkinson, 1984). Most measurements have been made using a variety of biomass harvest techniques which have been shown to produce estimates of plant productivity that can exceed the physiological capacity of *S. alterniflora* (Morris *et al.*, 1984; Dai and Wiegert, 1996). Fewer data are available for tidal freshwater marshes, due in part to their high diversity, seasonally variable species composition, and patchy distribution of belowground biomass. Reported

16

annual net aboveground production varies by species, averaging 900 gdw $m^{-2} yr^{-1}$ for

Peltandra virginica to 1900 gdw $m^{-2} yr^{-1}$ for *Phragmites australis* (Whigham *et al.*,

1978). Although few studies have included belowground production. Booth (1989)

reported approximately equal rates of aboveground and belowground production (1634

and 1568 gdw $m^{-2} yr^{-1}$, respectively) for a monospecific stand of *P. virginica* in Virginia.

When belowground components are included, it appears that freshwater marshes are as

productive as salt marshes.

Determining community production in tidal freshwater marshes is, at best, a difficult

proposition due to the diverse and seasonally changing species composition and the

extensive yet patchy distribution of belowground biomass (de la Cruz, 1978; Whigham *et*

al., 1978). Most commonly, aboveground production has been measured using either

single or multiple harvests where production is either equal to peak biomass (i.e.

Doumlele, 1981) or biomass adjusted by a mortality or turnover factor (i.e. Pickett, 1984;

Wohlgemuth, 1988; Booth, 1989). Few studies have attempted to measure belowground

production in tidal freshwater marshes, especially those dominated by *Peltandra*

virginica which have rhizomes that extend to a depth of 1 to 2 meters (Booth, 1989,

Chanton *et al.*, 1992). Complete excavation of belowground material and subsequent

separation of live and dead roots is a laborious, inexact, and time-consuming effort and

does not provide necessary information on turnover rates. An additional level of

complexity is added because turnover rates for both above and belowground tissues vary

depending on the species (Pickett, 1984) and tissue type (Schubauer and Hopkinson,

1984). In systems dominated by perennial plants, there can be significant translocation of

17

nutrients and energy from belowground to aboveground components in the spring, and in the reverse direction late in the growing season as aboveground tissues senesce (Lytle and Hull, 1980a, b; Hopkinson and Schubauer, 1984; Booth 1989). Because translocation is not accounted for in harvest methods, summing aboveground and belowground production will not provide an accurate estimate of true macrophyte productivity.

As an alternative to harvest methods, fluxes of CO_2 and CH_4 have been used to estimate gross and net macrophyte productivity under ambient field conditions (Blum *et al.*, 1978; Giurgevich and Dunn, 1978; Howes et al., 1984; Whiting and Chanton, 1996) or under experimental conditions such as elevated atmospheric CO_2 concentrations (Drake, 1984; Curtis *et al.*, 1989; Azcón-Bieto *et al.*, 1994) or manipulated soil salinities (Pezeshki, 1991; Hwang and Morris, 1994). The carbon gas flux technique integrates processes that occur within and between aboveground and belowground compartments (e.g. turnover and translocation) and therefore provides a more reliable estimate of total production than harvest methods. If carbon fluxes from the sediments are measured, *in situ* sediment microalgal production can also be calculated (Anderson *et al.*, 1997).

Marsh macrophyte and microalgal organic matter (carbon) can undergo several potential fates: biotic remineralization to CO_2 and CH_4, retention in the marsh system (as accumulated biomass or sediments), consumption by herbivores, or export to adjacent riverine and estuarine environments as particulate or dissolved organic matter. The outwelling hypothesis, which proposes that marsh-derived materials can support

18

secondary production in nearby aquatic communities, requires a net export of organic materials from the marsh (e.g. Teal, 1962; Odum, 1968; Gosselink *et al.*, 1973). Although historically developed for estuarine and salt marsh systems, the outwelling hypothesis is also applicable to tidal freshwater environments. Ecological simulation (i.e. Buzzelli, 1996) or mass balance models (Chalmers *et al.*, 1985; Hopkinson, 1988; Anderson *et al.*, 1997) can be used to predict overall carbon or nitrogen balances in a marsh system, but accurate production estimates must first be obtained. Sediment microalgae are highly productive (Sullivan and Moncreiff, 1988; Pinckney and Zingmark, 1993), can be suspended and exported from the marsh by tidal waters (Gallagher, 1975), and are often an important food source in aquatic systems (Sullivan and Moncreiff, 1990; Hamilton *et al.*, 1992; Currin *et al.*, 1995; Deegan and Garritt, 1997). Therefore, any study that attempts to couple marsh productivity and food web dynamics must include sediment microalgae.

In this study, we describe a carbon gas flux technique for determining macrophyte and sediment microalgal productivity in tidal freshwater marshes. We present estimates of total macrophyte productivity and rates of carbon cycling measured using the gas exchange technique and compare this with several traditional harvest methods. Additionally, we report the first known measurements of sediment microalgal productivity in a tidal freshwater marsh system. These data represent a first step in developing coupled carbon and nitrogen process-based mass balance models for a mid-Atlantic (Virginia) tidal freshwater marsh.

19

MATERIALS AND METHODS

Study Site: Sweet Hall marsh is an extensive emergent tidal freshwater marsh located on the Pamunkey River, approximately 69 km from the mouth of the York River, Virginia. The marsh is within the Chesapeake Bay National Estuarine Research Reserve system in Virginia (CB-NERRVA), and is bordered by non-tidal hardwood bottomland forests on the mainland side and submerged riverine mud flats along the Pamunkey River. Nearby upland areas on the Pamunkey River include agricultural fields, mixed hardwood and pine forests, and a pine plantation. A tidal channel and the Pamunkey River isolate the majority of the marsh from direct upland and groundwater influences.

Our study site was located along the western branch of Hill's Ditch, a tidal creek that drains into the Pamunkey River on the south end of Sweet Hall marsh. The tidal range is approximately 80 cm and much of the marsh is flooded on high tides. The study site (and on average, the entire marsh) is dominated by the broadleaf macrophytes *Peltandra virginica* and *Pontederia cordata* through most of the summer while the grass *Zizania aquatica* becomes abundant late in the growing season. To minimize disturbances due to repeated sampling, three boardwalks (30 m) were built into the interior of marsh in May 1996, roughly perpendicular to the tidal creek. All sampling was conducted from these boardwalks.

Carbon Flux Measurements: Marsh community CO_2 and CH_4 flux studies were performed by enclosing an area of marsh (0.69 m^2), including both plants and sediments,

20

within a large temperature-controlled chamber ("community chamber", 696 L, Figure 1), as described by Whiting *et al.* (1992). Belowground metabolism (no aboveground plants) was measured using a smaller chamber ("sediment chamber", 79 cm^2, 0.8 L). During spring 1996, six aluminum collars for the community chamber were installed along one transect and left in place for the duration of the study. Collars, embedded 10 cm into the sediment, provided an air-tight seal between the marsh and community chamber. Holes in each collar at the sediment surface allowed tidal inundation and drainage. Prior to making flux measurements, drainage holes were plugged; the community chamber was clamped to a collar; and the system allowed to equilibrate for 10 to 15 minutes. Sediment chambers were placed adjacent to each community collar. Fluxes were measured during June, September, and November 1996 and March, April, May, July, and September 1997. With the exception of the September 1997 study (see below), all measurements were made only during daytime low tides. To maximize light intensities for flux measurements, sampling dates were chosen so that slack low water occurred between 11:00 and 13:00 h, and sampling did not take place on excessively cloudy or rainy days. Flux measurements in the community chamber were made in full light and dark and at intermediate light levels (using shade cloths; 6 to 7 meshes cm^{-1} window screen) in order to construct photosynthesis vs. irradiance curves. Benthic metabolism was measured only in the light and dark. Flux measurements at all light levels (including dark) for a given chamber were made on the same day; it generally took two to three days to sample all chambers. To maintain community chamber temperature at ± 2°C of ambient, ice water was pumped through a heat exchanger within the chamber and the headspace air

21

**Community Chamber
(696 L)**

Syringe for gas samples

Air flow to LI-COR

LI-COR IRGA

Sediment
Chamber
(0.8 L)

Return to chamber

$[CO_2]$

Datalogger

Cooling system

Collar

Sediment
temp.

Interior & exterior temperature; Incident & canopy irradiance
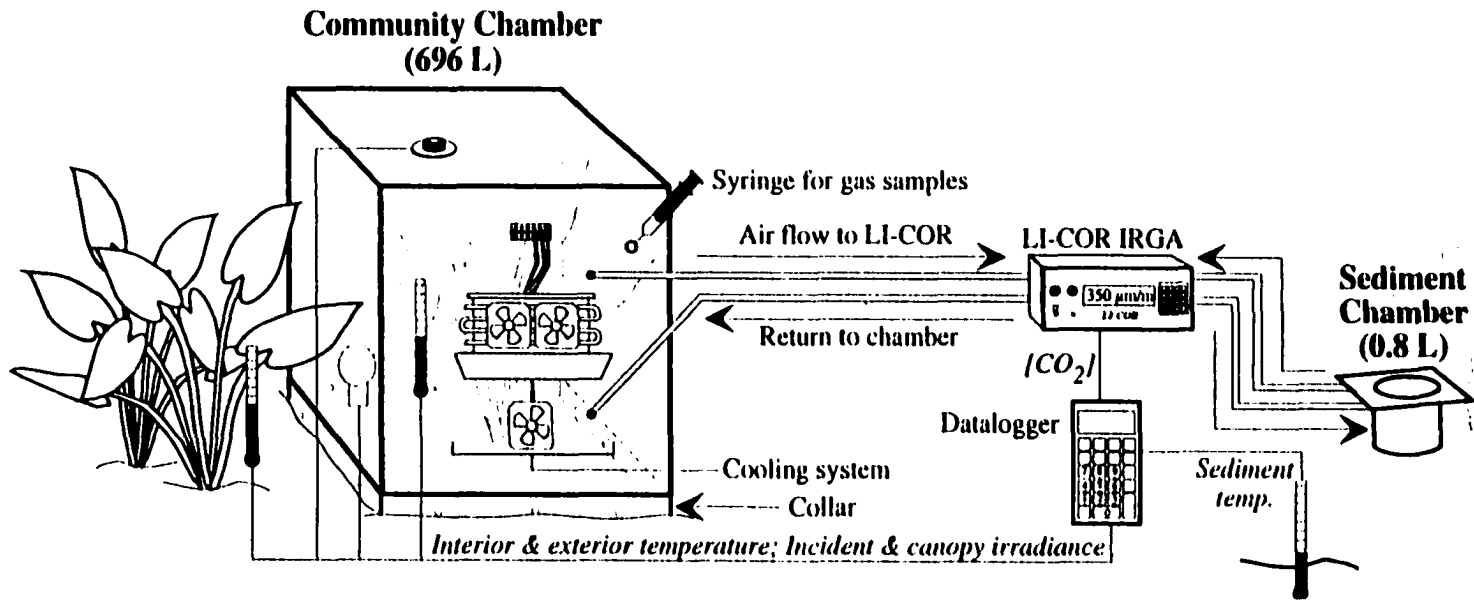
Figure 1: Schematic of community and sediment chambers used for gas flux measurements

stirred by three fans. The sediment chambers, which were generally shaded by macrophytes, did not have a cooling system.

CO_2 concentrations in each chamber were measured in the field using a LI-COR model 6252 infrared gas analyzer (IRGA; LI-COR Inc., Lincoln, NE). Prior to field measurements, the IRGA was zeroed for 15 to 30 minutes with N_2 passed sequentially through soda lime (to remove CO_2), Nafion tubing (Type 815 DuPont perflourinated polymer, Perma Pure Inc., Toms River, NJ) packed in silica gel (to remove water) and magnesium perchlorate $(Mg(ClO_4)_2$, to remove water). The instrument was then calibrated with gas standards containing 350, 408, or 1000 ppmv CO_2 in N_2 (Scott Specialty Gases, Inc., Plumsteadville, PA). In the field, air was circulated (500 ml min^{-1}; LI-COR model 6262-04 reference pump) from the chamber through the IRGA and back to the chamber; CO_2 concentrations were measured and recorded at one minute intervals using a LI-COR model 1000 datalogger. Five to fifteen measurements were made at each light level. Chamber CO_2 concentrations were always between 280 and 350 ppmv – preliminary studies in June 1996 indicated that there was no effect of CO_2 concentration on net photosynthetic rate within this range.

To determine CH_4 fluxes, 60 ml of gas were withdrawn from the community chamber at ten minute intervals. During November 1996 and September 1997, samples were also taken from the sediment chamber at 5 to 7 minute intervals. Thirty-five ml of the sample were used to flush, and the remainder to pressurize a gas-tight Hungate tube (12.8 ml). Tubes were stored inverted in brine to reduce gas leakage. Upon return to the

23

lab. 200 μl samples were injected into a Hewlett Packard model 5890 gas chromatograph equipped with a molecular sieve 13x column and flame ionization detector (oven @ 80°C, detector @ 220° C). A single point calibration of the instrument was performed routinely before and during analyses using a 9.02 ppmv CH_4 in N_2 standard (Scott Specialty Gases, Inc.). Rates of CH_4 flux were linear and showed no response to short term changes in light.

Concurrent with gas flux measurements, incident irradiance was measured using a LI-COR 2π light sensor placed on top of each chamber, and a 4π sensor within the plant canopy, 15 cm above the sediment surface. Temperatures were measured using thermistors positioned inside and outside the chamber and in the sediment (10 to 15 cm). Light and temperature data were logged at one-minute intervals on a LI-COR model 1000 datalogger.

Tidal effects on CO_2 and CH_4 fluxes were determined during September 1997. Sampling was conducted over one full tidal cycle, with measurements made during day and night, on both low and high tides, as described above. When the marsh was flooded, CO_2 and CH_4 fluxes in the chamber headspace and concentrations of dissolved CH_4 in overlying water were measured. Gaseous CO_2 and CH_4 fluxes were measured as above. For dissolved CH_4, 30 ml water samples were shaken for 30 seconds with an equal volume of CH_4-free argon in a 60 ml syringe. The gas was transferred to a 30 ml syringe with stopcock and analyzed as above within two days of collection. CH_4 concentrations in water were calculated using the Ostwald solubility coefficient (0.037 @ 20°C; Weiss,

24

1974). Dissolved CO_2 concentrations were not directly measured. Instead, we assumed

that air and water CO_2 concentrations were in equilibrium, with the concentration of

dissolved CO_2 calculated using chamber headspace CO_2 concentrations and the Ostwald

solubility coefficient for CO_2 (0.938 @ 20°C; Weiss, 1974). Differences in CO_2 and CH_4

respiration rates due to seasonal, diurnal and tidal effects were statistically tested using

ANOVA and Tukey's HSD multiple comparison tests (Zar, 1996).

Belowground Respiration (Nitrogen Mineralization): In freshwater marsh systems,

molecular diffusion or convective throughflow of sediment gases through plant tissues is

greater than direct sediment-atmosphere diffusion (Chanton *et al.*, 1992; Chanton and

Whiting, 1996; Whiting and Chanton, 1996). Thus, gas fluxes measured with sediment

chambers may underestimate true belowground respiration rates (Morris and Whiting,

1986). To account for this we used the sediment gross nitrogen mineralization rate as a

proxy for belowground respiration, with N mineralized converted to carbon units using

measured sediment C/N ratios and bacterial growth efficiencies (after Linley and Newell,

1984; Hart *et al.* 1994). Although there are potential errors with this approach (see

discussion), we believe this estimate will be more accurate than one based solely on CO_2

and CH_4 efflux into sediment chambers. Gross nitrogen mineralization was determined

by $^{15}NH_4^+$ isotope pool dilution as described in Anderson *et al.* (1997). Sediment cores

(10 cm deep) were collected seasonally in triplicate at five randomly selected points

along each transect using polycarbonate core tubes (20 cm tall by 25.5 cm^2). Each core

was uniformly injected with 4.0 ml of argon-sparged ^{15}N-labeled ammonium sulfate

(($^{15}NH_4$)$_2SO_4$, 10 mM, 99.7 atom percent, Isotec Inc., Miamisburg, OH) to an

25

approximate final concentration of 1 mM and 30 atom percent ^{15}N in porewater. Cores

were incubated at ambient temperature in the dark for either 0, 24, and 48 hr (November

96) or 0, 6, and 24 hr (September 96 and April 97). After each incubation period, one of

each set of three cores was sacrificed by addition of an equal volume of KCl (255 ml, 2

M) to extract the total exchangeable NH_4^+ pool. Sediment slurries were shaken in Whirl-

Pak bags for 1 hour on a rotary shaker at room temperature and centrifuged.

Supernatants were filter sterilized (0.45 μm Gelman Supor Acrodiscs) and stored frozen

in Whirl-Pak bags until analyzed for NH_4^+ using the technique of Solorzano (1969).

Remaining supernatants were transferred to sterile, disposable specimen cups.

Magnesium oxide (MgO, 0.2 g) was added to reduce $NH_4^+{}_{(aq)}$ to $NH_3{}_{(g)}$ which was trapped

on acidified (KHSO$_4$, 10 μl, 2.5 M) paper filters (Whatman #3, 7 mm) for six days, as

described by Brooks et al. (1989). Disks were dried overnight in a desiccator over

concentrated sulfuric acid (H$_2$SO$_4$), wrapped in tin capsules, and analyzed for %N and ^{15}N

enrichment using an elemental analyzer coupled to an isotope ratio mass spectrometer at

the University of California at Davis. Rates of N-mineralization were determined using a

model described by Wessel and Tietema (1992) which takes into account both the change

in atom percent enrichment of the ^{15}N-labeled NH_4^+ pool as well as the change in total

concentration of the NH_4^+ pool.

Sediment Characterization: Sediment cores (55 cm^2 by 30 cm deep) were collected

seasonally and sectioned into 0 to 2, 2 to 5, 10 to 13, 18 to 21, and 27 to 30 cm intervals.

Samples were dried at 50° C for 3 to 4 weeks. A portion of each sample was ground in a

Wiley mill (#40 screen), weighed into ashed silver cups and acidified with 1 to 2 drops of

26

10% HCl to remove carbonates. Samples were placed on a hot plate to evaporate excess acid. The acidification step was repeated and samples allowed to dry overnight in a 50° C drying oven. Total carbon and nitrogen were measured using a Fison model EA 1108 elemental analyzer.

Aboveground Macrophyte Biomass: Seasonally, aboveground macrophyte biomass was clipped at five points along each of two transects in the marsh. Each transect was divided into five zones (0 to 2, 2 to 8, 8 to 15, 15 to 23, and 23 to 30 m from tidal creek) and a sampling point within each zone was randomly selected. The two zones nearest the creek covered the front and back sides, respectively, of a natural levee, while the three interior zones were slightly lower in elevation. A 0.11 m^2 ring was blindly dropped at each sampling point; all vegetation rooted within the ring was clipped and returned to the lab for sorting. Samples were sorted by species into living (50 to 100% green), dying (0 to 50% green), and dead fractions, dried at 50°C for 3 to 4 weeks, and weighed. Percents carbon and nitrogen were measured as above without the acidification steps. From these data aboveground macrophyte productivity was estimated using the peak biomass (i.e. Whigham *et al.*, 1978; Doumlele, 1981) and Smalley harvest methods (Smalley, 1958). The peak aboveground biomass (converted to g C m^{-2}) of each species was summed to calculate productivity. Because different species have their peak biomass at different times of the year, multiple harvests allow a better estimation of aboveground productivity than does a single harvest. Smalley production was calculated by taking into account changes in both the live and combined dying plus dead fractions of biomass for all species over the course of the year (Smalley, 1958). To account for leaf mortality and

27

decomposition between sampling dates, we applied a turnover factor of 2.24 yr^{-1} (Wohlgemuth, 1988) to our estimates obtained from each method. Seasonal trends in live, dead, and total biomass were analyzed using one-way ANOVA followed by Tukey's HSD multiple comparison tests.

Sediment Chlorophyll *a*: For analysis of sediment microalgal biomass, sediment was collected using 2 cm diameter core tubes to a depth of at least 1 cm. Triplicate cores were taken from the same areas sampled for macrophyte biomass, plugged with rubber stoppers, and stored in the dark until processed. The 0 to 5 mm section of each core was removed and stored frozen. Analysis was performed according to the protocol of Lorenzen (1967), as modified by Pinckney *et al.* (1994) to include extraction of the sediment (unground) with 10 ml of extractant (45% methanol, 45% acetone, 10% DI water) at -15° C for 72 hours. Differences in monthly chlorophyll concentrations were analyzed using ANOVA and Tukey's HSD multiple comparison tests.

RESULTS AND CALCULATIONS

Carbon Flux Measurements: Mean short-term community CO_2 respiration measured as dark CO_2 flux (CR; see Table 1 for list of abbreviations) ranged from a low of 0.28 mg C m^{-2} min^{-1} in March 1997 to a high of 6.51 mg C m^{-2} min^{-1} in September 1997 (Figure 2). CR was highest during the summer when temperatures and aboveground macrophyte biomass (AGB) were greatest. While there was considerable variability between sampling sites on any given day, average community CH_4 fluxes (ME) were highest in

28

Table 1: List of abbreviations used throughout this paper

Abbreviation	Explanation	Units
GCP	Gross community photosynthesis	mass C m^{-2} time^{-1}
GMaP	Gross macrophyte photosynthesis	mass C m^{-2} time^{-1}
GMiP	Gross microalgal photosynthesis	mass C m^{-2} time^{-1}
TCR	Total community respiration (CO_2 plus CH_4)	mass C m^{-2} time^{-1}
CR	Community respiration (CO_2 only)	mass C m^{-2} time^{-1}
ME	Community respiration (CH_4 only)	mass C m^{-2} time^{-1}
BGR	Belowground respiration	mass C m^{-2} time^{-1}
MaR	Macrophyte respiration	mass C m^{-2} time^{-1}
MiR	Microalgal respiration	mass C m^{-2} time^{-1}
GNM	Gross sediment nitrogen mineralization	mass N m^{-2} time^{-1}
AGB	Aboveground macrophyte biomass	mass C m^{-2} or gdw m^{-2}
BGE	Bacterial growth efficiency	%
MOM	Sediment macro-organic matter	—

29
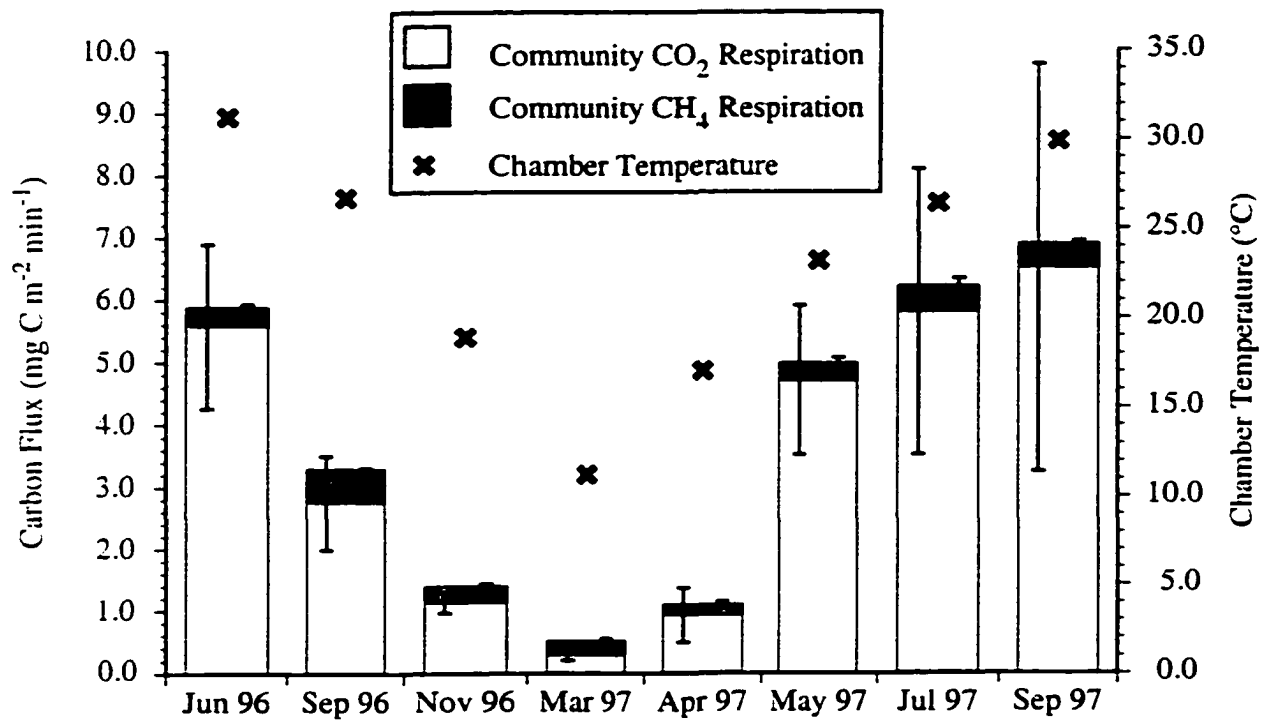
Figure 2: Seasonal community CO_2 and CH_4 fluxes (mg C m^{-2} min^{-1}), and air temperature within the chamber. Bars are additive; thus combined CO_2 + CH_4 flux = TCR. Error bars are ± 1 standard deviation; n = 3 to 7

30

September 1996 (0.54 mg C m^{-2} min^{-1}) and lowest during April 1997 (0.16 mg C m^{-2} min^{-1}; Fig. 2). Sediment CH$_4$ fluxes were a small percentage (generally <5%) of the total ME flux (data not shown). Community ME rates accounted for five (May, June 1996; September 1997) to forty-six (March 1997) percent of short-term total community respiration (TCR; CR+ME; Fig. 2). TCR followed the same general trend as CR: rates were highest between May and September, and significantly lower from November to April (Fig. 2; ANOVA, F = 18.09, p < 0.0001; Tukey's HSD, p < 0.05).

During September 1997, studies were conducted over one full tidal cycle. Mean CR ranged from 4.02 (nighttime high tide) to 9.00 mg C m^{-2} min^{-1} (nighttime low), but there were no statistical differences in CR over the tidal cycle (Fig. 3A; ANOVA, F = 2.68, p = 0.14). In contrast, there were large changes in ME over the tidal cycle (Fig. 3A). All treatments (nighttime low, nighttime high, daytime high) were significantly different than ME measured during daytime low tides (ANOVA, F = 18.18, p < 0.01; Tukey's HSD, p < 0.05). ME was higher during the day than at night, and low tide release rates were higher than when the marsh was flooded. Gross photosynthesis also varied with the tidal cycle (Fig. 3B).

Belowground Respiration (N-Mineralization): Gross N-mineralization in the upper 10 cm of the sediment was highest in September (20 mg N m^{-2} hr^{-1}; Table 2) and lowest in November (0.4 mg N m^{-2} hr^{-1}). Average sediment C/N ratios (g C / g N) in the upper 30 cm ranged from 11.6 to 12.1. Mineralization, the reduction of organic matter to NH$_4^+$, is largely confined to the live root zone. Our data indicate that sediment organic matter

31
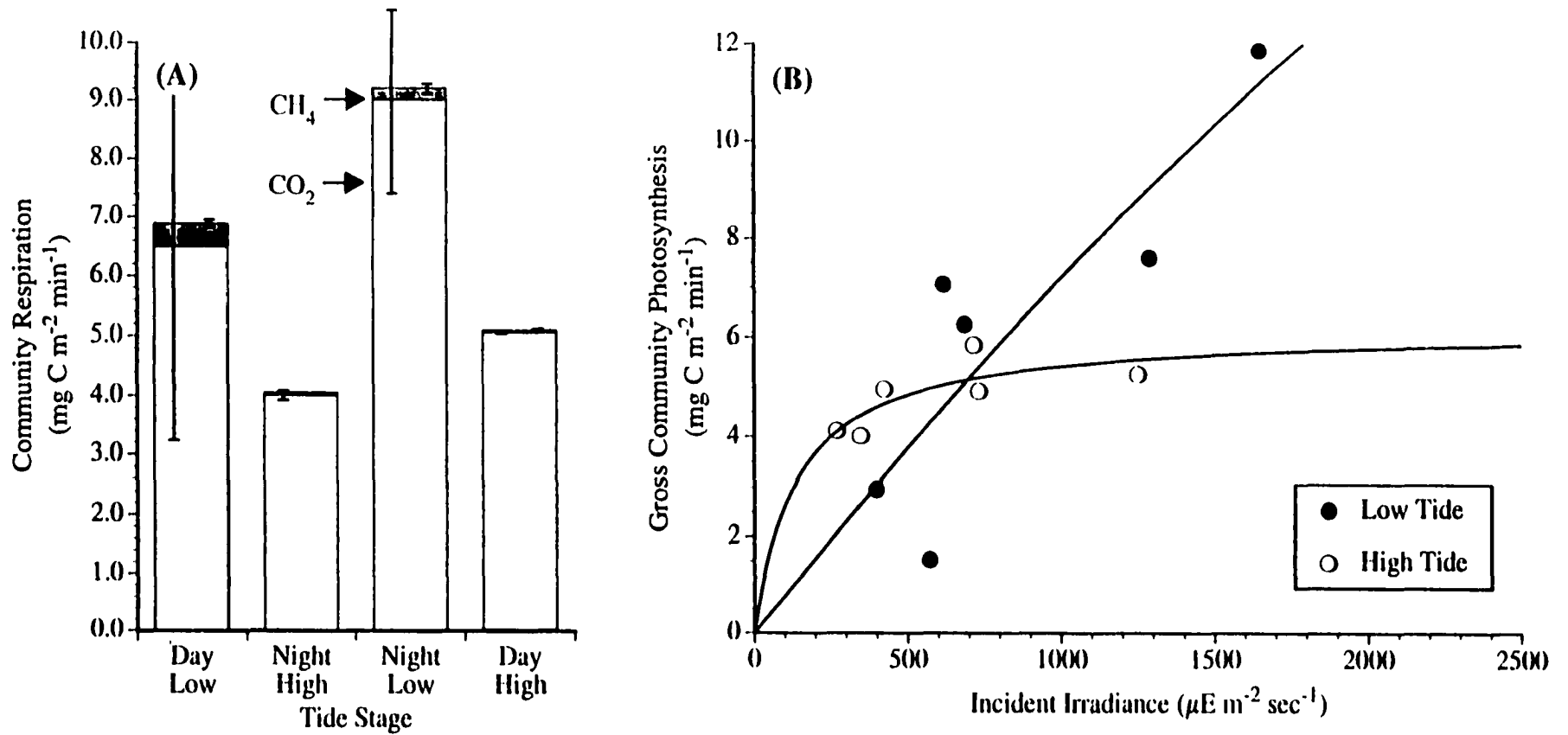
Figure 3: Tidal effects on community gas fluxes. (A) Community CO_2 and CH_4 respiration (mg C m^{-2} min^{-1}) measured in darkened

community chamber over 1 tidal cycle in Sep 1997. Error bars are $\pm$ 1 standard deviation; n = 2 or 3. (B) Gross community

photosynthesis versus incident irradiance at high and low tides. Each data point is the slope of CO_2 concentration versus time for a 5

to 10 min sampling interval, minus measured dark respiration.

Table 2: Sediment carbon mineralization rates as calculated from measured gross nitrogen mineralization rates, C/N ratios (g/g), and estimates of bacterial growth efficiency (BGE). Rates were measured in April, September, and November and extrapolated to seasons as defined below. All rates integrated through the upper 30 cm of the sediment column. n = 16 to 30 for mineralization rates; n = 9 to 29 for sediment C/N.

Season	# days	N-Mineralization (mg N m^{-2} hr^{-1})	Sediment C/N (g/g)	C-Mineralization (g C m^{-2} season^{-1}) BGE = 0.5	BGE = 0.4	BGE = 0.3
"growth" (Mar to Jul)	153	11.32	11.66[a]	243[b]	291	340
"senescence" (Aug to Oct)	92	20.01	12.06	266	320	373
"winter" (Nov to Feb)	120	0.43	11.60	7	9	10
Annual totals (g C m^{-2} yr^{-1})				516	620	723

[a] Sediment C/N values are averages of seasonal C/N values for 0 to 2, 2 to 5, 10 to 13, 18 to 21, and 27 to 30 cm sediment sections.

[b] Calculated by multiplying N-mineralization x number of hours per season x sediment C/N x (1 – BGE).

concentrations were fairly uniform (average 19.6% ± 7.0 SD; n=294) through the top 30

cm of sediment. The high standard deviation reflects occasional high organic matter

concentrations (50 to 80%) in the upper 2 cm. In *Peltandra virginica* marshes, the

highest organic matter content and root concentrations are observed in the upper 30 cm

(Booth. 1989; Chambers and Fourqurean, 1991; Hussey and Odum, 1992; Harvey *et al.*,

1995), although live roots and high concentrations of sediment organic matter (15 to

20%) can be present to greater than 1 m (Booth, 1989; S.C. Neubauer, unpublished). In

our calculations, we extrapolated our measured rates of N mineralization (top 10 cm) to

30 cm depth.

Aboveground Biomass and Sediment Chlorophyll *a*: There was considerable

variability in aboveground biomass (AGB) along each transect with highest live biomass

observed near the tidal creek. All sampling locations were generally dominated by

Peltandra virginica and *Pontederia cordata*, with *Zizania aquatica* increasing in

abundance at the end of the growing season. Live biomass was highest during May and

June and lowest in November (Fig. 4; ANOVA, F=25.63, p < 0.0001; Tukey's HSD, p <

0.05). AGB was not measured during winter when few standing stems were observed.

Dead and dying biomass peaked in July (ANOVA, F=6.84, p < 0.001; Tukey's HSD, p <

0.01); nearly 70% of this material was *P. virginica* or *P. cordata*, while 20% was

unidentifiable detritus or wrack. Macrophyte C/N ratios ranged from 11.5 (*P. cordata*,

June) to 26.0 (*Z. aquatica*, November) and increased during the growing season.

Sediment chlorophyll *a* concentrations in the top 5 mm were highest in May (Fig. 4;

ANOVA, F=19.35, p<0.0001; Tukey's HSD, p<0.01).

34
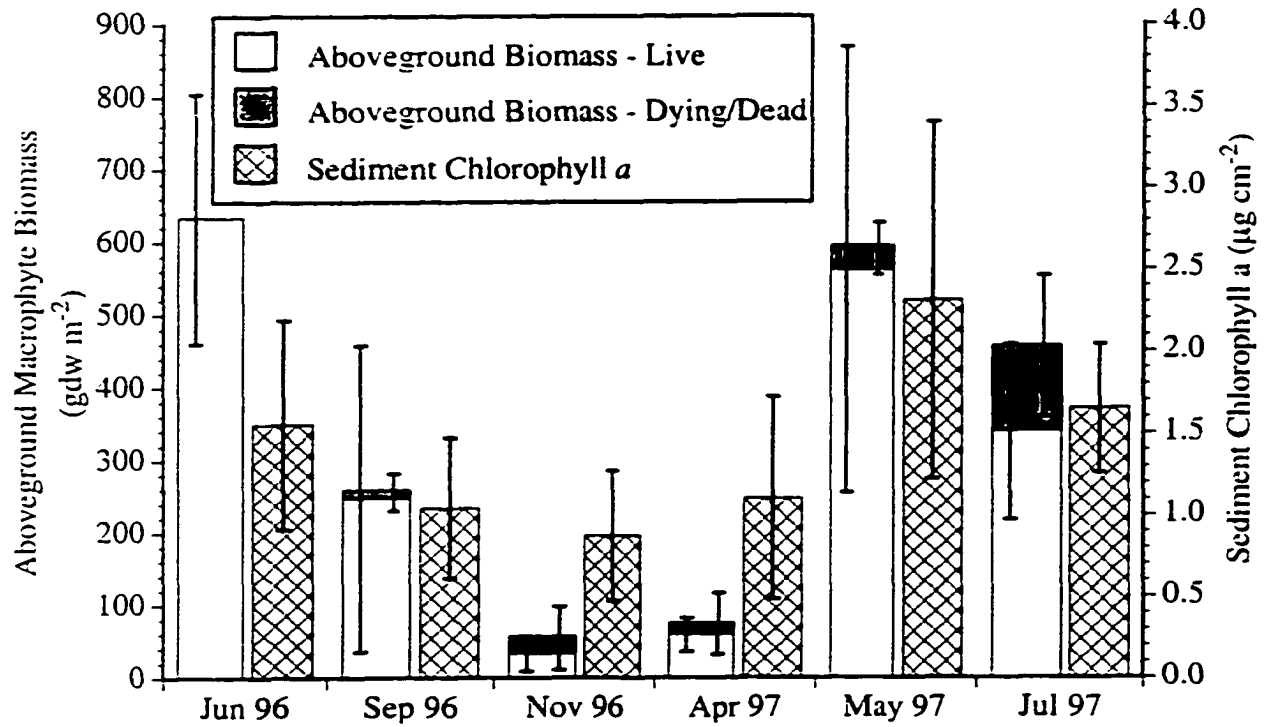
Figure 4: Aboveground macrophyte biomass and sediment chlorophyll. Error bars are ±

1 standard deviation; n = 10 for macrophyte biomass; n = 30 for sediment chlorophyll

GASEOUS CARBON FLUX MODEL

As a first step in constructing coupled carbon and nitrogen process-based mass balance models for Sweet Hall marsh, we developed a carbon gas flux model to determine annual rates of macrophyte and microalgal carbon fixation, and community and belowground respiration. To do this, it was necessary to scale our short-term field measurements of community and sediment CO_2 and CH_4 fluxes to daily, monthly, and annual rates. Our model is driven by these seasonal rates, which, in turn, are controlled by hourly changes in irradiance and temperature (measured at the Virginia Institute of Marine Science (VIMS), ~50 km from Sweet Hall; VIMS, 1997) and predicted tidal inundation of the marsh (modeled with a sine curve; 12 to 13 hr flooding per day).

Carbon fluxes were estimated for the two-year period from January 1996 through the end of December 1997. For the model, we made the assumption that photosynthesis vs. irradiance (P vs. I) and respiration vs. temperature (R vs. T) relationships (see below) did not change from year to year. Thus, interannual variations in modeled carbon fluxes are primarily due to changes in incident irradiance and temperature. For months where field data were not collected, flux rates were estimated by linear interpolation.

Model Construction and Assumptions

Gross Community Photosynthesis: Measurements of gross community photosynthesis (GCP) were made during eight months of the two year modeling period, with data

36

collected at a range of light levels (dark to full light) in each season. GCP was calculated

from field measurements of net community photosynthesis (light and shaded CO_2 fluxes)

plus community respiration (CR; dark CO_2 fluxes) taken immediately following the light

measurements. To determine changes in GCP over the course of a day or month in

response to changing light levels, GCP vs. irradiance (I) curves were developed. Data

from six chambers, placed along a transect extending from creekbank to marsh interior

were used to generate a GCP vs. I curve for each season. Hyperbolic curves (after

Whiting *et al.*, 1992) were fit to the data using the Levenberg-Marquardt iterative method

(DeltaPoint, 1996). Hourly GCP was modeled as:

$$GCP_t = \left[\frac{a \times I}{b + I} \right]$$

where GCP_t is calculated gross community photosynthesis (mg C m^{-2} hr^{-1}); I is average

hourly incident irradiance measured at VIMS (μE m^{-2} sec^{-1}); and *a* and *b* are empirically

derived constants with units of mg C m^{-2} hr^{-1} and μE m^{-2} sec^{-1}, respectively. Hourly GCP_t

rates were summed to determine daily and monthly fluxes.

When data for individual chambers were analyzed, ambient irradiance and GCP were

highly correlated (i.e. $r^2 = 0.84$ to 1.00 for April 1997; Fig. 5A). However, when a

month's data for all chambers were pooled (Fig. 5A), the correlation coefficient dropped

considerably ($r^2 = 0.30$ for April 1997 to 0.88 for July 1997), reflecting variability in

AGB and species composition along the transect. In spite of this, aggregated GCP vs. I

curves for each month were used to model the integrated response of the entire, spatially

variable, marsh community to changing light conditions (Fig. 5B).

37
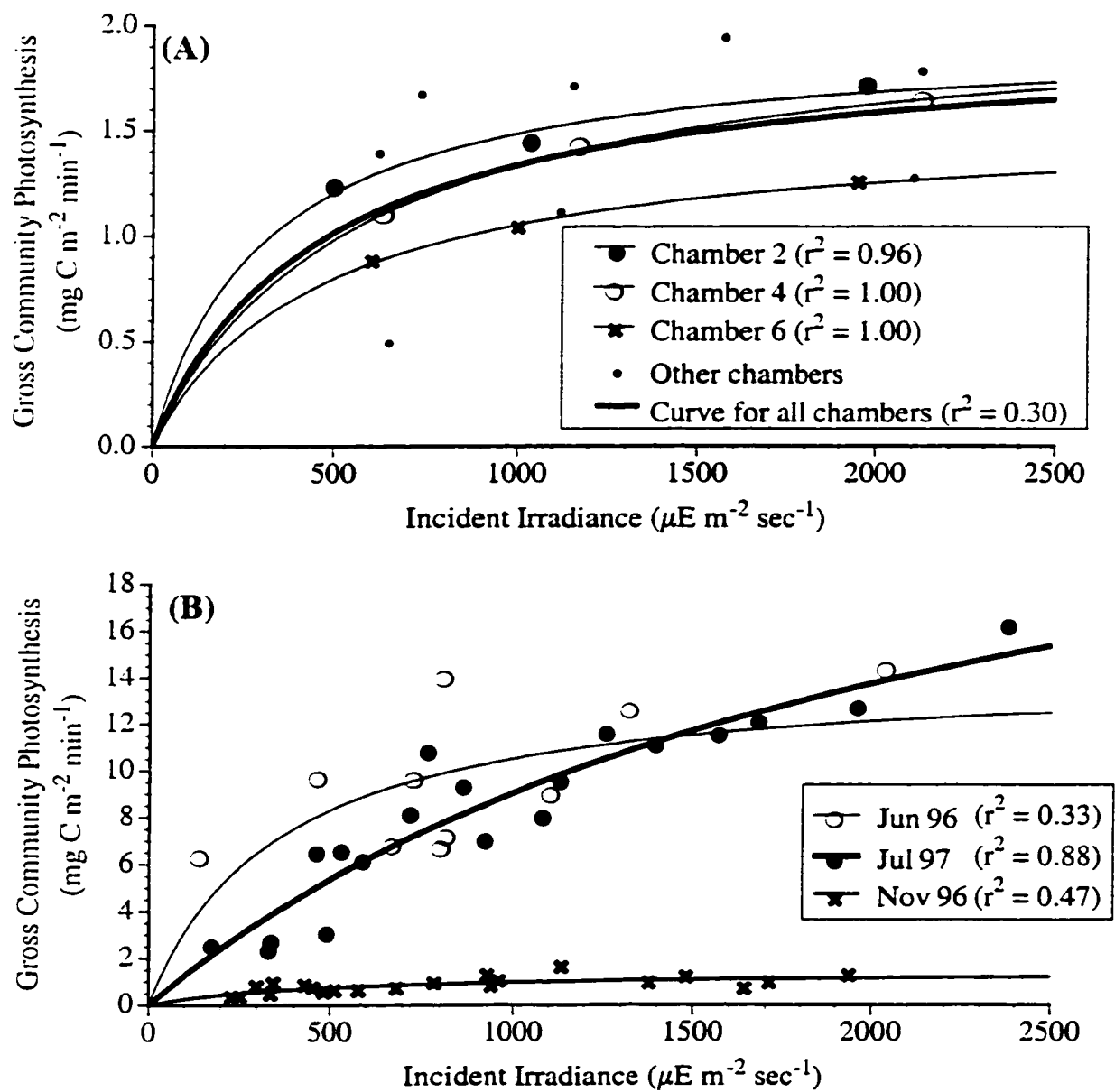
Figure 5: Photosynthesis versus irradiance curves. (A) Relationship between incident irradiance (I) and gross community photosynthesis (GCP) for April 1997, showing strong correlation for individual chambers, but much lower correlation when all chambers are considered. (B) Representative GCP versus I curves used in carbon gas flux model

38

Curves of GCP vs. I measured under flooded and non-flooded conditions were markedly different (Fig. 3B). However, when these curves were used to calculate GCP for the entire month of September 1997 (hypothetically assuming the marsh was always flooded or always dry), there was only a small difference between calculated monthly high and low tide GCP (106 vs. 108 g C m^{-2} month^{-1}, respectively). Therefore, we assumed that there was no change in GCP due to tidal flooding.

Gross Microalgal Photosynthesis: Because of a lack of low light intensity measurements during field studies (less than 200 μE m^{-2} sec^{-1}), gross microalgal photosynthesis (GMiP) vs. I curves could not be developed. To scale short-term rates to daily and monthly fluxes, we assumed maximum GMiP at irradiances greater than 500 μE m^{-2} sec^{-1}. Between 0 and 500 μE m^{-2} sec^{-1}, there was a linear increase from zero to full GMiP. Holmes and Mahall (1982) showed that net CO_2 exchanges for water-saturated intertidal sediments from California plateaued between 500 and 750 μE m^{-2} sec^{-1}. Similarly, Darley et al. (1981) observed saturating irradiances in a Spartina alterniflora marsh of 500 μE m^{-2} sec^{-1} during summer and 100 μE m^{-2} sec^{-1} in winter. Whitney and Darley (1983) and Pinckney (1994) reported saturating irradiances ranging from 500 to greater than 1000 μE m^{-2} sec^{-1}, depending on the habitat (i.e. creekbank vs. marsh interior). Short-term GMiP rates were multiplied by 60 to obtain hourly rates which were then summed to determine daily and monthly rates.

-

39

In our tidal inundation study, we were unable to calculate GMiP during high tide. Using the data of Holmes and Mahall (1982), we calculated that gross CO_2 uptake rates decreased by an average of 49 percent when the sediments were flooded with only a few millimeters of water. Pinckney and Zingmark (1993) calculated that microalgal production decreased by less than 25 percent during periods of flooding. To be conservative, we applied the 49 percent relative decrease from Holmes and Mahall (1982) to simulate a depression in Sweet Hall GMiP rates due to increased light attenuation and vertical migration (downward) of microalgae during tidal flooding (Pinckney and Zingmark, 1993; Pinckney, 1994). When modeling tidal effects on carbon flux rates, we assumed that the depth of water overlying the marsh did not affect process rates; the important factor was whether the marsh was "wet" or "dry."

Community Respiration: In April, July and September, Q_{10} values were calculated from plots of respiration vs. air temperature (CR vs. T). Values ranged from 1.94 (July) to 3.2 (April). In other months there was not a significant CR vs. T relationship, so values from April, July or September were substituted based on similarities in overall vegetation characteristics (AGB and species composition).

Monthly Q_{10} values were combined with hourly weather data measured at VIMS and average monthly respiration rates to calculate hourly CR rates:

$$CR_t = CR_i \times Q_{10}^{\left[\frac{t_t - t_i}{10}\right]}$$

where CR_t is calculated hourly respiration (mg C m^{-2} hr^{-1}); CR_i is the average CR rate during season i (mg C m^{-2} hr^{-1}); Q_{10} varies seasonally; and t_t and t_i are air temperatures

40

(°C) at time t and the time the field measurements were made, respectively. There were no tidal effects on CR (Fig. 3; ANOVA, $F = 2.68$, $p = 0.14$). Respiration was calculated 24 hours per day; hourly rates were summed to obtain daily and monthly CR rates.

Methane Release: Community CH_4 release (ME) was not significantly related to either air or sediment temperature; thus we assumed that the rates we measured were applicable throughout a month. The tidal effects study indicated that there were significant differences in ME over a tidal cycle (Fig. 3; ANOVA, $F = 18.18$, $p < 0.01$; Tukey's HSD, $p < 0.05$). Nighttime rates were fifty percent of daytime rates, suggesting that a light-dependent process was responsible for some of the CH_4 transport. For modeling purposes, night was defined as any time when average hourly irradiance was less than 50 μE m^{-2} sec^{-1}. Rates at high tide were only twelve percent of corresponding low tide rates. Hourly rates of CH_4 release were calculated as:

$$ME_t = ME_i \times (0.50)^* \times (0.12)^*$$

where ME_t is calculated CH_4 release rate (mg C m^{-2} hr^{-1}); ME_i is average ME rate during season i (mg C m^{-2} hr^{-1}); and the factors 0.5 and 0.12 are added (*as needed) to convert daytime low tide rates in response to diurnal or tidal changes, respectively. Hourly rates were summed to obtain daily and monthly fluxes.

Belowground Respiration: Gross N-mineralization (GNM) rates measured in April, September, and November were integrated over a sediment depth of 30 cm. Rates of GNM were converted to carbon units using sediment C/N ratios and estimated bacterial

41

growth efficiencies (BGE. or microbial growth yield) of 30 to 50% (Linley and Newell. 1984: Hart *et al.* 1994):

$$\text{Belowground C Respiration} = \left(\frac{C}{N}\right)_{substrate} \times \text{Gross N Mineralization} \times (1 - \text{BGE})$$

To convert rates from discrete seasons to an annual rate, seasons were defined based on vegetation processes. Early spring to summer (March to June) was defined as the "growth" period since AGB rises from near zero in March to maximum values in mid-June. Large amounts of *Peltandra virginica* and *Pontederia cordata* biomass begin to die in July (Fig. 4), and total community AGB continues to decline through the end of the growing season. Thus, July to September was classified as the period of "senescence." From November to February ("winter"), AGB was near zero. Within a season, no corrections were made for changes in sediment temperature.

Model Results

Photosynthesis: Total gross community photosynthesis (GCP) averaged 1062 ($\pm$102 SD) g C m^{-2} yr^{-1} over the 1996 to 1997 model period. Results from the sediment chambers show that 66 ($\pm$12 SD) g C m^{-2} yr^{-1} were fixed by sediment microalgae (GMiP). By difference, the remaining 996 ($\pm$114 SD) g C m^{-2} yr^{-1} was gross macrophyte photosynthesis (GMaP). GCP was low during winter and early spring, but increased from 26 to 174 g C m^{-2} month^{-1} between April and May (Fig. 6). This large increase in GCP was reflected in the large accumulation of AGB during the same period (Fig. 4), although measured photosynthetic rates were not sufficient to explain the entire biomass accumulation (see discussion below). Following a maximum in June, and coincident with decreases in AGB, there was a steady decline in GCP through the end of the

42
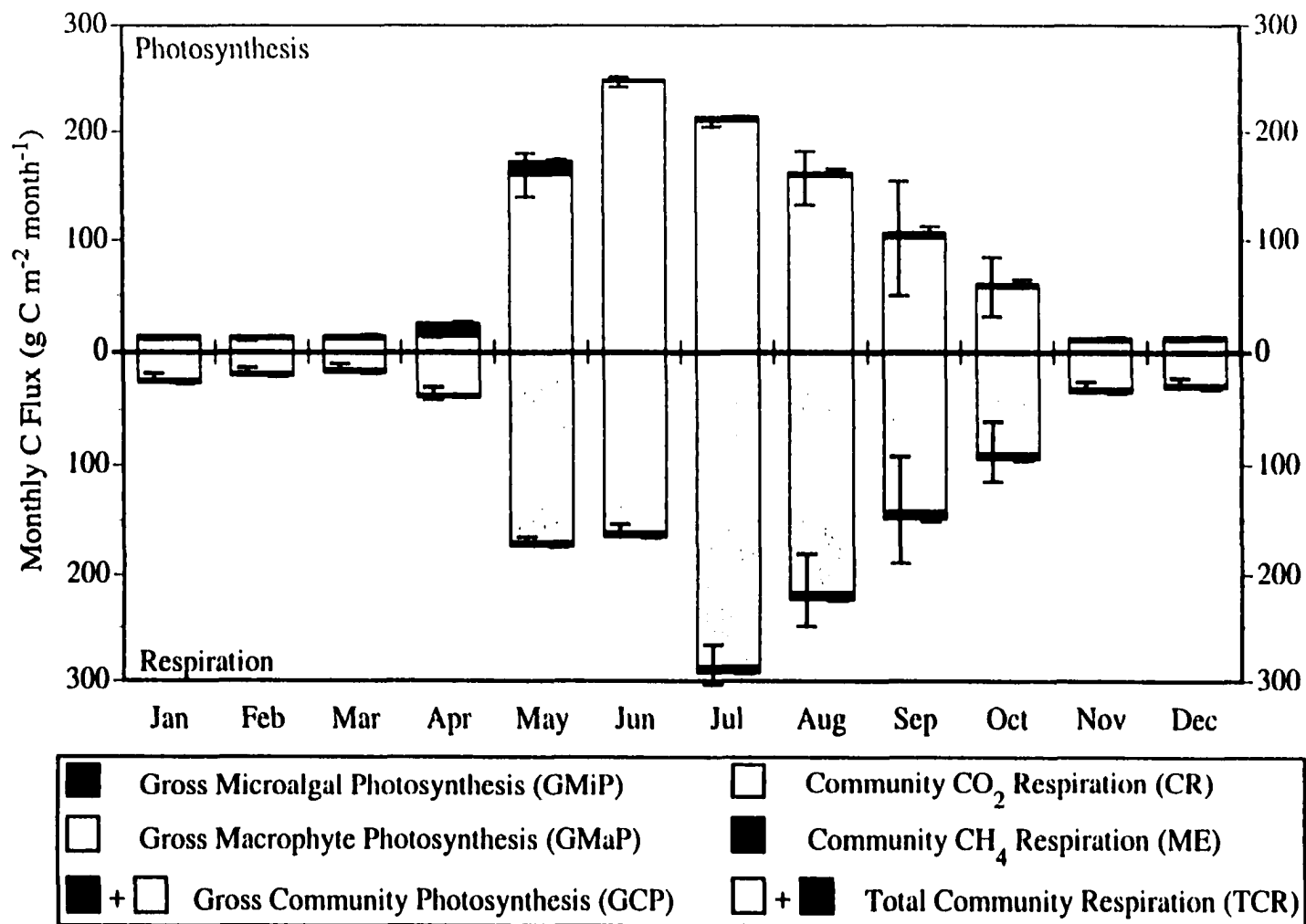
Figure 6: Carbon flux model output. Monthly rates of gross macrophyte and microalgal photosynthesis and community CO_2 and CH_4

respiration (g C m^{-2} mo^{-1}) from carbon gas flux model. Values are averages of 1996 and 1997 model output ($\pm$ 1 standard deviation;

error bars do not include prediction error of the P vs. I or R vs. T regressions)

growing season. GCP rates during winter were relatively constant (12 to 14 g C m^{-2} month^{-1}), reflecting low AGB during this time. Statistically, GCP rates were significantly higher (p < 0.05) during the summer (May to September) than during the rest of the year (November to April). Highest GMiP rates occurred in May (14.3 g C m^{-2} month^{-1}), before the growth of dense macrophyte biomass restricted light penetration to the sediment surface. In June, GMiP rates were the lowest of the year (2.1 g C m^{-2} month^{-1}; Fig. 6). GMiP rates again increased toward the end of the growing season, possibly due to senescence of the dense *Peltandra virginica* and *Pontederia cordata* cover and subsequent replacement by the tall. thin grass *Zizania aquatica*, which allowed more light to reach the sediment surface.

Respiration: Total community carbon respiration (TCR; CR+ME) exceeded gross marsh photosynthesis (GCP), 1269 ($\pm$130 SD) vs. 1062 g C m^{-2} yr^{-1}. Although not the focus of this paper, we hypothesize that sedimentation during tidal flooding provided sufficient carbon to the marsh to account for the high respiration rates and maintain rates of marsh surface accretion. Alternately, if GCP and TCR vary annually and are out of phase, high autotrophic production in one year might not be decomposed until the following year leading to an imbalance between GCP and TCR. Total community respiration rates were significantly greater during the summer (p < 0.05; May to September) than during the remainder of the year. Of the community respiratory flux, 6 percent (72 $\pm$ 4 g C m^{-2} yr^{-1}) was due to CH$_4$ release (ME); the remaining ninety-four percent (1197 $\pm$ 134 g C m^{-2} yr^{-1}) was CO$_2$ efflux (CR). CR rates were highest during July (285 g C m^{-2} month^{-1}; Fig. 6), perhaps due to the large amount of dead and dying *Peltandra virginica* and *Pontederia*

44

cordata biomass (Fig. 4). ME rates were highest during the late growing season (Aug to Sep; 8.4 to 8.6 g C m^{-2} month^{-1}).

When hourly N-mineralization rates were extrapolated to seasonal rates and converted to carbon units using measured sediment C/N ratios and bacterial growth efficiencies ranging from 0.3 to 0.5, "growth" and "senescence" periods accounted for nearly equal amounts of belowground respiration (BGR; 243 to 340 and 266 to 373 g C m^{-2} season^{-1}, respectively; Table 2). Although "winter" accounted for 120 days of the year, BGR during this season (7 to 10 g C m^{-2} season^{-1}) was less than two percent of the annual total.

Total BGR estimated from sediment nitrogen mineralization was 516 to 723 g C m^{-2} yr^{-1}. In contrast, carbon respiration (CO$_2$ + CH$_4$) measured using sediment chambers was 75 ($\pm$2 SD) g C m^{-2} yr^{-1}, suggesting that over 85% of CO$_2$ and CH$_4$ produced in the sediments was transported through macrophytes before being released to the atmosphere. Methane release (72 g C m^{-2} yr^{-1}) accounted for 11 to 13% of total BGR. However, nearly all CH$_4$ passed through plant tissues; sediment CH$_4$ fluxes were generally <1% of total sediment chamber respiration (data not shown). While gross CH$_4$ production may be much larger than net release due to methane oxidation in the sediment (Yavitt, 1997), gas transport through plant stems appears to provide a more efficient mechanism of releasing CH$_4$ to the atmosphere than direct sediment-atmosphere diffusion.

45

The difference between TCR and BGR (546 to 753 g C m^{-2} yr^{-1}) can be divided

among marsh macrophyte and microalgal respiration (MaR and MiR, respectively).

Pomeroy (1959) stated that MiR was less than ten percent of GMiP. Using this value, we

calculated a MiR rate of 7 g C m^{-2} yr^{-1} and a net microalgal photosynthesis rate of 60

($\pm$10) g C m^{-2} yr^{-1}. This will underestimate total microalgal production to the extent that

the algae utilize porewater DIC in addition to atmospheric CO_2. The remaining 539 to

747 g C m^{-2} yr^{-1} of respiration was due to macrophyte growth and respiration costs and

decomposition.

Macrophyte Carbon Budget: On an annual basis, 996 g C m^{-2} yr^{-1} (Table 3) were fixed by

marsh macrophytes (GMaP). During the early growing season (March to June), there

was little decaying AGB (Fig. 4); therefore, measured TCR included MaR necessary for

growth and maintenance and BGR. MaR, calculated as TCR – BGR – MiR, was

subtracted from GMaP to give a net macrophyte photosynthesis rate of 232 to 309 g C m^{-2}

($\overline{X}$ = 271 g C m^{-2}; March to June only). As the growing season progresses,

decomposition of AGB makes up an increasing proportion of TCR. To calculate MaR

while accounting for decomposition, we assumed that growth and maintenance

respiration costs were a constant percentage of GMaP, regardless of the time of year.

During March to June, we calculated that macrophyte respiration was 28 to 46% of

GMaP. Based on this estimate MaR for the remainder of the year would range from 159

to 261 g C m^{-2} yr^{-1} ($\overline{X}$ = 210); the remaining 259 to 287 g C m^{-2} ($\overline{X}$ = 273 g C m^{-2}) would

result from plant decomposition. Annual net macrophyte photosynthesis was thus

calculated to range from 536 to 715 g C m^{-2} yr^{-1} ($\overline{X}$ = 625 g C m^{-2} yr^{-1}). Based on studies

46

Table 3: Model output and sensitivity analysis for conceptual carbon flux model (Fig. 7). Case 1 to 3: variations in the bacterial growth efficiency from 30 to 50%. Cases 4 and 5: variations in the ratio of macrophyte respiration (MaR) to gross macrophyte photosynthesis (GMaP)

	Case 1	Case 2	Case 3	Case 4	Case 5
	Bacterial Growth Efficiency (%) =			MaR / GMaP (%) =	
	50	40	30	40	50
System Gas Fluxes					
Gross Macrophyte Photosynthesis	996	996	996	996	996
Macrophyte Respiration	459	370	281	398	497
Macrophyte Decomposition	287	273	259	277	293
Macro. Resp. / Gross Photo. (%)	46	37	28	40	50
Belowground Respiration	516	620	723	587	472
Carbon Inputs					
Net Macrophyte Photo.	536	625	715	597	498
DIC Uptake	21	21	21	21	21
Internal Cycling					
Spring Translocation	444	405	367	417	461
Autumn Translocation	460	460	460	460	460
Carbon Outputs					
Dissolved losses (leaching terms)	66	66	66	66	66
Particulate losses ("other losses")	204	307	410	275	160
Maximum C for export (dissolved plus particulate)	270	374	477	341	226

by Hwang and Morris (1992) in a *Spartina alterniflora* marsh, 5 to 37 g C m^{-2} yr^{-1} ($\overline{X}$ = 21 g C m^{-2} yr^{-1}) were fixed via DIC uptake by the roots (0.5 to 3.7% of GMaP). Therefore, net macrophyte production (net photosynthesis + DIC uptake) was 557 to 736 g C m^{-2} ($\overline{X}$ = 646 g C m^{-2}; Fig. 7).

Early summer translocation of carbon from belowground rhizomes to aboveground tissue is critical to support accumulation of aboveground biomass (AGB). Production of peak AGB required a total of 676 g C m^{-2} between the start of the growing season (March) and the time of peak biomass (June; calculated from peak AGB, species-specific % carbon values, and a turnover of 2.24 yr^{-1}). During this four month period, net photosynthesis accounted for only 35 to 45 percent of the carbon required. The remaining 367 to 444 g C m^{-2} ($\overline{X}$ = 405 g C m^{-2}) was likely supplied by translocation from below to aboveground tissues. Following peak biomass, AGB disappeared from the surface of the marsh. Possible fates include: respiration to CO_2 or CH_4, leaching as DOC during tidal flooding, translocation to belowground tissues, and other losses which include herbivory, deposition on the sediment surface or export from the marsh. Using our carbon gas flux model, some literature values, and a few simplifying assumptions, we have completed a conceptual carbon flux model, described below, for macrophytes in *Peltandra virginica* dominated tidal freshwater marshes (Fig. 7).

Leaching of DOC from plant tissues can occur both during tidal submergence and aerial exposure (Gallagher *et al.*, 1976; Turner, 1978; Pakulski, 1986; Moran and Hodson, 1990; Turner, 1993; Mann and Wetzel, 1996). Working in *Spartina alterniflora*

48
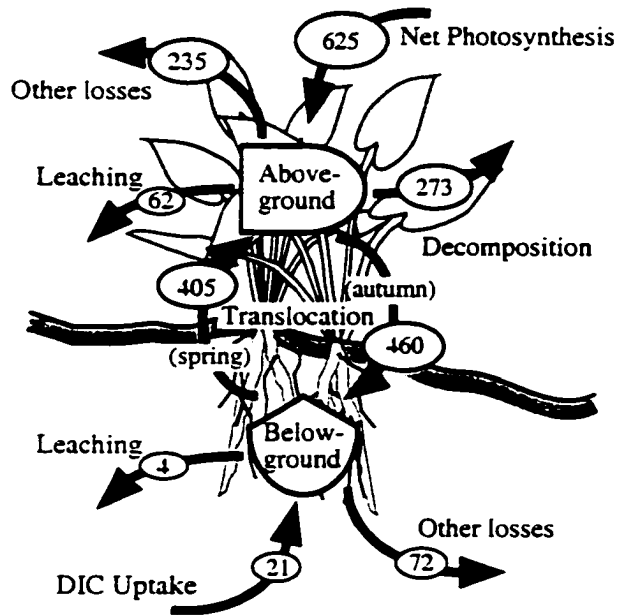
Figure 7: Conceptual model of carbon fluxes in a *Peltandra virginica* dominated tidal freshwater marsh. Bacterial growth efficiencies from 30 to 50% were used in the calculations presented in the text. For visual simplicity, only results using a median efficiency of 40% are shown here. Units are $g\ C\ m^{-2}\ yr^{-1}$.

49

salt marshes, Turner (1993) calculated that 5 to 10% of total aboveground production was leached from plant tissues. From our biomass harvests, seasonal and species-specific percent carbon data, and an annual live biomass turnover of 2.24 yr^{-1} (Wohlgemuth, 1988), we calculated aboveground macrophyte productivities using the peak biomass (845 g C m^{-2} yr^{-1}) and Smalley methods (776 g C m^{-2} yr^{-1}). Combined with Turner's (1993) data, we estimated a leaching rate of 41 to 85 g C m^{-2} yr^{-1} ($\overline{X}$ = 62 g C m^{-2} yr^{-1}). Using Booth's (1989) nitrogen leaching rates for *Peltandra virginica* and a C/N ratio of 16.3 for aboveground tissues (this study), 34 g C m^{-2} yr^{-1} were leached from aboveground tissues. Both of these values are likely underestimates of true leaching rates as *S. alterniflora* is more resistant to degradation than fleshy plants like *P. virginica* (Odum and Heywood, 1978; Webster and Benfield, 1986), and Booth's (1989) study examined only live standing leaves; leaching rates are higher from dead and dying tissues (Mann and Wetzel, 1996).

We assumed that DIC uptake occurred at a constant rate of 1.75 g C m^{-2} $month^{-1}$, for an annual total of 21 g C m^{-2}. Belowground leaching rates (4 g C m^{-2} yr^{-1}) were estimated from Rovira (1969) who reported that root leaching rates from a range of species are rarely more than 0.4% of GMaP. Combined root and rhizome mortality (defined here as loss to sediment macro-organic matter (MOM)) was estimated based on Booth (1989). Total loss of root matter during the early growing season (March to June) was 474 g C m^{-2}. Of this, 33 to 110 g C m^{-2} ($\overline{X}$ = 72 g C m^{-2}) were transferred from belowground biomass to the sediment MOM pool (474 g C m^{-2} total loss – 367 to 444 g C m^{-2} translocation loss – 3 g C m^{-2} leaching loss + 7 g C m^{-2} DIC uptake), although the

50

ultimate fate (e.g. respiration to CO_2 and CH_4, export from the marsh) of this MOM is unclear. Because belowground biomass standing stocks are similar at the beginning and end of the year (Booth, 1989), we balanced all inputs to the belowground compartment (DIC uptake and fall translocation) with outputs (leaching, spring translocation, and other losses) to calculate an autumn translocation rate of 460 g C m^{-2} yr^{-1}. Similarly, we balanced all inputs and outputs from the aboveground compartment (assuming that AGB is zero at the beginning and end of the year) and determined that 171 to 300 g C m^{-2} yr^{-1} ($\overline{X} = 235$ g C m^{-2}) of AGB was lost by herbivory, detritus deposition on the sediment surface, or export from the marsh by tidal waters. The partitioning between these loss terms is currently unknown.

DISCUSSION

The gas exchange technique described herein provides a non-destructive means of determining total macrophyte and microalgal production. Because production numbers are based on actual process modeling, a relatively large amount of data (e.g. GCP vs. I, CR vs. T curves) are needed to construct a robust model. Additionally, there are a series of assumptions (see "model construction and assumptions" section) that must be made to successfully extrapolate short-term (5 to 30 minute) field measurements to monthly and annual budgets. However, if these process relationships can be described and all assumptions confidently justified, a gas flux modeling approach can provide a degree of process-related insight into differences in primary productivity over the course of several years or between different marshes in the same year.

51

Gas Exchange versus Harvest Techniques: Annual net macrophyte production (557 to

736 g C m^{-2} yr^{-1}) determined using our gas flux model was lower than that based on AGB

harvest methods (776 to 845 g C m^{-2} yr^{-1}) adjusted by a turnover rate of 2.24 yr^{-1}

(Wohlgemuth, 1988). As previously discussed, harvest techniques tend to bias

production estimates by failing to account for seasonal translocation while the gas

exchange technique implicitly includes translocation and biomass turnover in production

calculations.

Several studies have measured both aboveground macrophyte biomass and

production in tidal freshwater marshes (Fig. 8). Because there is a wide range in

aboveground productivity depending on marsh species composition (Whigham *et al.*,

1978), we limited our comparison to *Peltandra virginica* and *Pontederia cordata*, the two

dominant species at our study site. In order to compare annual production values, we

converted literature production values from gdw m^{-2} yr^{-1} to g C m^{-2} yr^{-1} assuming a

percent carbon of 48.5% (our data, *P. virginica*, June). Our values of peak aboveground

biomass fall within the wide range of values reported for other east coast *P. virginica* and

P. cordata dominated tidal freshwater marshes (Fig. 8), while our annual production is

among the highest reported. This reflects the high biomass at our site, but also indicates

the sensitivity of the production estimate to the assumed rate of biomass turnover. The

studies reported in Whigham *et al.* (1978), Doumlele (1981), and the peak biomass and

Smalley methods of Wohlgemuth (1988) do not account for complete turnover of leaf

material during the growing season. These studies will underestimate true macrophyte

52
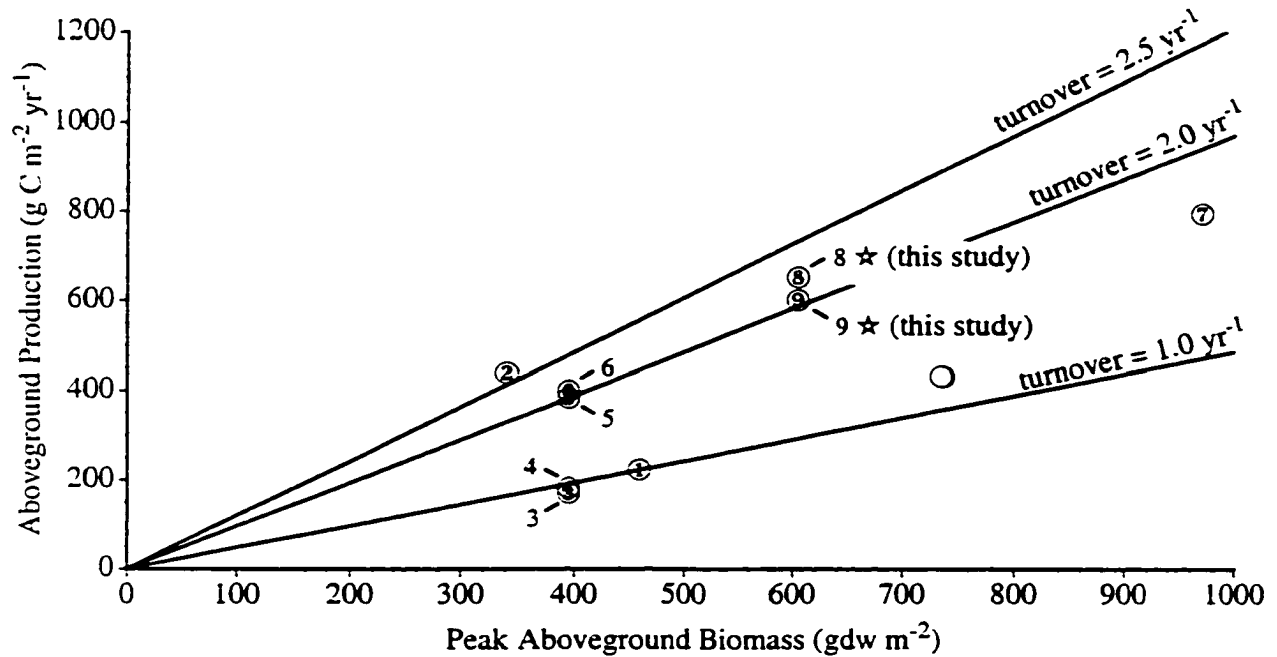
Figure 8: Aboveground production versus peak biomass for *Peltandra virginica* and/or

Pontederia cordata only in tidal freshwater marshes. Symbols as follows: O Whigham

et al. (1978); ①Doumlele (1981); ② Pickett (1984); ③ Wohlgemuth's (1988) peak

biomass, ④ Smalley, ⑤ mortality, and ⑥ Allen curve methods; ⑦ Booth (1989); ⑧this

study's peak biomass, and ⑨ Smalley methods. Lines indicate turnover (production /

peak biomass) of 1, 2, and 2.5 yr^{-1}.

53

production as *P. virginica* leaves can lose up to 50% of their dry weight after only nine

days of immersion (Odum and Heywood, 1978). The remaining data points on Figure 8,

with the exception of Booth (1989), fall between the lines indicating a turnover

(production / peak biomass) of 2 and 2.5 yr^{-1} and represent a more accurate estimate of

aboveground marsh production.

Microalgal Production: Sediment microalgal production rates measured in this study

fall in the wide range of 30 to 200 g C m^{-2} yr^{-1} reported for salt marshes and intertidal

habitats (Table 4). Estimates from a *Spartina alterniflora* salt marsh show that, given the

assumptions and limitations inherent in each approach, the gas exchange and

ecophysiological techniques provide similar production rates (Anderson *et al.*, 1997).

Nitrogen Mineralization: In spite of the uncertainties associated with using N

mineralization rates to calculate belowground C respiration, we believe that this method

is more accurate than directly measuring CO_2 and CH_4 gas effluxes into sediment

chambers. Few studies have simultaneously measured both carbon respiration and gross

nitrogen mineralization; none have done so in tidal marshes. Working in grassland and

cropland soils in North Dakota, Schimel (1986) reported no correlation between CO_2

evolution and gross N mineralization over the course of a four day laboratory incubation

and attributed this to changes in substrate quality (i.e. C/N ratio) during the incubation.

In contrast, studies in an old-growth forest in Oregon (Hart *et al.*, 1994) and a pine

plantation in New Zealand (Scott *et al.*, 1998) found strong correlations between CO_2

evolution and gross N mineralization rates. Hart *et al.* (1994) calculated the C/N ratio of

54

Table 4: Benthic microalgal production rates for intertidal marsh and sand/mudflat habitats

Location	Marsh Type	Method	Annual Production $(g\ C\ m^{-2}\ yr^{-1})$	Source
Delaware	salt marsh	O_2	61–99	Gallagher & Daiber (1974)
Tijuana Estuary, California	salt marsh	^{14}C	185–341	Zedler (1980)
global survey	intertidal and shallow coastal sediments	^{14}C and O_2	50–200	Colijn & de Jonge (1984) and references therein
East Galveston Bay, Texas	salt marsh	^{14}C	71	Hall & Fisher (1985)
Graveline Bay, Missisippi	salt marsh	^{14}C	28–151	Sullivan & Moncreiff (1988)
Sheepscot River Estuary, Maine	intertidal sand/mudflats	O_2	28–29	Cammen (1991)
North Inlet, South Carolina	salt marsh	O_2 microelectrode, Ecophysiological model	56–234	Pinckney & Zingmark (1993)
Goodwin Islands, Virginia	salt marsh	Process-based simulation model	101–169	Buzzelli (1996)
Phillips Creek marsh, Virginia	salt marsh	Ecophysiological model Ecophysiological model CO_2 gas flux	27.8 $4.9\ g\ C\ m^{-2}$; July only $3.8\ g\ C\ m^{-2}$; July only	Anderson et al. (1997)
Upper Brownsville marsh, Virginia	salt marsh	CO_2 gas flux	24–68	Miller (1998)
Sweet Hall marsh, Virginia	tidal freshwater marsh	CO_2 gas flux	59	this study

the respired substrate as 10 to 12, compared with a C/N ratio of 26.8 for forest soils. This difference suggests the presence of two sediment organic pools, one that is labile and rapidly mineralized (i.e. proteins and sugars) and another more recalcitrant pool (i.e. cellulose and lignin). Because emergent marsh macrophytes contain less cellulose and lignin than woody terrestrial plants (Odum and Heywood, 1978), the C/N ratio of respired marsh organic matter will be similar to that of marsh sediments. Thus, we converted N mineralization rates to C respiration using the C/N ratio of the sediments (11.6 to 12.1). Our measure of belowground respiration (516 to 723 g C m^{-2} yr^{-1}) may include some root respiration since no attempts were made to separate fine roots from the sediment matrix prior to the N mineralization studies.

Based on belowground biomass and sediment organic matter profiles for Sweet Hall and other *Peltandra virginica* dominated freshwater marshes, we assumed that mineralization was constant through the top 30 cm of the sediment column. Bowden *et al.* (1991) measured depth profiles of sediment mineralization in peat sediments along the North River, Massachusetts, and observed minimal N production or consumption between 10 and 30 cm. However, their study location was dominated by *Zizania aquatica*, *Carex* spp., and *Typha latifolia* - species with relatively shallow root distributions. Bowden *et al.* (1991) observed a distinct organic matter minimum at 30 cm; we observed constant concentrations (15 to 20%) to greater than 1 meter. These factors suggest that mineralization will occur to a greater depth at Sweet Hall than observed by Bowden *et al.* (1991), but this assumption needs to be experimentally verified. However, it is a daunting task to determine mineralization rates over a 1 meter

sediment profile in an extremely patchy environment where rates can be expected to vary both spatially (horizontally and vertically) and temporally.

There are few estimates of bacterial growth efficiency on marsh plants or sediment organic matter. In the absence of exogenous nutrient sources, the theoretical maximum microbial growth yield is equal to the C/N ratio of bacteria divided by the C/N ratio of the substrate (Linley and Newell. 1984). Assuming a bacterial C/N of 5 and measured sediment C/N ratios for Sweet Hall (11.6 to 12.1), bacterial growth efficiency is theoretically no greater then ~40%. However, in the presence of available nitrogen (e.g. DIN) in excess of that present in the substrate, actual growth efficiencies can be greater than the theoretical maximum (Newell *et al.*, 1983; Benner and Hodson, 1985; Benner *et al.*, 1988; Bano *et al.*, 1997, del Giorgio and Cole, 1998). Because fleshy emergent freshwater marsh plants are lower in lignin and humic compounds than salt marsh or woody plants and generally have lower C/N ratios, they are degraded more easily (Odum and Heywood, 1978; Odum *et al.*, 1984; Webster and Benfield, 1986) and may be expected to support microbial communities with higher growth efficiencies. Therefore, we used a range of bacterial growth efficiencies ranging from 30 to 50% ("theoretical" maximum ± 10%) to convert sediment N mineralization to C respiration.

Model Sensitivity Analysis: We performed sensitivity analyses to determine how our conceptual model responds to variations in bacterial growth efficiency (BGE) and macrophyte respiration rates (Table 3). When BGEs used in our analyses were varied from 30 to 50% (cases 1 to 3), calculated belowground respiration (BGR) varied by over

57

200 g C m^{-2} yr^{-1}. Although a BGE of 30% (case 3) is most similar to microbial yields on plant detritus (del Giorgio and Cole, 1998), it may overestimate the true BGR rate since macrophyte respiration (281 g C m^{-2} yr^{-1}) is only 28% of GMaP. In contrast, the ecophysiological model of Dai and Wiegert (1996) calculated total macrophyte respiration rates of 43 to 50% of GMaP for *Spartina alterniflora*. Because BGR and MaR are directly linked in our calculations, overestimating BGR will underestimate MaR and reduce the apparent respiration/photosynthesis ratio. Alternatively, it is possible that the BGR rates in case 3 are accurate since respiration costs are proportionally higher in salt marsh than freshwater plants due to salt (Cavalieri and Huang, 1981; Mendelssohn and Burdick, 1987) and sulfide stresses (King *et al.*, 1982). Cases 4 and 5 forced annual MaR to 40 to 50% of GMaP (the range reported by Dai and Wiegert, 1996) by increasing MaR (rather than by decreasing GMaP). The results from these cases were similar to those obtained from BGE estimates of 40 and 50%, suggesting that these growth yields are close to the true values for this system.

To further constrain our results, we estimated rates of GMaP and MaR using leaf-only gas flux measurements. In *Peltandra virginica*, there is restricted gas transport along the length of the petiole (Frye, 1989; Chanton *et al.*, 1992). Instead of passing through leaves, CH_4 and sediment-produced CO_2 diffuse directly from the petioles to the atmosphere. Therefore, measuring gas fluxes from leaves provides an independent means of measuring growth and maintenance respiration and partitioning BGR and MaR. Using mid-summer (July) leaf-only flux rates measured in a mixed *Zizania aquatica* and *P. virginica* tidal freshwater marsh on the Edisto River, South Carolina (C. Nietch, pers.

58

comm.) and Sweet Hall biomass numbers (this study), we calculated an average GMaP

rate of 310 g C m^{-2} (July only) and a leaf respiration rate of 154 g C m^{-2}. These rates

were higher than measured at Sweet Hall using the community chamber (Fig. 6).

Because photosynthesis and respiration rates are higher in leaves than in petioles and

stems, using leaf-only flux measurements and total AGB (leaves + stems + petioles) will

tend to overestimate rates. With this approach, macrophyte respiration was 50% of gross

photosynthesis. For comparison, using a BGE of 50% to convert gross sediment N

mineralization to C respiration (Table 3, case 1) produced a macrophyte respiration to

photosynthesis ratio of 46%. The similarity of these numbers is additional evidence that

our conversion of gross N mineralization to C respiration using sediment C/N ratios and

bacterial growth efficiencies was valid.

Macrophyte Carbon Budget: Our conceptual model of macrophyte-mediated carbon

flows in *Peltandra virginica* dominated tidal freshwater marshes is the first effort of this

type. Few studies have attempted to couple aboveground productivity with belowground

biomass (translocation and re-translocation), thereby limiting their utility in a larger

ecological context. The production of aboveground biomass is supported by net

macrophyte photosynthesis ($\overline{X}$ = 625 g C m^{-2} yr^{-1}; range 536 to 715 g C m^{-2} yr^{-1}) and the

spring translocation of "recycled" carbon stored in belowground rhizomes ($\overline{X}$ = 405 g C

m^{-2} yr^{-1}; range 367 to 444 g C m^{-2} yr^{-1}). In autumn, a slightly larger quantity of carbon

(462 g C m^{-2} yr^{-1}) is moved back to belowground tissues as plants senescence, contrasting

with N cycling where significantly greater quantities of nitrogen are translocated

aboveground in the spring than belowground in the autumn (Walker, 1981; Hopkinson

59

and Schubauer, 1984; Booth, 1989). Presumably this difference reflects the dominant

sources of carbon (atmospheric fixation) and nitrogen (belowground uptake) to the plants.

We have attempted to examine the fates of net macrophyte production as a first step

in determining the role that these highly productive plants play in supporting detrital or

microbially based food webs in adjacent tidal waters. We estimate that 66 g C m^{-2} yr^{-1}

(combined above + belowground) are leached from standing stems, roots, and rhizomes.

This leachate may be potentially important as a source of dissolved organic carbon

(DOC) to microbial food webs in adjacent tidal waters or it may be respired *in situ* and

form a portion of measured belowground respiration. Labile DOC leached from *Spartina*

alterniflora has been correlated with enhanced rates of water column community

respiration in waters adjacent to Georgia salt marshes (Turner, 1978; Pakulski, 1986),

while Mann and Wetzel (1996) demonstrated high rates of bacterial production on

leachates from aquatic macrophytes. Thus, marsh macrophytes can contribute to

microbially-based food webs in adjacent ecosystems.

The ultimate fate of 204 to 410 g C m^{-2} yr^{-1} ($\overline{X}$ = 307 g C m^{-2} yr^{-1}; combined above

and belowground "other loss" terms) is unknown. These plant tissues are either

consumed by herbivores, deposited as detritus on the sediment surface or macro-organic

matter in the sediment matrix, or exported from the marsh as dissolved or particulate

carbon. With the exception of a couple of species (notably *Hibiscus moscheutos*), direct

consumption of plant tissues by insects and birds is reportedly minimal, accounting for

less than ten percent of plant production (Odum *et al.*, 1984; Cahoon and Stevenson,

60

1986). The particulate carbon that is not directly consumed by herbivores falls to the sediment surface and enters the detrital pool where it contributes to belowground respiration, vertical marsh accretion, or is exported from the system. Interestingly, the relative lability (high nitrogen and low cellulose/lignin content) of freshwater marsh macrophyte tissues may limit their importance in aquatic food webs. Utilization of a food source by a consumer depends not only on the quality of the food item, but also on the availability of that food. If decomposition and leaching are rapid enough to remove detritus (as CO_2, CH_4 or DOC) before particulate matter can be exported from the marsh, labile detritus may play only a small role in supporting secondary production (Findlay *et al.*, 1990). Because the partitioning between these fates has important implications in the role of marsh macrophytes as sources of energy and nutrients to riverine food webs, further research should address the cycling of carbon both within tidal freshwater marshes and between these marshes and adjacent ecosystems.

61

LITERATURE CITED

Anderson IC, Tobias CR, Neikirk BB, Wetzel RL 1997. Development of a process-based nitrogen mass balance model for a Virginia (USA) *Spartina alterniflora* salt marsh: implications for net DIN flux. *Mar. Ecol. Prog. Ser.* 159:13-27.

Azcón-Bieto J, Gonzalez-Meler MA, Doherty W, Drake BG 1994. Acclimation of respiratory O_2 uptake in green tissues of field-grown native species after long-term exposure to elevated atmospheric CO_2. *Plant Physiol.* 106:1163-1168.

Bano N, Moran MA, Hodson RE 1997. Bacterial utilization of dissolved humic substances from a freshwater swamp. *Aquat. Microb. Ecol.* 12:233-238.

Benner R, Hodson RE 1985. Microbial degradation of the leachable and lignocellulosic components of leaves and wood from *Rhizophora mangle* in a tropical mangrove swamp. *Mar. Ecol. Prog. Ser.* 23:221-230.

Benner R, Lay J, K'nees E, Hodson RE 1988. Carbon conversion efficiency for bacterial growth on lignocellulose: implications for detritus-based food webs. *Limnol. Oceanogr.* 33(6 part 2):1514-1526.

Blum U, Seneca ED, Stroud LM 1978. Photosynthesis and respiration of *Spartina* and *Juncus* salt marshes in North Carolina: some models. *Estuaries* 1(4):228-238.

Booth PM 1989. *Nitrogen and phosphorus cycling strategies in two tidal freshwater macrophytes, Peltandra virginica and Spartina cynosuroides.* PhD dissertation, College of William and Mary, Virginia Institute of Marine Science, Gloucester Point

Bowden WB, Vörösmarty CJ, Morris JT, Peterson BJ, Hobbie JE, Steudler PA, Moore III B 1991. Transport and processing of nitrogen in a tidal freshwater wetland. *Water Resour. Res.* 27(3):389-408.

Brooks PD, Stark JM, McInteer BB, Preston T 1989. Diffusion method to prepare soil extracts for automated nitrogen-15 analysis. *Soil Sci. Soc. Am. J.* 53:1707-1711.

Buzzelli, CP 1996. *Integrative analysis of ecosystem processes in the littoral zone of lower Chesapeake Bay: a modeling study of the Goodwin Islands National Estuarine Research Reserve.* PhD dissertation, College of William and Mary, Virginia Institute of Marine Science, Gloucester Point.

Cahoon DR, Stevenson JC 1986. Production, predation, and decomposition in a low-salinity *Hibiscus* marsh. *Ecology* 67(5):1341-1350.

Cammen LM 1991. Annual bacterial production in relation to benthic microalgal production and sediment oxygen uptake in an intertidal sandflat and an intertidal mudflat. *Mar. Ecol. Prog. Ser.* 71:13-25

Cavalieri AJ, Huang AHC 1981. Accumulation of proline and glycinebetaine in *Spartina alterniflora* in response to NaCl and nitrogen in the marsh. *Oecologia* 49:224-228.

Chalmers AG, Wiegert RG, Wolf PL 1985. Carbon balance in a salt marsh: interactions of diffusive export, tidal deposition and rainfall-caused erosion. *Est. Coast. Shelf Sci.* 21:757-771.

Chambers RM, Fourqurean JW 1991. Alternative criteria for assessing nutrient limitation of a wetland macrophyte (*Peltandra virginica* (L) Kunth). *Aquat. Bot.* 40:305-320.

Chanton JP, Whiting GJ 1996. Methane stable isotopic distributions as indicators of gas transport mechanisms in emergent aquatic plants. *Aquat. Bot.* 54:227-236.

Chanton JP, Whiting GJ, Showers WJ, Crill PM 1992. Methane flux from *Peltandra virginica*: stable isotope tracing and chamber effects. *Global Biogeochem. Cycles* 6(1):15-31.

Colijn F, de Jonge VN 1984. Primary production of microphytobenthos in the Ems-Dollard estuary. *Mar. Ecol. Prog. Ser.* 14:185-196.

Currin CA, Newell SY, Paerl HW 1995. The role of standing dead *Spartina alterniflora* and benthic microalgae in salt marsh food webs: considerations based on multiple stable isotope analysis. *Mar. Ecol. Prog. Ser.* 121:99-116.

Curtis PS, Drake BG, Leadley PW, Arp WJ, Whigham DF 1989. Growth and senescence in plant communities exposed to elevated CO_2 concentrations on an estuarine marsh. *Oecologia* 78:20-26.

Dai T, Wiegert RG 1996. Estimation of the primary productivity of *Spartina alterniflora* using a canopy model. *Ecography* 19(4):410-423.

Darley WM, Montague CL, Plumley FG, Sage WW, Psalidas AT 1981. Factors limiting edaphic algal biomass and productivity in a Georgia salt marsh. *J. Phycol.* 17:122-128.

63

de la Cruz AA 1978. Primary production processes: summary and recommendations. In: Good RE, Whigham DF, Simpson RL (eds) *Freshwater wetlands: ecological processes and management potential.* Academic Press, New York, p 79-86.

del Giorgio PA, Cole, JJ 1998. Bacterial growth efficiency in natural aquatic systems. *Ann. Rev. Ecol. Syst.* 29:503-541.

Deegan LA, Garritt RH 1997. Evidence for spatial variability in estuarine food webs. *Mar. Ecol. Prog. Ser.* 147:31-47.

DeltaPoint Inc 1996. DeltaGraph version 4.0 users guide. Monterey, California.

Doumlele DG 1981. Primary production and seasonal aspects of emergent plants in a tidal freshwater marsh. *Estuaries* 4(2):139-142.

Drake BG 1984. Light response characteristics of net CO_2 exchange in brackish wetland plant communities. *Oecologia* 63(2):263-270.

Findlay S, Howe K, Austin HK 1990. Comparison of detritus dynamics in two tidal freshwater wetlands. *Ecology* 71(1):288-295.

Frye JP 1989. *Methane movement in* Peltandra virginica. MS thesis, University of Virginia, Charlottesville.

Gallagher JL 1975. The significance of the surface film in salt marsh plankton metabolism. *Limnol. Oceanogr.* 20(1):120-123.

Gallagher JL, Daiber F 1974. Primary production of edaphic algal communities in a Delaware salt marsh. *Limnol. Oceanogr.* 19:390-395.

Gallagher JL, Pfeiffer WJ, Pomeroy LR 1976. Leaching and microbial utilization of dissolved organic carbon from leaves of *Spartina alterniflora. Est. Coast. Mar. Sci.* 76(4):467-471.

Giurgevich JR, Dunn EL 1978. Seasonal patterns of CO_2 and water vapor exchange of *Juncus Roemerianus* Scheele in a Georgia salt marsh. *Am. J. Botany* 65(5):502-510.

Gosselink JG, Odum EP, Pope RM 1973. *The value of the tidal marsh.* Work Paper No. 3. Wetland Resoures Institute, Louisiana State University, Baton Rouge.

Hall SL, Fisher Jr FM 1985. Annual productivity and extracellular release of dissolved organic compounds by the epibenthic algal community of a brackish marsh. *J. Phycol.* 21:277-281.

64

Hamilton SK, Lewis Jr WM, Sippel SJ 1992. Energy sources for aquatic animals in the Orinoco River floodplain: evidence from stable isotopes. *Oecologia* 89:324-330.

Hart SC, Nason GE, Myrold DD, Perry DA 1994. Dynamics of gross nitrogen transformations in an old-growth forest: the carbon connection. *Ecology* 75(4): 880-891.

Harvey JW, Chambers RM, Hoelscher JR 1995. Preferential flow and segregation of porewater solutes in wetland sediment. *Estuaries* 18(4):568-578.

Holmes RW, Mahall BE 1982. Preliminary observations on the effects of flooding and dessication upon the net photosynthetic rates of high intertidal estuarine sediments. *Limnol. Oceanogr.* 27(5):954-958.

Hopkinson CS 1988. Patterns of organic carbon exchange between coastal ecosystems: the mass balance approach in salt marsh ecosystems. In: Jansson BO (ed) *Coastal-offshore ecosystem interactions: lecture notes on coastal and estuarine studies,* Volume 22. Springer-Verlag, Berlin, p 122-154.

Hopkinson CS, Schubauer JP 1984. Static and dynamic aspects of nitrogen cycling in the salt marsh graminoid *Spartina alterniflora. Ecology* 65(3):961-969.

Howes BL, Dacey JWH, King GM 1984. Carbon flow through oxygen and sulfate reduction pathways in salt marsh sediments. *Limnol. Oceanogr.* 29(5):1037-1051.

Hussey BH, Odum WE 1992. Evapotranspiration in tidal marshes. *Estuaries* 15(1):59-67.

Hwang YH, Morris JT 1992. Fixation of inorganic carbon from different sources and its translocation in *Spartina alterniflora* Loisel. *Aquat. Bot.* 43:137-147.

Hwang YH, Morris JT 1994. Whole plant gas exchange responses of *Spartina alterniflora* (Poaceae) to a range of constant and transient salinities. *Am. J. Botany* 81:659-665.

King GM, Klug MJ, Wiegert RG, Chalmers AG 1982. Relation of soil water movement and sulfide concentration to *Spartina alterniflora* production in a Georgia salt marsh. *Science* 218:61-63.

Linley EAS, Newell RC 1984. Estimates of bacterial growth yields based on plant detritus. *Bull. Mar. Sci.* 35(3):409-425.

Lorenzen C 1967. Determination of chlorophyll and phaeopigments: spectrophotometric equations. *Limnol. Oceanogr.* 12:343-346.

Lytle RW, Hull RJ 1980a. Photoassimilate distribution in *Spartina alterniflora* Loisel, I Vegetative and floral development. *Agronomy J.* 72:933-938.

Lytle RW, Hull RJ 1980b. Photoassimilate distribution in *Spartina alterniflora* Loisel, II Autumn and winter storage and spring regrowth. *Agronomy J.* 72:938-942.

Mann CJ, Wetzel RG 1996. Loading and utilization of dissolved organic carbon from emergent macrophytes. *Aquat. Bot.* 53:61-72.

Mendelssohn IA, Burdick DM 1987. The relationship of soil parameters and root metabolism to primary production in periodically inundated soils. In: Hook DD, McKee Jr. WH, Smith HK, Gregory J, Burrell VG, DeVoe MR, Sojka RE, Gilbert S, Banks R, Stolzy LH, Brooks C, Matthews TD, Shear TH (eds) *The ecology and management of wetlands*. Timber Press, Portland, p 398-428.

Miller WD 1998. *The effects of increased inundation and wrack deposition on photosynthesis and respiration in a Virginia salt marsh*. MA thesis, College of William and Mary, Williamsburg.

Moran MA, Hodson RE 1990. Contributions of degrading *Spartina alterniflora* lignocellulose to the dissolved organic carbon pool of a salt marsh. *Mar. Ecol. Prog. Ser.* 62:161-168.

Morris, JT, Houghton RA, Botkin DB 1984. Theoretical limits of belowground production by *Spartina alterniflora*: an analysis through modeling. *Ecol. Model.* 26:155-175.

Morris JT, Whiting GJ 1986. Emission of gaseous carbon dioxide from salt-marsh sediments and its relation to other carbon losses. *Estuaries* 9(1):9-19.

Newell RC, Linley EAS, Lucas MI 1983. Bacterial production and carbon conversion based on salt marsh plant debris. *Est. Coast. Shelf Sci.* 17(4):405-419.

Odum EP 1968. *A research challenge: evaluating the productivity of coastal and estuarine water*. Proceedings of the Second Sea Grant Conference, University of Rhode Island, Providence p 63-64.

Odum WE, Heywood MA 1978. Decomposition of intertidal freshwater marsh plants. In: Good RE, Whigham DF, Simpson RL (eds) *Freshwater wetlands: ecological processes and management potential*. Academic Press, New York, p 89-98.

Odum WE, Smith III TJ, Hoover JK, McIvor CC 1984. *The ecology of tidal freshwater marshes of the United States east coast: a community profile.* US Department of the Interior, Fish and Wildlife Service, FWS/OBS-83/17.

Pakulski JD 1986. The release of reducing sugars and dissolved organic carbon from *Spartina alterniflora* Loisel in a Georgia salt marsh. *Est. Coast. Shelf Sci.* 22:385-394.

Perry III JE 1991. *Analysis of vegetation patterns in a tidal freshwater marsh.* PhD dissertation, College of William and Mary, Virginia Institute of Marine Science. Gloucester Point.

Pezeshki SR 1991. Population differentiation in *Spartina patens*: gas exchange responses to salinity. *Mar. Ecol. Prog. Ser.* 72(1-2):125-130.

Pickett JR 1984. *Community composition and net primary production of emergent macrophytes in a South Carolina tidal freshwater marsh ecosystem.* MS thesis, University of South Carolina, School of Public Health, Columbia.

Pinckney JL 1994. Development of an irradiance-based ecophysiological model for intertidal benthic microalgal production. In: Krumbein WE, Paterson DM, Stal LJ (eds) *Biostabilization of sediments.* Carl von Ossietzky Universität, Oldenburg, Germany, p 55-83.

Pinckney JL, Papa R, Zingmark RG 1994. Comparison of high-performance liquid chromatographic, spectrophotometric, and fluorometric methods for determining chlorophyll *a* concentrations in estuarine sediments. *J. Microbiol. Methods* 19:59-66.

Pinckney JL, Zingmark RG 1993. Modeling the annual production of intertidal benthic microalgae in estuarine ecosystems. *J. Phycol.* 29:396-407.

Pomeroy LR 1959. Algal productivity in salt marshes of Georgia. *Limnol. Oceanogr.* 4:386-397

Rovira AD 1969. Plant root exudates. *Bot. Rev.* 35:35-57.

Schimel, DS 1986. Carbon and nitrogen turnover in adjacent grassland and cropland ecosystems. *Biogeochem.* 2:345-357.

Schubauer JP, Hopkinson CS 1984. Above- and belowground emergent macrophyte production and turnover in a coastal marsh ecosystem, Georgia. *Limnol. Oceanogr.* 29(5):1052-1065.

Scott NA, Parfitt RL, Ross DJ, Salt GJ 1998. Carbon and nitrogen transformations in New Zealand plantation forest soils from sites with different N status. *Can. J. For. Res.* 28:967-976.

Smalley AE 1958. *The role of two invertebrate populations,* Littorina irrorata *and* Orchelimum fidicinium, *in the energy flow of a salt marsh ecosystem.* PhD dissertation, University of Georgia, Athens.

Solorzano L 1969. Determination of ammonia in natural waters by the phenolhypochlorite method. *Limnol. Oceanogr.* 14:799-801.

Sullivan MJ, Moncreiff CA 1988. Primary production of edaphic algal communities in a Mississippi salt marsh. *J. Phycol.* 24:49-58.

Sullivan MJ, Moncreiff CA 1990. Edaphic algae are an important component of salt marsh food- webs: evidence from multiple stable isotope analyses. *Mar. Ecol. Prog. Ser.* 62:149-159.

Teal JM 1962. Energy flow in the salt marsh ecosystem of Georgia. *Ecology* 43:614- 624.

Turner RE 1978. Community plankton respiration in a salt marsh estuary and the importance of macrophyte leachates. *Limnol. Oceanogr.* 23(3):442-451.

Turner RE 1993. Carbon, nitrogen, and phosphorus leaching rates from *Spartina alterniflora* salt marshes. *Mar. Ecol. Prog. Ser.* 92:135-140.

VIMS 1997. *York River ambient monitoring data: VIMS scientific data archive.* Virginia Institute of Marine Science, College of William and Mary, Gloucester Point (accessed: 12 March 1999); available at http://www.vims.edu/data_archive.

Walker R 1981. *Nitrogen, phosphorus and production dynamics for* Peltandra virginica *(L) Kunth in a southern New Jersey freshwater tidal marsh.* PhD dissertation, Rutgers University, New Brunswick.

Webster JR, Benfield EF 1986. Vascular plant breakdown in freshwater ecosystems. *Ann. Rev. Ecol. Syst.* 17:567-594.

Weiss RF 1974. Carbon dioxide in water and seawater: the solubility of a non-ideal gas. *Mar. Chem.* 2:203-215.

Wessel WW, Tietema A 1992. Calculating gross N transformation rates of ^{15}N pool dilution experiments with acid forest litter: analytical and numerical approaches. *Soil Biol. Biochem.* 24:931-942.

Whigham DF, McCormick J, Good RE, Simpson RL 1978. Biomass and primary production in freshwater tidal wetlands of the middle Atlantic Coast. In: Good RE, Whigham DF, Simpson RL (eds) *Freshwater wetlands: ecological processes and management potential*. Academic Press, New York, p 3-20.

Whiting GJ, Bartlett DS, Fan S, Bakwin PS, Wofsy SC 1992. Biosphere/atmosphere CO_2 exchange in tundra ecosystems: community characteristics and relationships with multispectral surface reflectance. *J. Geophys. Res.* 97(D15):16,671-16,680.

Whiting GJ, Chanton JP 1996. Control of the diurnal pattern of methane emission from emergent aquatic macrophytes by gas transport mechanisms. *Aquat. Bot.* 54:237-253.

Whitney DE, Darley WM 1983. Effect of light intensity upon salt marsh benthic microalgal photosynthesis. *Mar. Biol.* 75(2-3):249-252.

Wohlgemuth M 1988. *Estimation of net aerial primary production of* Peltandra virginica *(L) Kunth using harvest and tagging techniques*. MA thesis, College of William and Mary, Virginia Institute of Marine Science, Gloucester Point.

Yavitt JB 1997. Methane and carbon dioxide dynamics in *Typha latifolia* wetlands in central New York state. *Wetlands* 17(3):394-406.

Zar JH 1996. *Biostatistical analysis*, 3rd edition. Prentice-Hall, Upper Saddle River, New Jersey.

Zedler JB 1980. Algal mat productivity: comparisons in a salt marsh. *Estuaries* 3(2):122-131.

SECTION II

Sedimentation in a Mid-Atlantic Tidal Freshwater Marsh[*]

[*] To be submitted to *Estuarine Coastal and Shelf Science* with Scott C. Neubauer, José A. Constantine, Iris Cofman Anderson and Steven A. Kuehl as authors.

ABSTRACT

Sediment deposition and accretion rates in a Virginia tidal freshwater marsh were measured to provide insight into the processes and time scales that are important for maintaining marsh surface elevation. Short term sediment deposition rates (biweekly to monthly) measured using sediment collection tiles were spatially and temporally variable. Rates were greatest near a tidal creek and decreased along a transect extending toward the marsh interior. When integrated across the entire marsh, annual sediment deposition averaged 517 ± 353 g C m^{-2} y^{-1} and was sufficient to balance the effects of relative sea level rise and marsh respiration rates. At the creekbank, the highest deposition rates were measured during summer while rates were relatively constant over time at the interior sites. Similar spatial and temporal patterns were obtained when deposition rates were calculated from ^{7}Be inventories (monthly time scale). Seasonal sediment inventories of ^{7}Be were greater than atmospherically supported ^{7}Be inventories, indicating that the spatial patterns of sedimentation were not due to sediment erosion and redistribution within the marsh. Accretion rates calculated from ^{137}Cs (decadal scale) and ^{14}C dating (centuries to millennia) were substantially less than annual deposition rates, with a steady decrease in accretion rate with increasing time scale. Mineralization rates of recently deposited sediments (measured as O_2 consumption) indicated that sediment metabolism could potentially remove ~30% of recently deposited carbon within one month of deposition. The metabolism of a labile sediment fraction could explain a portion of the observed decrease in accretion rate with increasing time scale, with the remainder due to periodic storm-induced erosion and historical variability in sediment deposition rates.

71

INTRODUCTION

Because of their location at the head of estuaries where watershed influences are concentrated, tidal freshwater marshes are among the first systems to interact with, and potentially remove watershed-derived sediments, nutrients, and pollutants. Sediment deposition onto the marsh surface occurs when water column turbulent energy is reduced following flooding of the marsh itself (Leonard & Luther 1995), while removal of dissolved materials can take place via direct uptake by organisms in the marsh or sorption onto sediment particles with subsequent deposition (Olsen et al. 1982; Froelich 1988; Hedges and Keil 1999). In contrast to infrequently flooded marshes where the retention of autochthonous production is responsible for the bulk of vertical accretion, marshes that are regularly inundated rely on both autochthonous production and the deposition of mineral sediments to maintain marsh elevation relative to a rising sea level (Bricker-Urso et al. 1989; Craft et al. 1993).

While tidal salt marsh sedimentation has been well studied (see reviews in Frey & Basan 1985; Stevenson et al. 1988; Friedrichs & Perry 2000), relatively few studies have examined sediment dynamics in tidal freshwater wetlands. Pasternack and Brush (1998) measured seasonal patterns in sediment deposition across freshwater marsh habitat types using sediment collection tiles, while Ledwin (1988) studied annual deposition and erosion rates using a combination of marker horizons, sediment traps and graduated stakes. Childers et al. (1993) used a sedimentation-erosion table (SET) to examine spatial and temporal variability in sedimentation along an estuarine gradient. Short term

72

measurements, which are usually collected at relatively high frequency (i.e. weekly to monthly), are useful in determining seasonal patterns in sediment deposition due to variations in sediment supply or marsh sediment trapping efficiency. Sediment accretion rates (decades to centuries) in tidal freshwater marshes have been calculated using palynology (pollen analysis; e.g. Orson et al. 1990, 1992; Khan & Brush 1994), modeling (Morris & Bowden 1986), and ^{137}Cs, ^{210}Pb, and ^{14}C radioisotope dating (e.g. Orson et al. 1990; Campana 1998; Cornwell & Zelenke 1998). Unlike short term deposition rates, accretion rates integrate processes that occur over many years and can therefore be useful in detecting historical patterns in sedimentation due to changes in land use and sediment delivery from the watershed.

Rates of sediment deposition and accretion are linked. For instance, greater rates of sediment deposition can lead to enhanced preservation and accretion (Hedges & Keil 1995). Similarly, sediment accretion rates influence the frequency and duration of tidal flooding which subsequently affects deposition rates (Bricker-Urso et al. 1989; Cahoon & Reed 1995; Leonard 1997). Examining sedimentation rates over a range of time scales provides insight into the factors that control marsh elevation and sedimentation processes. In this study, biweekly to monthly measurements of deposition onto sediment collection tiles were used to estimate annual sediment deposition rates for a mid-Atlantic (Virginia) tidal freshwater marsh. Depth profiles of ^{137}Cs were used to calculate decadal accretion rates, while long term (centuries to millennia) rates were estimated using ^{14}C dating. Sediment inventories of the radioisotope ^{7}Be were used to assess the role of erosion in marsh sediment dynamics, and seasonal measurements of sediment respiration examined

73

the importance of biological utilization of sediment-associated carbon in controlling sedimentation rates.

STUDY AREA

The Pamunkey River drains 3768 km^2 in southeastern Virginia before converging with the Mattaponi River at West Point, Virginia to form the York River (Fig. 1A). The Pamunkey River watershed is predominately undeveloped (65% forested, 6% tidal + non-tidal wetlands), with 27% as grass and croplands and <2% urbanized (EPA 1996). Tidal marshes along the lower Pamunkey River range in size from small pocket and fringing marshes less than 0.5 ha to expansive marshes up to 587 ha (Doumlele 1979; Silberhorn & Zacherle 1987). Global eustatic sea level rise is occurring at 1 to 1.5 mm yr^{-1} (Gornitz et al. 1982; Gorniz & Lebedeff 1987). When combined with locally high rates of subsidence (3 to 5 mm yr^{-1}; Holdahl & Morrison 1974) due to groundwater withdrawal and post-glacial crustal rebound, relative sea level in the lower Pamunkey River is rising at a rate of 4 to 6.5 mm yr^{-1}.

This study was conducted at Sweet Hall, a 401 ha tidal freshwater marsh located 35 km by river from West Point, VA (Fig. 1A). The marsh is a site within the Chesapeake Bay National Estuarine Research Reserve System in Virginia (CB-NERRVA). Long-term average salinity at Sweet Hall is 0.5 (Brooks 1983) although the average salinity in 1999 was 2.8 (range 0.0 to 15.9; CB-NERRVA unpublished data). High salinity and the increasing presence of the oligohaline species *Spartina cynosuroides* in the marsh may be

74
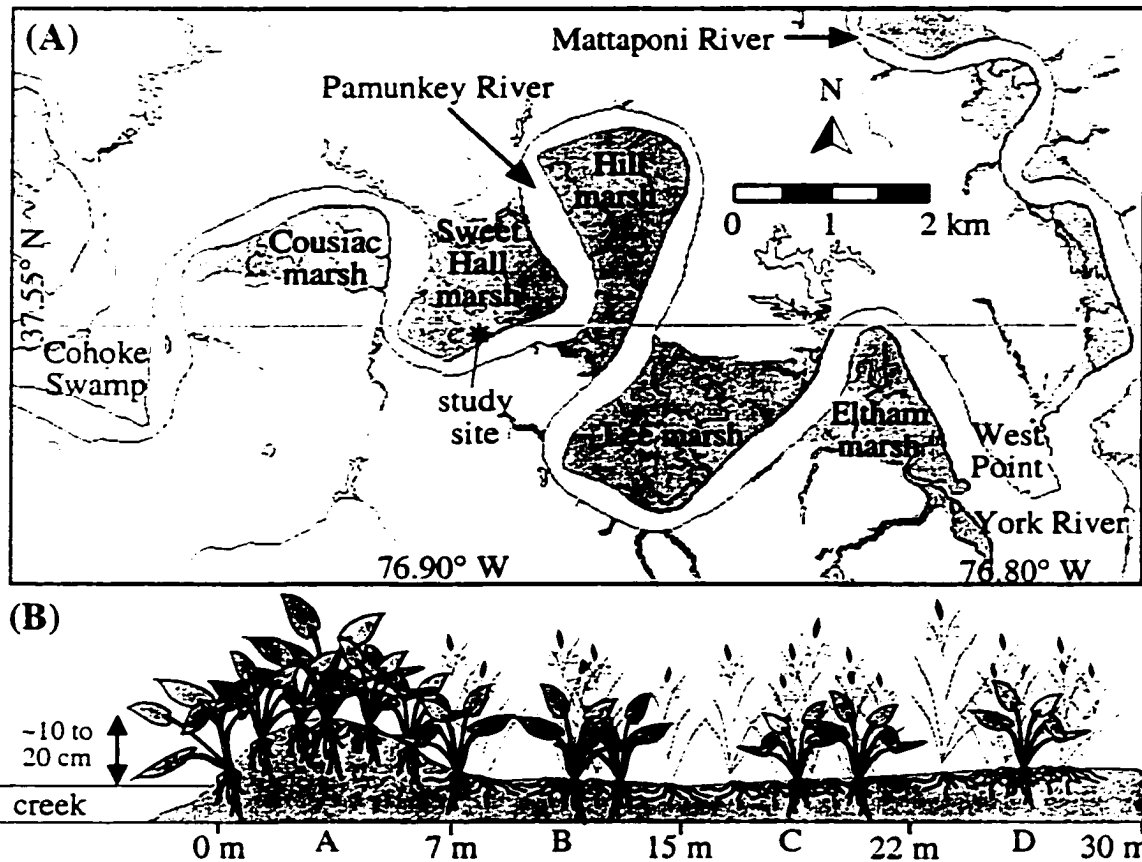
Figure 1: Sweet Hall marsh study site. (A) Map of Pamunkey River, Virginia showing

location of Sweet Hall and other tidal marshes (shaded areas). Tidal marsh areas were

redrawn from Doumlele (1979) and Silberhorn and Zacherle (1987). Approximately

2400 ha of tidal marsh in the Pamunkey River (out of 3000 ha total) are shown on this

map; the remainder are farther upriver. (B) Generalized cross-section of study site

showing 10 to 20 cm elevated creekbank levee and location of sampling blocks within the

marsh. Not to scale.

75

indicative of a long-term shift from freshwater to oligohaline conditions (Perry & Hershner 1999). At Sweet Hall, the Pamunkey River is microtidal, with a mean tidal range of 70 cm (neap tide) to 90 cm (spring tide). To minimize disturbance to the marsh surface, all sampling was conducted from three boardwalks (30 m) which extended roughly perpendicular to the western branch of Hill's Ditch, a tidal creek draining the southern portion of the marsh. Each boardwalk traversed a creekside levee (~10 to 20 cm elevated above the surrounding marsh) before extending into the marsh interior (Fig. 1B).

MATERIALS AND METHODS

Sedimentation Measurements

Sediment Collection Tiles: Between February 1998 and August 1999, net rates of marsh sediment deposition were measured using 117 cm^2 ceramic sedimentation tiles positioned flush with the marsh surface (after Pasternack & Brush 1998; Christiansen et al. 2000; JT Morris, U. South Carolina, pers. comm.). Tiles were deployed along one 30 m transect, the transect was divided into four blocks (0 to 7, 7 to 15, 15 to 22, and 22 to 30 m from the creekbank; Fig. 1B), and four tiles were positioned at a random location in each block (total of 16 tiles). Tile deployment and retrieval took place when the marsh surface was exposed to air and occurred every other week during the summer of 1998 and monthly thereafter. After removing fallen dead stems and roots from each tile, deposited sediments were scraped and washed with deionized water into clean, preweighed plastic specimen cups. Samples were dried at 50°C and weighed to calculate mass sedimentation

76

rates. Subsamples were processed for organic content and percent carbon and nitrogen as described below.

The carbon content of each sample and surface sediment bulk density (see "sediment characterization" section) were used to calculate annual rates of carbon deposition and vertical marsh accretion, respectively. To account for interannual variability in deposition on the marsh, rates were integrated from May 1998 (start of study) to April 1999, and September 1998 to August 1999 (end of study). Additionally, average 1998 and 1999 summer (May to August) deposition rates plus measured rates for the remainder of the year (September 1998 to April 1999) were used to provide a third estimate of annual deposition. Errors for annual rate calculations due to variations in deposition rates, carbon content, and bulk density were propagated following Skoog and West (1963).

Beryllium-7: Sediment inventories of ^{7}Be ($t_{1/2}$ = 53.3 d) were used to estimate marsh sediment deposition and erosion rates on a time scale of months (after He & Walling 1996, Goodbred & Kuehl 1998). The inventory approach assumes that any radioisotope activity above that supplied by atmospheric fallout is due to sediment input (Walling et al. 1992) and that atmospheric inputs are evenly distributed across the study area (i.e. there is no "focusing" of fallout ^{7}Be due to land topography). In June and October 1998 and January 1999, 15.2 cm diameter sediment cores were taken to a depth of ~15 cm and sectioned at 1 to 5 cm intervals. Each section was homogenized and a subsample was gamma counted (477 keV) for 24 hours using a high-purity germanium detector. Total core ^{7}Be inventories (I_{total}; dpm cm^{-2}) were calculated as:

77

$$I_{total} = \frac{\sum_{i=1}^{n}(A_i \times W_i)}{SA},$$ (1)

where n is the number of intervals between the sediment surface and base of the core; A_i is the specific activity of interval i (dpm g^{-1}); W_i is the total dry mass of interval i (g) and SA is the core surface area (cm^2). The sediment accumulation rate (R; $g\ cm^{-2}\ d^{-1}$) is calculated as:

$$R = \lambda_{Be} \times \left(\frac{I_{total} - I_{atm}}{A_{catch}}\right),$$ (2)

where λ_{Be} is the ^7Be decay constant (0.013 d^{-1}); I_{total} is total sediment ^7Be inventory (dpm cm^{-2}; from equation 1); I_{atm} is local atmospheric fallout inventory (dpm cm^{-2}); and A_{catch} is a mean ^7Be activity for catchment derived sediments (dpm g^{-1}). Total atmospheric ^7Be deposition (wet + dry) has been measured at the Virginia Institute of Marine Science (VIMS; ~50 km from Sweet Hall marsh) since April 1997 (SA Kuehl, unpublished data). At Sweet Hall, the marsh is flooded for 12 to 13 hr d^{-1}. Therefore, we assumed that the actual ^7Be deposition (I_{atm}) to the marsh surface was 50 to 100% of that measured at VIMS. This range represents the extremes of no fallout (50% case) or all fallout (100% case) reaching the sediment when the marsh is flooded. In October and November 1998, particle specific ^7Be activity (A_{catch}) was estimated by concentrating (via settling and centrifugation) and measuring the ^7Be activity of particles in approximately 70 L of creek water collected adjacent to the marsh study site near low tide.

Cesium-137: The ^{137}Cs profile ($t_{1/2}$ = 30.17 y) in a marsh core was used to determine sediment accretion rates over the last 30 to 50 years. In February 1998, a core was taken

78

to a depth of 1.3 m using a 10.2 cm diameter PVC tube. Total compaction of 8 cm (6%) over the length of the core was measured; no corrections for this compaction were made in subsequent calculations. One cm thick sections of the core were gamma counted for 24 hours using a high-purity germanium detector. The area of the ^{137}Cs photopeak (661.62 keV) was quantified and converted to ^{137}Cs activity (dpm g^{-1}) using known detector efficiency factors. The depths corresponding to the first appearance (1954) and maximum activity (1963) of ^{137}Cs were identified and average annual accretion rates calculated (DeLaune et al. 1978). Vertical accretion (mm yr^{-1}) was converted to a carbon accretion rate using measured sediment bulk densities and carbon content:

$$CA = \frac{\sum_{i=1}^{n}(d_i \times B_i \times C_i)}{t}, \qquad (3)$$

where CA is carbon accretion (g C m^{-2} yr^{-1}); n is the number of intervals between the sediment surface and the ^{137}Cs peak; d_i is thickness of interval i (m); B_i is interval bulk density (g sediment m^{-3}), C_i is interval percent carbon, and t is time since ^{137}Cs peak horizon deposition (34 yr). For intervals where bulk density and percent carbon were not measured (see "sediment characterization" section), these properties were estimated by averaging adjacent intervals.

Carbon-14: In November 1998, an aluminum core tube (7.5 cm diameter) was driven into the marsh to a depth of 6.7 m using a vibracorer. Compaction was minimal (15.3 cm or 2%) and no corrections were made in accretion calculations. Samples from 3.1 and 6.5 m were sent to Beta Analytic, Inc. (Miami, FL) for ^{14}C dating. Radiocarbon ages (BP) were converted to calendar years (Cal AD/BC) using calibration curves in Stuiver et al. (1998).

79

Additional samples were taken every 15 cm for analysis of organic content and percents carbon and nitrogen as described below, and the entire core was described for color, texture, and the character of visible organic detritus.

Sediment Characterization: Sediment bulk density and organic and carbon contents were measured over the course of the study. Surface samples (0 to 0.5 cm) were collected using 2 cm diameter core tubes at all locations and times when sedimentation tiles were retrieved. Deeper sediments (to 30 cm) were collected in June, August, and November 1996 and April 1997 using 4.2 cm diameter core tubes. These cores were collected from five locations along each of three parallel 30 m transects (15 cores per season) and sectioned at 0 to 2, 2 to 5, 10 to 13, 18 to 21, and 27 to 30 cm intervals. Samples were dried at 50°C and weighed to calculate dry bulk density (g cm^{-3}).

A fraction of each dried sediment sample from tiles and cores was combusted at 500°C for 5 hours and reweighed. Organic content was calculated as the weight loss-on-ignition. A second fraction of each dried sediment sample was ground in a Wiley mill (#40 screen) or by mortar and pestle for determination of carbon and nitrogen content. A portion of dried, ground sediments was weighed into ashed silver cups, acidified with 1-2 drops of 30% HCl to remove carbonates, and redried overnight at 50°C. Organic carbon and total nitrogen were measured using a Fison model EA 1108 elemental analyzer. The average precision for duplicate samples was ± 0.08% C and ± 0.02% N.

80

Sediment Lability: In June, August, and November 1999, the reactivity of freshly deposited sediment was examined. Four sediment traps (plastic specimen cups; 7.7 cm diameter opening, 150 ml) were deployed around a randomly selected point in each block (16 traps total). To reduce bed load transport of sediments into the traps, each trap was pushed into the sediments so the lip of the trap was slightly (<5 mm) above the surface of the marsh. Furthermore, each trap was filled with marsh creek water to minimize turbulence effects on deposition during marsh flooding. After 24 hours, the traps were recovered and returned to the lab. Collected sediments from each block were combined and filtered through window screening (6 to 7 meshes cm^{-1}) to remove large detritus. Window-screen filtered marsh creek water was added to the sediments to bring the total volume to ~1200 ml. This sediment-water slurry was subdivided among three 300 ml darkened biological oxygen demand (BOD) bottles per block. Triplicate BOD bottles were filled with creek water to serve as a water blank. Duplicate 100 ml samples from each block and the creek were filtered through precombusted GF/F filters and weighed when dry to calculate total sediment mass per bottle. A subsample of each filter was analyzed for percent carbon using a Fison model EA 1108 elemental analyzer.

All BOD bottles were incubated in the dark at ambient sediment temperatures (June: 21°C; August: 29°C; November: 13°C) for 5 days (June, August) or >1 month (November). To prevent oxygen gradients within the BOD bottles, all samples were gently mixed (170 rpm) throughout the incubation. Dissolved oxygen concentrations were regularly measured in each BOD bottle using an Orbisphere model 2604 multichannel oxygen probe (Orbisphere Laboratories, Geneva, Switzerland). Dissolved

81

oxygen levels over the course of each incubation were fit to the exponential decay equation:

$$DO_t = a \times \left(1 - e^{-b \times t}\right) + c,$$ (4)

where DO_t is dissolved oxygen concentration (mg l^{-1}) at time t, and a, b, and c are empirically determined constants. Oxygen utilization rates over 5 days (all months) and 30 days (November only) were calculated and corrected for water blank oxygen utilization. Rates were converted to carbon units assuming a respiratory quotient of 1 (1 mole CO_2 produced per 1 mole O_2 consumed) and normalized to the mass of carbon in each BOD bottle at the start of the incubation.

RESULTS

Sedimentation Rates

<u>Sediment Collection Tiles</u>: Direct measures of deposition using ceramic tiles revealed considerable spatial and temporal variability (Fig. 2). Deposition rates were consistently higher on the creekbank (block A) than at the three interior sampling blocks (blocks B, C, D), especially during the growing season (roughly April to October). Average rates on the creekbank ranged from 0.1 g sediment m^{-2} d^{-1} during winter (Nov 1998 to Jan 1999) to 284.2 g sediment m^{-2} d^{-1} for Jul to Aug 1999. In the marsh interior, sediment accumulation rates were more consistent between stations and over the course of the year. Mean rates ranged from 1.2 g sediment m^{-2} d^{-1} between Feb and Mar 1999 (block D) to 56.5 g sediment m^{-2} d^{-1} for Sep to Oct 1998 (block B). Although all tiles in a given block were within 0.5 m of each other, deposition rates within a block were highly variable
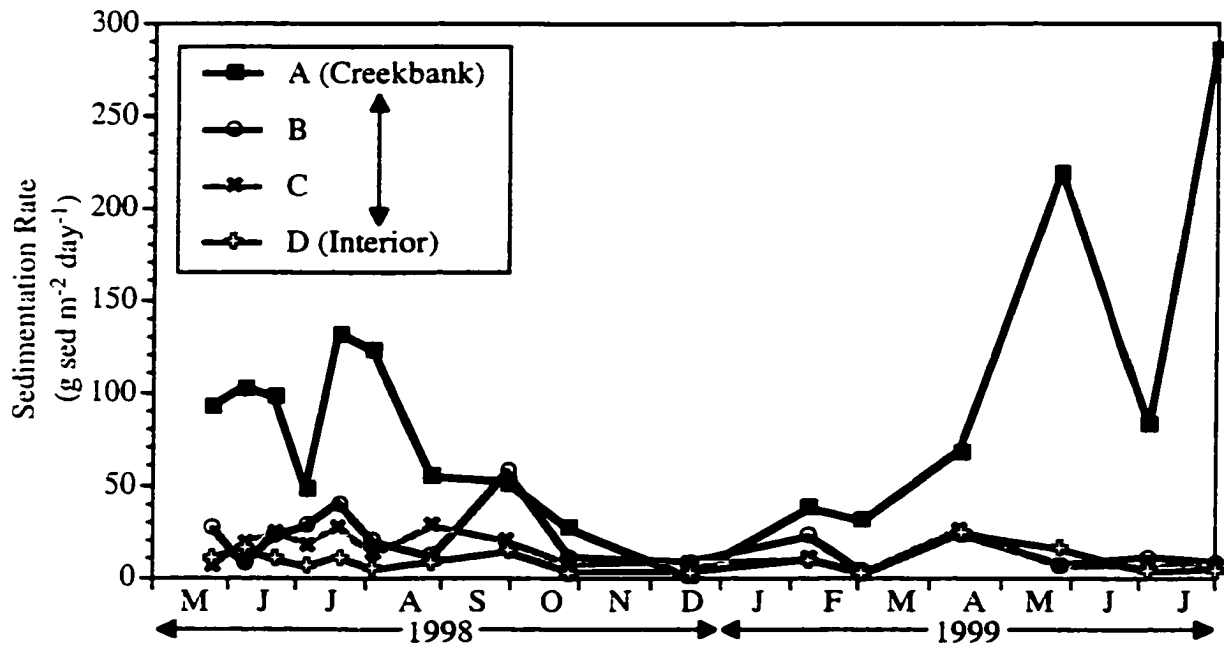
Figure 2: Sediment deposition rates onto ceramic tiles deployed in marsh for 2 to 4 week periods. Data are plotted at the midpoint of each sampling period. All points are the mean of 4 plates, with error bars omitted for clarity. The median coefficient of variation (standard deviation / mean) for all samples was 36% (range 6 to 171%).

83

with coefficients of variation (standard deviation / mean) ranging from 6 to 171%

(median = 36%). The carbon content of recently deposited sediments averaged 5.96 ±

0.95% C and was lowest at the creekbank site (5.31 ± 0.43% C; ANOVA, $p < 1 \times 10^{-7}$;

Tukey's HSD, $p < 0.001$). Surface (0 to 5 mm) sediment bulk density for all months

averaged 0.324 ± 0.096 g sed cm^{-3} (Table 1). Creekbank bulk density (0.407 ± 0.095 g

sed cm^{-3}) was significantly higher than at the interior sites (0.289 to 0.303 g sed cm^{-3};

ANOVA. $p < 1 \times 10^{-7}$; Tukey's HSD. $p < 0.00001$).

Average carbon accumulation rates onto ceramic tiles ranged from 1268 ± 329 g C

m^{-2} yr^{-1} at the creekbank to 199 ± 67 g C m^{-2} yr^{-1} at site D, while vertical accretion ranged

from 64.7 ± 19.2 mm yr^{-1} at the creekbank to 10.6 ± 3.7 mm yr^{-1} at site D (Table 2).

Regardless of the time period of integration, sedimentation and vertical accretion rates

were greatest at the creekbank with a gradual decrease from sites B through D. When

averaged across all locations and calculation periods, carbon accumulation and vertical

accretion were 517 ± 353 g C m^{-2} yr^{-1} and 28.4 ± 21.3 mm yr^{-1}, respectively.

Beryllium-7: Average sediment ^{7}Be inventories ranged from 1.8 to 16.5 dpm cm^{-2} and

varied with season and transect location (Table 3). The study period was characterized by

lower than average atmospheric ^{7}Be fallout, with atmospherically supported inventories

at VIMS ranging from 1.29 to 2.41 dpm cm^{-2} versus a longer-term average of 2.52 ± 1.30

dpm cm^{-2} (July 1997 to Dec 1999; SA Kuehl unpublished data). In 9 out of 11 cores, the

sediment ^{7}Be inventory was greater than could be supported by atmospheric fallout onto

84

Table 1: Sediment characterization with depth – bulk density, percent organic matter (loss-on-ignition) and carbon content. Values are means ± 1 standard deviation and have been averaged across season and location in marsh. For the 0 to 0.5 cm depth, bulk density was measured on 2 cm diameter cores while percents organic matter and carbon are from sediments collected on tiles

Depth Interval (cm)	Bulk Density n	(g cm⁻³)	Percent Organic n	(%)	Percent Carbon n	(%)
0 to 0.5	172	0.324 (±0.095)	259	16.48 (±2.07)	257	5.96 (±0.95)
0 to 2	60	0.353 (±0.125)	60	20.73 (±12.34)	19	5.81 (±1.44)
2 to 5	59	0.380 (±0.132)	59	17.00 (±2.75)	20	5.57 (±1.11)
10 to 13	60	0.427 (±0.153)	60	18.37 (±3.98)	4	5.97 (±1.73)
18 to 21	59	0.433 (±0.143)	59	21.06 (±5.75)	4	7.44 (±3.31)
27 to 30	56	0.393 (±0.144)	56	20.81 (±5.02)	4	7.36 (±3.29)

Table 2: Annual marsh carbon accumulation and vertical accretion rates for blocks A (creekbank) to D (marsh interior)

Carbon Accumulation (g C m^{-2} yr^{-1})

Time period	A	B	C	D	Transect Mean
May 1998 to Apr 1999	1096 (± 145)[a]	395 (± 56)	300 (± 37)	210 (± 40)	500 (± 164)
Sep 1998 to Aug 1999	1413 (± 248)	290 (± 54)	197 (± 29)	181 (± 38)	521 (± 258)
summer average	1293 (± 161)	350 (± 54)	267 (± 31)	205 (± 37)	529 (± 176)
Average, all methods	1268 (± 329)	345 (± 94)	255 (± 56)	199 (± 67)	517 (± 353)

Vertical Accretion (mm yr^{-1})

Time period	A	B	C	D	Transect Mean
May 1998 to Apr 1999	51.5 (± 7.7)	23.7 (± 4.4)	17.6 (± 2.6)	10.6 (± 2.2)	25.9 (± 9.5)
Sep 1998 to Aug 1999	77.7 (± 15.1)	19.9 (± 4.2)	15.0 (± 2.3)	10.6 (± 2.0)	30.8 (± 16.0)
summer average	65.0 (± 8.9)	21.8 (± 4.2)	16.4 (± 2.3)	10.7 (± 2.0)	28.5 (± 10.3)
Average, all methods	64.7 (± 19.2)	21.8 (± 7.4)	16.4 (± 4.2)	10.6 (± 3.7)	28.4 (± 21.3)

[a] Values in parentheses are ± 1 standard deviation and were calculated by propogating errors associated with seasonal sediment deposition rates, carbon content and surface sediment bulk density

Table 3: Calculated beryllium-7 sedimentation rates, including sediment and atmospheric inventories, by month and distance from creekbank.

Date	Distance (m)	n	I_{total} (dpm cm^{-2})	I_{atm} [a] (dpm cm^{-2})	Sedimentation Rate[b] (g sed m^{-2} d^{-1})
29 Jun 1998	2.4	1	16.45	1.21 to 2.41	128.0 to 139.0
	13.7	1	3.19	1.21 to 2.41	7.1 to 18.0
	25.0	1	1.80	1.21 to 2.41	-5.6 to 5.4
15 Oct 1998	1.5	3	5.16 (±1.94)[c]	0.75 to 1.51	33.3 to 40.2 (±17.7)[c]
	11.6	2	2.24 (±0.11)	0.75 to 1.51	6.6 to 13.5 (±1.0)
	25.3	2	3.46 (±4.28)	0.75 to 1.51	17.8 to 24.7 (±39.0)
25 Jan 1999	1.2	1	4.47	0.64 to 1.29	29.0 to 34.9

[a] Range in I_{atm} assumes that 50 to 100% of ^{7}Be fallout measured at Virginia Institute of Marine Science directly reaches the marsh surface, with reductions due to interception of fallout by tidal waters during marsh flooding (12 to 13 hr d^{-1}).

[b] Calculated using equation 2, with A_{catch} estimated as 14.3 dpm g^{-1}, the median particle-specific ^{7}Be activity reported in the literature for particles and recently deposited sediments in estuarine and shallow coastal systems. Range in sedimentation rates is due to the range in I_{atm}. Positive rates indicate net deposition; negative rates indicate erosion.

[c] Mean ± standard deviation for replicate cores. The median counting error for I_{total} was ± 0.03 dpm cm^{-2}.

the marsh surface, indicating net sediment deposition (exceptions: June and October

cores at 25 m from creekbank). In October and November 1998, we measured particle

specific ^{7}Be activities of 2.26 and 9.13 dpm g^{-1}. Because ^{7}Be activities on particles can

vary twofold or more over a single tidal cycle (SA Kuehl & T Dellapenna, unpublished

data) and show a much wider range over several months (e.g. Olsen et al. 1986; Dibb &

Rice 1989; Baskaran et al. 1997), we calculated a median value of 14.3 dpm g^{-1} (4.2 to

21.5 for 25th to 75th percentiles) for suspended particles (this study; SA Kuehl & T

Dellapenna unpublished; Olsen et al. 1986; Dibb & Rice 1989; Baskaran et al. 1997) and

recently deposited sediments (Canuel et al. 1990) in estuarine and shallow coastal waters.

Using this median value, we calculated deposition rates of –6 to 139 g sed m^{-2} d^{-1} in June

1998, 7 to 40 g m^{-2} d^{-1} in October 1998, and 29 to 35 g m^{-2} d^{-1} in January 1999 (Table 3).

Cesium-137: Cesium-137 activities ranged from undetectable below 37 cm to a

maximum of 3.21 dpm g^{-1} at 29 cm, for average accretion rates of 8.4 and 8.5 mm yr^{-1}

since 1954 and 1963, respectively. These calculations will underestimate the actual

accretion rates if compaction was confined to the upper 30 cm of the core (RL Wetzel,

pers. comm.) and not evenly distributed throughout the core. Sediment bulk density was

significantly higher in the 10 to 13 and 18 to 21 cm intervals than in surface and deeper

sediments (Table 1; ANOVA, p = 0.011; Tukey's HSD, p < 0.05). There was a general

but non-significant trend (ANOVA, p = 0.165) of increasing percent carbon with

increasing depth (Table 1). Organic content was significantly higher in the 0 to 2 cm

interval than the 2 to 5 cm section (ANOVA, p = 0.003; Tukey's HSD, p < 0.05), perhaps

due to inputs of organic detritus or the presence of shallow adventitious roots. Between

10 and 30 cm depth, there were no significant differences in organic content (Tukey's HSD, $p > 0.30$). Using equation 3, we calculated an average carbon accretion rate of 224 ($\pm$ 45) g C m^{-2} yr^{-1} since 1963.

Vibracore and Carbon-14: In the marsh vibracore, organic content and percent carbon in the root zone (0 to ~125 cm; Booth 1989; SC Neubauer field observations) were relatively constant (Fig. 3; 13.50 $\pm$ 1.35% and 4.78 $\pm$ 0.35%, respectively). Below this depth, to about 250 cm, organic and carbon concentrations were homogenous (11.30 $\pm$ 0.60% and 3.34 $\pm$ 0.36%, respectively), but significantly lower than in the root zone (t-test, $p < 0.001$). From 250 cm to the base of the core, there were large variations in both organic matter (12.49 to 55.82%) and carbon content (4.48 to 34.31%). Throughout the core, organic matter and carbon contents were highly correlated ($r^2 = 0.94$). Sediment C/N ratios (mol C / mol N) averaged 16.3 ($\pm$ 2.3 SD) from 0 to 250 cm with no difference between the 0 to 125 and 125 to 250 cm intervals (t-test, $p = 0.15$). Carbon to nitrogen ratios were higher below 250 cm (23.9 $\pm$ 3.4; t-test, $p < 1 \times 10^{-10}$). Sediment color varied from light to medium brown in surface sediments through gray to black at the base of the core. In the upper 3 m of the core, organic matter was disseminated through the sediments or preserved as fibrous material. A high density of wood fragments was observed between 106 and 140 cm. Below 323 cm, the sediment matrix was densely fibrous with wood fragments present from 366 to 665 cm. A more complete description of core color, organic content, and texture is available from the authors. Based on radiocarbon dating of samples from 3.1 m (630 $\pm$ 70 BP; Cal AD 1270 to 1430) and 6.5
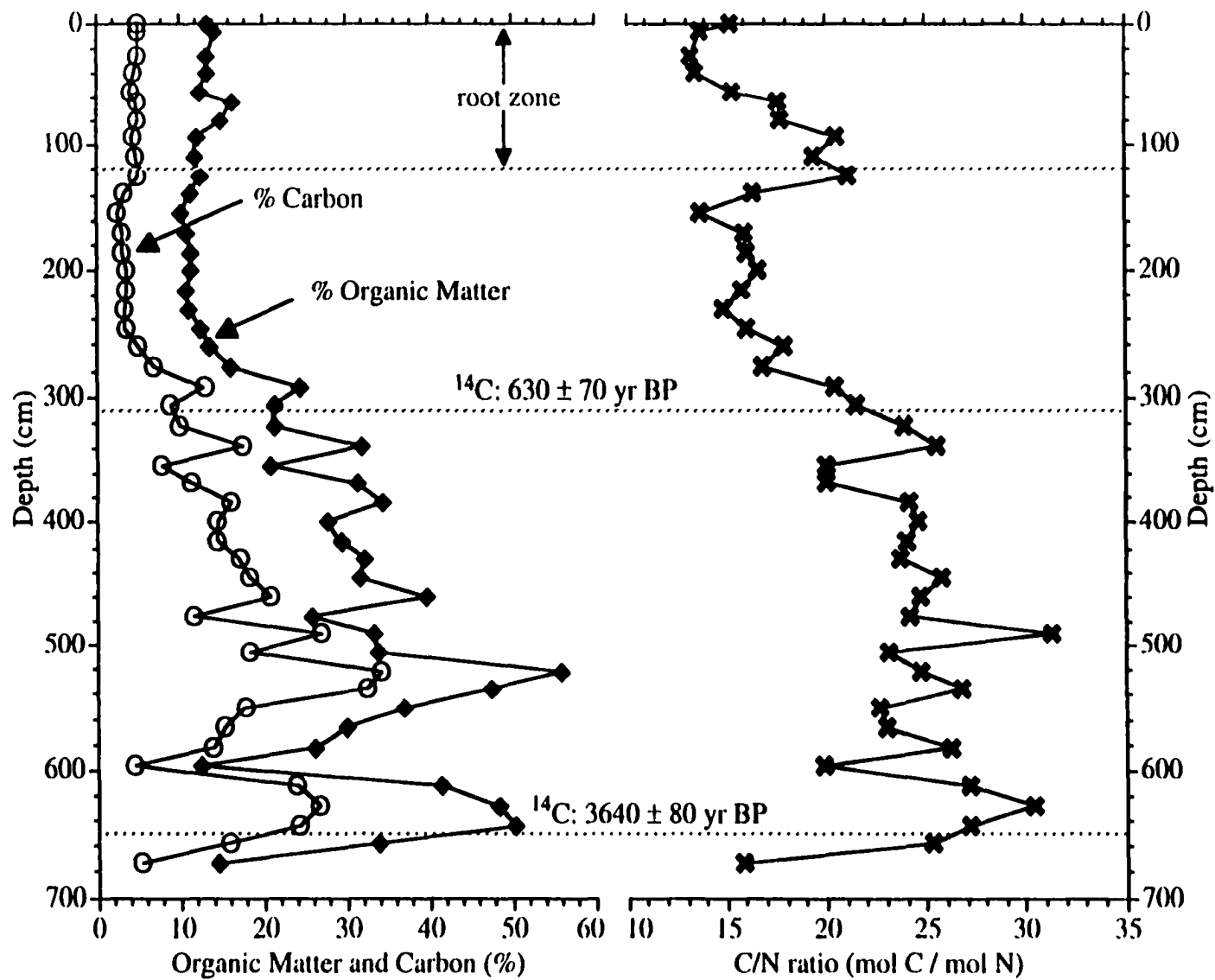
Figure 3: Marsh vibracore characterization with sediment organic content, percent carbon, carbon to nitrogen ratios and ^{14}C dates.

m (3640 ± 80 BP; Cal BC 2210 to 1770), average accretion rates were 4.3 to 5.5 mm yr^{-1}

(0 to 3.1 m) and 1.5 to 1.7 mm yr^{-1} (0 to 6.5 m).

Sediment Lability: Oxygen levels during sediment incubations decreased exponentially

(Equation 4) with regression coefficients (r^2) of 0.95 to 1.00 (Fig. 4). Due to variations in

marsh sedimentation rates, the amount of sediment in each BOD bottle varied along the

transect as well as between months (June: 65 to 188; Aug: 61 to 286; and Nov: 20 to 216

mg dry sediment bottle^{-1}). Incubated sediments averaged $5.8 \pm 1.1\%$ carbon and did not

significantly vary by date or transect block (2-way ANOVA, $p = 0.085$ for date; $p =$

0.322 for block). In all months, average respiration rates for the first 5 days of the

incubation were lowest at the creekbank site (ca. 0.04 mg C respired (mg sediment C)$^{-1}$,

or 4% sediment C respired; Fig. 4). Overall, mean respiration rates increased from June

($\overline{X} = 4.8 \pm 2.3\%$ C respired) to November ($\overline{X} = 12.6 \pm 7.5\%$ C respired; Fig. 4). When

calculated over 30 days, respiration rates in November ranged from 5.9 to 45.4% C

respired ($\overline{X} = 27.5 \pm 11.1\%$), an average increase of 209% compared to 5 day rates.

DISCUSSION

Sediment Deposition: Tidal marshes can be sites of active yet spatially and temporally

variable sedimentation. Across marsh habitat types (e.g. low marsh to high marsh),

sediment deposition rates are largely a function of the duration of inundation: sites that

are flooded more frequently and for a longer time tend to exhibit higher deposition rates

(Reed 1990; Cahoon & Reed 1995; Leonard 1997). However, near tidal creeks, this

91
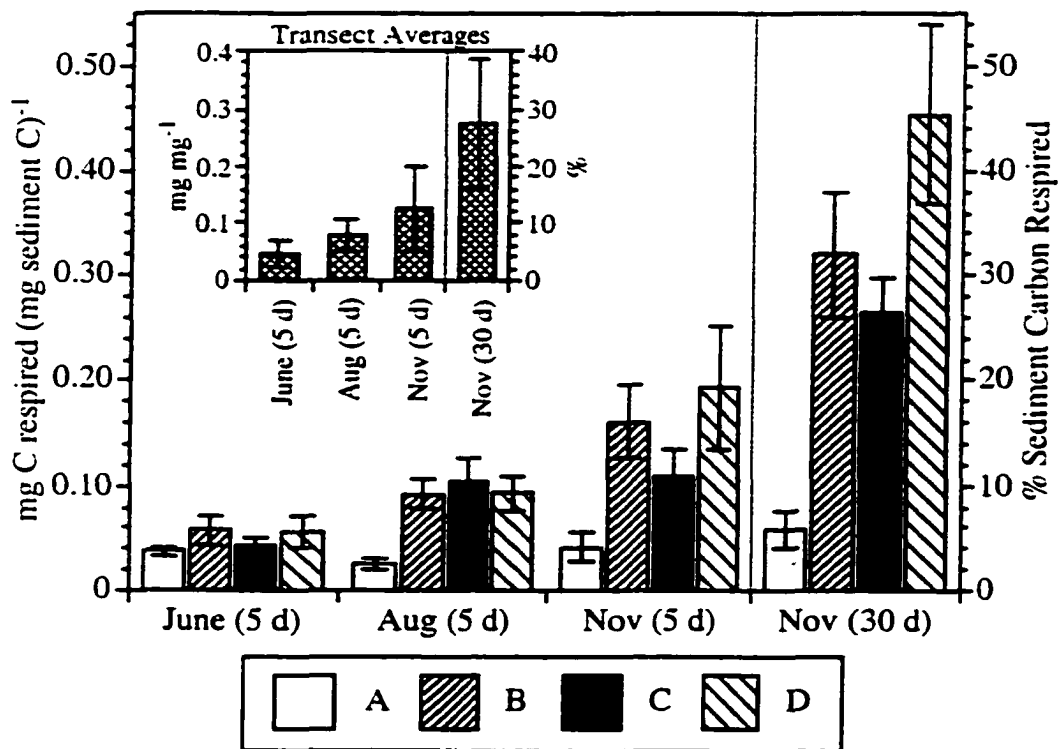
Figure 4: Average sediment respiration rates by date and location. Samples were collected along a 30 m transect from block A (creekbank) to D (marsh interior). Values are mean rates for 3 replicate incubations (± 1 standard deviation). Inset shows seasonal respiration rates averaged across all locations (n = 12)

relationship breaks down and highest rates are measured on topographically high levees

immediately adjacent to the creek (French & Spencer 1993; Esselink et al. 1998). This

occurs because the rapid decrease in turbulent energy as water starts to flood the marsh

causes sediments to fall out of suspension close to the creekbank. At Sweet Hall, this

pattern was especially pronounced from April to November (Fig. 2) when plant stems

further reduced water velocities and enhanced deposition (Leonard et al. 1995; Leonard

& Luther 1995). We did not observe the same dependence of sedimentation on time of

year at the interior sites. In part, plant production was lower at these stations (S.C.

Neubauer, unpublished data) so there was less frictional resistance to sediment transport

(Leonard et al. 1995). Also, and perhaps more importantly, the interior sites are farther

from the sediment source (i.e. the creek). Although the marsh interior was flooded first

and for a longer period than the creekbank levee, water that floods the marsh interior

must first travel through small channels that incise the levee and then across the inner

marsh flat. During this transport from creek to channel to marsh interior, sediments were

constantly being deposited (French & Spencer 1993; Leonard 1997). By the time the

interior marsh floods, suspended sediment concentrations and flood water velocity were

low enough that additional frictional resistance from plant stems did not significantly

affect deposition rates.

Marsh fauna also influence patterns of sediment deposition. Burrow excavation by

fiddler crabs (*Uca* spp.) can bring buried sediments to the surface and increase the

apparent sedimentation rate if these sediments are deposited on a collection tile.

However, deposition rates calculated from [7]Be inventories would not be affected by

vertical sediment mixing. At Sweet Hall, fiddler crabs were most abundant near the

creekbank (SC Neubauer, pers. observation). In January 1999, several sedimentation tiles

fell into a collapsed muskrat (*Ondatra zibethica*) tunnel and were buried by 6 to 10 cm

sediment (versus ~2 mm for all other tiles). These extreme results were not included in

sedimentation calculations, but illustrate that marsh biology can influence total

sedimentation rates by creating regions of intense deposition. Alternately, muskrat eatout

of a dense marsh root mat can lower the marsh surface (Garbisch, 1994).

The magnitude and temporal patterns of sedimentation measured in this study are

similar to those observed by Pasternack and Brush (1998) for a tidal freshwater marsh in

Maryland, although Pasternack and Brush documented significant net erosion (~50 to 190

g sediment m^{-2} day^{-1}) from low marsh sites during winter 1997. We suggest that erosion

was not a significant factor during our study. During the growing season, when 70 to

90% of the annual sediment deposition occurs, high plant stem density slows water flow

across the marsh (Leonard et al. 1995; Shi et al. 1996) so sediment erosion and

redistribution across the marsh are unlikely (Christiansen et al. 2000). Our seasonal [7]Be

inventories provide further evidence of net accretion throughout the year, as sediment

inventories were greater than atmospherically supported [7]Be inventories in 9 of 11 cores.

In contrast, Ledwin (1988) measured net erosion of 0 to 8 mm during a 14 month study at

an exposed riverbank site at Sweet Hall and also observed local resuspension and

redeposition of glitter placed on the sediment surface. This suggests that processes

controlling sediment deposition and erosion can differ between an exposed high energy

94

riverbank site (Ledwin 1988) and a more protected creekbank site (this study) within the same marsh.

Beryllium-7 Sedimentation: When calculated using a median particle activity of 14.3 dpm g^{-1}, ^{7}Be-based deposition rates were similar in magnitude to those measured using sediment tiles. For example, rates measured using sediment tiles at the creekbank site in June 1998 ranged from 62 to 140 g sed m^{-2} d^{-1} versus 128 to 139 g sed m^{-2} d^{-1} calculated from ^{7}Be inventories. Some variation between methods was expected because ^{7}Be inventories (Table 3) and sediment tile deposition rates (Fig. 2) were measured on different transects and at different distances from the creekbank. Additionally, ^{7}Be derived rates were integrated over several months (mean ^{7}Be lifetime for radioactive decay, τ, = 77 d), while sediment tile measurements were averaged over 14 to 30 days. In spite of these differences, both methods reported greatest sedimentation rates at the creekbank with lower rates in the marsh interior. Additionally, deposition rates at the creekbank decreased from summer to winter with each technique.

The calculation of sedimentation rates using ^{7}Be inventories is strongly influenced by estimates of particle specific ^{7}Be activity (A$_{catch}$, equation 2). In estuaries, there can be considerable spatial and temporal variability in particle associated ^{7}Be activity due to variations in atmospheric ^{7}Be fallout, suspended particle concentrations and residence time in the water column, water salinity, and pH (Olsen et al. 1986; Dibb & Rice 1989). The literature values of particle activity (median = 14.3 dpm g^{-1}; range: undetectable to >150 dpm g^{-1}) that we used as an estimate of A$_{catch}$ were greater than our October and

95

November 1998 measurements of 2.3 and 9.1 dpm g^{-1}. For example, in June the activity of surface sediments ranged from 10.9 dpm g^{-1} at the creekbank (0-2 cm) to 8.8 and 2.7 dpm g^{-1} in the marsh interior (0-1 cm). Based on our tile sedimentation measurements, we estimated that recent sediment deposition (within 1 ^{7}Be half-life of sampling) accounted for only 20 to 50% of the sediment in these surface intervals during June (and a smaller fraction in October and January). Because the total ^{7}Be activity in the surface represented inputs from recently deposited (^{7}Be-enriched) as well as older (^{7}Be-depleted) sediments, the actual activity of recently deposited sediments would be greater than the mean ^{7}Be activity in surface sediments. Based on this, we suggest that the mean activity of recently deposited sediments (A$_{catch}$) was closer to 14.3 dpm g^{-1} (literature median) than 2.3 and 9.1 dpm g^{-1} (measured, this study). Preferential binding of ^{7}Be to inorganic over organic particles or fine-grained versus sandy particles may explain our relatively low particle-specific ^{7}Be activities (Bloom & Crecelius 1983). At Sweet Hall, the maximum suspended particle concentrations and minimum percent of organic particles (20 to 25% organic; range for 10 tidal cycles) were measured approximately midway between slack tides – this was also near the time when the marsh was first flooded (Neubauer, unpublished data). Because we collected suspended particles near low tide when organic enrichment (23 to 52% organic) and possible dilution of activity by ^{7}Be-depleted organic matter were greatest, our measures of A$_{catch}$ may underestimate the actual activity of deposited particles.

Using ^{7}Be inventories to calculate sedimentation rates also requires measuring atmospheric ^{7}Be deposition. In intertidal systems, a fraction of ^{7}Be fallout may be

intercepted by tidal waters. Because Sweet Hall is flooded for 12 to 13 hr d^{-1}, we

estimated the minimum atmospheric ^{7}Be deposition to the marsh as 50% of that measured

at the Virginia Institute of Marine Science ($I_{atm. Sweet Hall} = 0.5 \times I_{atm. VIMS}$). Inherent in this

estimation are the assumptions that ^{7}Be fallout is evenly distributed between periods of

high and low tide, and that fallout which occurs during high tide does not directly reach

the marsh surface. If any atmospheric ^{7}Be fallout during high tide sorbs to particles which

then settle to the marsh surface, this input would be measured as sediment deposition.

However, in a shallow, well-mixed water column (such as that overlying a microtidal

marsh), a fraction of dissolved atmospheric beryllium may also directly sorb to

submerged sediments (Olsen et al. 1986; Dibb & Rice 1989). Therefore, we estimated a

maximum value for I_{atm} by assuming that atmospheric beryllium delivery was not affected

by tidal stage (i.e. $I_{atm. Sweet Hall} = I_{atm. VIMS}$). In all samples, this range in I_{atm} caused

variability in calculated sedimentation rates of ~6 to 11 g sed m^{-2} d^{-1}, but did not cause a

change from net deposition to erosion (exception: 25 m core from June 1998; Table 3).

Marsh plants may also intercept atmospheric fallout and reduce delivery to

underlying sediments. Russell et al. (1981) estimated that forests with leaf area indices of

3 to 10 (LAI = m^2 leaf area per m^2 subtended land) can reduce atmospheric radionuclide

flux by 5 to 20%. At Sweet Hall, we calculated a LAI of 3 to 11 in June 1996 and 0 to <2

in September (SC Neubauer, unpublished data) and suggest that atmospheric deposition

of ^{7}Be to the sediment surface may be further reduced during early to mid summer when

macrophyte leaf area and biomass are greatest. By not accounting for this effect, we are

effectively providing a conservative estimate of sediment deposition since further reducing the atmospheric flux will increase calculated deposition rates (equation 2).

Sediment Lability and Marsh Carbon Budget: Using a process-based carbon gas flux model based on measured field fluxes of CO_2 and CH_4, Neubauer et al. (2000) calculated rates of total community photosynthesis and respiration at Sweet Hall marsh. Annually, community respiration (1269 g C m^{-2}) exceeded gross photosynthesis (1062 g C m^{-2}). In the absence of an external carbon source, this "excess" respiration implies that some fraction of sediment carbon is being mineralized to CO_2 or CH_4 and lost from the marsh. Simultaneously, a relative sea level rise of 4 to 6.5 mm yr^{-1} may potentially lower marsh elevation relative to mean tidal level. Because tidal marsh plant zonation is affected by the frequency and depth of tidal flooding (Odum et al. 1984; Perry 1991) and the distribution of plant assemblages at Sweet Hall has not changed significantly since 1937 (Perry 1991), we assume that the marsh imports enough carbon to overcome the combined effects of respiration and relative sea level rise on marsh elevation. Converting relative sea level (RSL) rise to carbon units using surface bulk density and percent carbon data, we estimate a required C input of 284 to 332 g C m^{-2} yr^{-1} (207 g C m^{-2} yr^{-1} "excess" respiration + 77 to 125 g C m^{-2} yr^{-1} RSL) to balance these factors. Based on a measured annual sedimentation rate of 517 g C m^{-2} yr^{-1} (Table 2), the deposition of sediment-associated carbon during tidal flooding is sufficient to counteract the effects of respiratory marsh loss and relative sea level rise.

In order to explain measured respiration rates, freshly deposited sediments must contain a sufficient quantity of labile carbon. We used average respiration rates (Fig. 4) and annual sediment deposition rates (Table 2) for each block to calculate that 22 to 44 g C m^{-2} yr^{-1} of recently deposited sediment organic carbon was mineralized on time scales less than 5 days, with 54 to 71 g C m^{-2} yr^{-1} metabolized within 30 days of deposition. This accounts for 26 to 35% of the measured "excess" respiration of 207 g C m^{-2} yr^{-1}. An additional fraction can be explained by the turnover of sediment carbon on time scales longer than 1 month as natural sediment carbon is composed of compounds that are remineralized on time scales from hours (e.g. free amino acids: k > 7500 yr^{-1}) to centuries (e.g. sterols: k = 0.015 yr^{-1}) or longer (e.g. hydrocarbons: k < 0.001 yr^{-1}; lignin: k = 0 yr^{-1}; see references in Henrichs 1993). Inputs of relatively labile organic matter from marsh primary producers (macrophytes, microalgae) or sediment deposition may promote the degradation of more refractory organic matter due to the effects of co-metabolism. The mineralization of "old" detritus from autotrophic production in previous years may account for some measured respiration, while anaerobic metabolism of sediment carbon is also likely to be important.

Sediment Accretion: Our ^{137}Cs-based estimates of sediment accretion rates (8.4 to 8.5 mm yr^{-1}) are higher than estimated rates of relative sea level rise (4.5 to 6 mm yr^{-1}) at Sweet Hall marsh. Working in *Spartina cynosuroides* and *Phragmites australis* stands elsewhere at Sweet Hall, Campana (1998) measured accretion rates of 4.9 to 6.0 mm yr^{-1} using ^{137}Cs activity profiles. The difference between our rates and those of Campana (1998) illustrates between habitat sedimentation differences. *S. cynosuroides* and *P.*

australis grow at slightly higher elevations and are therefore flooded less frequently than *Peltandra virginica* and *Pontederia cordata*, the dominant species at our study site (Perry 1991). Thus, sedimentation rates will be lower in these communities. The similarity between relative sea level (RSL) and accretion rates in the *S. cynosuroides* and *P. australis* communities suggests that they are accreting sediments at rates similar to RSL, while our study site is growing vertically at a faster rate than sea level rise. Over time, this will reduce the flooding duration at our site and cause a reduction in sedimentation rates until a morphodynamic equilibrium between marsh elevation and sea level is reached.

Using ^{14}C dating, we calculated long term average accretion rates of 4.3 to 5.5 mm yr^{-1} (0 to 3.1 m) and 1.5 to 1.7 mm yr^{-1} (0 to 6.5 m). The relative consistency in organic and carbon content above 250 cm (Fig. 3) indicates that deposition and preservation conditions throughout this portion of the sediment profile were similar to those in the modern tidal freshwater marsh. We therefore estimate that Sweet Hall has been a tidal freshwater marsh for approximately 450 to 580 years (250 cm / 0.43 to 0.55 cm yr^{-1} vertical accretion). Variability in sediment organic matter and carbon content below ~250 cm, the increase in sediment C/N ratio (Fig. 3), and the presence of wood fragments through much of the deep core suggest that Sweet Hall marsh may have been a non-tidal swamp or other wetland type in the past. Thus, caution must be applied when comparing accretion rates from this section of the core with shorter term measurements from the modern tidal freshwater marsh.

With this caveat in mind, we observed a decrease in sediment accumulation rate with increasing time scale, from years to decades to millennia (Table 4). A review of other studies that have examined accretion rates over a range of time scales revealed that this trend is a common feature in Chesapeake Bay marshes (Fig. 5) and in other sedimentary environments (e.g. McKee et al. 1983). Due to the high spatial variability in short-term (annual) deposition rates, the most significant decrease in accretion rates occurs when comparing annual and decadal rates with those averaged over centuries and millennia. As rates are integrated over longer time periods, there is a greater probability that the effects of significant sediment removal events (e.g. hurricanes and large storms) will be captured in the sediment record. An additional part of the difference in vertical accretion rates is likely due to compaction of deeper sediments. However, the concurrent reduction in carbon accumulation rate (this study, Table 4) indicates that compaction can not be the sole mechanism as sediment bulk density is included (and therefore compaction accounted for; equation 3) in the carbon accretion calculations. Land clearance associated with agricultural development in the 1600s increased sediment delivery to rivers and estuarine waters and may explain increased accretion rates in recent sediments (Brush 1989; Orson et al. 1990). Alternately, an increase in the frequency and duration of tidal inundation due to sea level rise or marsh subsidence could increase sedimentation rates (Bricker-Urso et al. 1989; Cahoon & Reed 1995; Leonard 1997).

We also suggest that a portion of the decrease in accretion rate with increasing time scale is due to the respiration of labile sediment carbon following deposition. For example, approximately 60% of the 517 g C m^{-2} deposited annually must be mineralized

Table 4: Variations in Sweet Hall marsh accretion rates at different time scales

Method	Time Scale	(mm yr^{-1}) Vertical Accretion	(g C m^{-2} yr^{-1}) Mass Accumulation
plates	annual	28.4 (±21.3)[a]	517 (±353)[a]
^{137}Cs	decades	8.4, 8.5[b]	229
^{14}C	centuries	4.3 to 5.5[c]	—[d]
^{14}C	millennia	1.5 to 1.7[c]	—[d]

[a] Average (± 1 standard deviation) for entire transect.

[b] Based on depths of first appearance and maximum activity of ^{137}Cs, respectively.

[c] Range represents analytical uncertainty associated with radiocarbon dating and conversion to calendar age.

[d] Insufficient bulk density data to convert mm yr^{-1} to g C m^{-2} yr^{-1}.

102
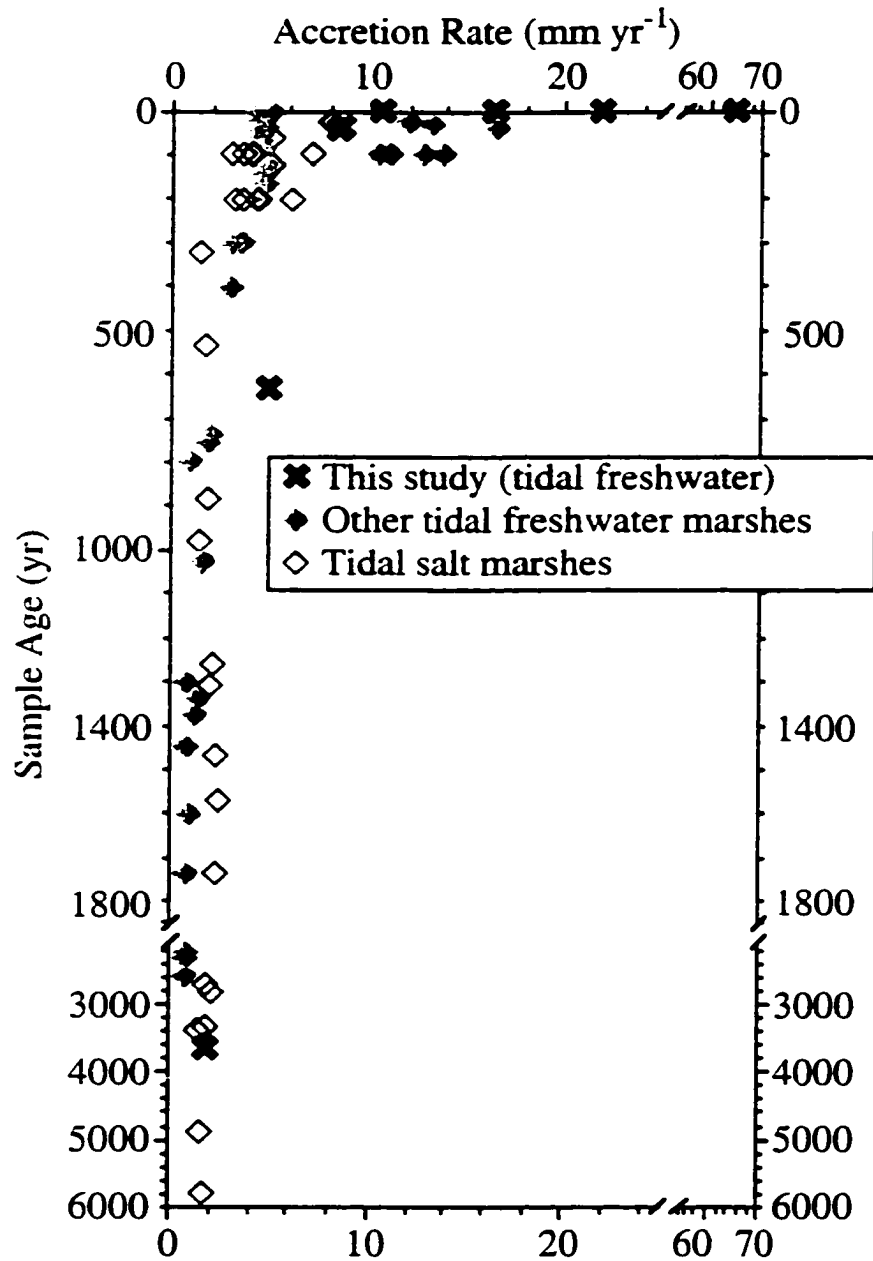
Figure 5: Accretion rate versus sample age for mid-Atlantic tidal marshes (USA). Data are presented from studies where accretion rates were measured over a range of time scales. Tidal freshwater marsh data points are from Orson et al. (1990; Delaware River), Khan and Brush (1994; Jug Bay, MD), and this study (Pamunkey River, VA). Salt marsh data points are from Ellison and Nichols (1976; James and Rappahannock Rivers, VA) and Kearney et al. (1994; Monie Bay, MD)

103

over ~30 years to produce a ^{137}Cs-based accretion rate of 224 g C m^{-2} yr^{-1}. Additionally, we suggest that sediment metabolism continues at gradually decreasing rates over hundreds or thousands of years as the remaining sediment carbon becomes more refractory. The importance of carbon mineralization over these time scales is reinforced by the significant decrease in carbon content from freshly deposited sediments (5.95% C) to sediments in the root zone (0-125 cm; 4.78% C) to deeper sediments (125-250 cm; 3.34% C; ANOVA, p < 1 x 10^{-7}; Tukey's HSD, p < 0.005). Overall, we hypothesize that a combination of mechanisms (including periodic storm-induced erosion, historical variability in sediment deposition, and the metabolism of a labile sediment fraction) is responsible for the decrease in apparent accretion rates with increasing time scale.

CONCLUSIONS

1) Short term sediment deposition rates in tidal freshwater marshes are spatially and temporally variable. Throughout the study period, rates were greatest near a tidal creek and progressively decreased into the marsh interior. At the creekbank, the highest deposition rates were observed during the growing season when the frictional effects of plant vegetation enhanced sediment deposition. Deposition rates were relatively constant throughout the year at the interior sites. When integrated over an entire year, sediment deposition provided sufficient carbon to the marsh to balance the effects of relative sea level rise and marsh respiration rates.

2) Sediment inventories of ^{7}Be were greater than atmospheric fallout inventories in 9 of 11 cores analyzed, indicating net sediment deposition throughout the year. Sedimentation rates calculated using a median literature value for particle-specific ^{7}Be activity were similar to those measured using sedimentation tiles, although direct comparisons are difficult because the methods integrate sediment deposition over different time scales. Both methods showed similar temporal and spatial trends in sediment deposition.

3) Depth profiles of ^{137}Cs and ^{14}C dating of deep sediments were used to calculate sediment accretion rates on decadal to millennial time scales. Accretion rates were substantially less than annual deposition rates. Characterization of a deep (6.7 m) sediment core suggested that the modern marsh extends to ~250 cm depth. The remainder of the core was highly variable in carbon and organic content, C/N ratios, and detritus character, indicating that the marsh may have been a non-tidal swamp or other wetland type in the past.

4) Mineralization rates of recently deposited sediments were spatially and seasonally variable. Rates were consistently lowest at the creekbank site and, when averaged across all locations, increased from June to August to November. Within 30 days of sediment deposition, sediment metabolism can remove ~30% of recently deposited carbon. We suggest that part of the difference between sediment deposition and accretion rates is due to periodic storm-induced erosion and historical variability in sedimentation rates, with a portion also due to the respiration of sediment-associated carbon following deposition.

105

LITERATURE CITED

Baskaran, M., Ravichandran, M. & Bianchi, T. S. 1997 Cycling of ^{7}Be and ^{210}Pb in a high
DOC, shallow, turbid estuary of south-east Texas. *Estuarine, Coastal and Shelf
Science* **45**, 165-176.

Bloom, N. & Crecelius, E. A. 1983 Solubility behavior of atmospheric ^{7}Be in the marine
environment. *Marine Chemistry* **12**, 323-331.

Booth, P. M. 1989 *Nitrogen and phosphorus cycling strategies in two tidal freshwater
macrophytes*, Peltandra virginica *and* Spartina cynosuroides Ph.D. dissertation,
College of William and Mary, Virginia Institute of Marine Science, Gloucester Point.

Bricker-Urso, S., Nixon, S. W., Cochran, J. K., Hirschberg, D. J. & Hunt, C. 1989.
Accretion rates and sediment accumulation in Rhode Island salt marshes *Estuaries*
12, 300-317.

Brooks, T. J. 1983 *Pamunkey River slack water data report: Temperature, salinity,
dissolved oxygen 1970-1980* Virginia Institute of Marine Science Data Report 20.

Brush, G. S. 1989 Rates and patterns of estuarine sediment accumulation *Limnology and
Oceanography* **34**, 1235-1246.

Cahoon, D. R. & Reed, D. J. 1995 Relationships among marsh surface topography,
hydroperiod, and soil accretion in a deteriorating Louisiana salt marsh. Journal of
Coastal Research **11**, 357-369.

Campana, M. L. 1998 *The effect of* Phragmites australis *invasion on community processes
in a tidal freshwater marsh* M.S. Thesis, College of William and Mary, Virginia
Institute of Marine Science, Gloucester Point.

Canuel, E. A., Martens, C. S., & Benninger, L. K. 1990 Seasonal variations in ^{7}Be
activity in the sediments of Cape Lookout Bight, North Carolina *Geochimica et
Cosmochimica Acta* **54**, 237- 245.

Childers, D. L., Sklar, F. H., Drake, B., & Jordan, T. 1993 Seasonal measurements of
sediment elevation in three mid-Atlantic estuaries *Journal of Coastal Research* **9**,
986-1003.

106

Christiansen, T., Wiberg, P. L. & Milligan, T. G. 2000 Flow and sediment transport on a tidal salt marsh surface *Estuarine Coastal and Shelf Science* **50**, 315-331.

Cornwell, J. C., & Zelenke, J. L. 1998 The role of oligohaline marshes in estuarine nutrient cycling *Concepts and controversies in tidal marsh ecology* conference, April 5-9, 1998, Vineland N.J.

Craft, C. B., Seneca, E. D. & Broome, S. W. 1993 Vertical accretion in microtidal regularly and irregularly flooded estuarine marshes *Estuarine Coastal and Shelf Science* **37**, 371-386.

DeLaune, R. D., Patrick Jr, W. H. & Buresh, R. J. 1978 Sedimentation rates determined by ^{137}Cs dating in a rapidly accreting salt marsh *Nature* **275**, 532-533.

Dibb, J. E. & Rice, D. L. 1989 The geochemistry of beryllium-7 in Chesapeake Bay *Estuarine, Coastal and Shelf Science* **28**, 379-394.

Doumlele, D. G. 1979 *New Kent County Tidal Marsh Inventory* Special Report No. 208 in Applied Marine Science and Ocean Engineering. Virginia Institute of Marine Science, Gloucester Point, Virginia.

Ellison, R. L. & Nichols, M. M. 1976 Modern and Holocene Foraminifera in the Chesapeake Bay Region *First International Symposium on Benthonic Foraminifera of Continental Margins*, Halifax, Nova Scotia, Canada. 131-151.

EPA. 1996 *Region III Land Cover Data Set* United States Environmental Protection Agency, Washington DC.

Esselink, P., Dijkema, K. S., Reents, S. & Hageman, G. 1998 Vertical accretion and profile changes in abandoned man-made tidal marshes in the Dollard estuary, the Netherlands *Journal of Coastal Research* **14**, 570-582.

French, J. R. & Spencer, T. 1993 Dynamics of sedimentation in a tide-dominated backbarrier salt marsh, Norfolk, UK *Marine Geology* **110**, 315-331.

Frey, R. W. & Basan, P. B. 1985 Coastal salt marshes. In *Coastal Sedimentary Environments* (Davis, R. A., ed). Springer-Verlag, New York, pp. 225-301.

Friedrichs, C. T. & Perry III, J. E. 2000 Tidal salt marsh morphodynamics *Journal of Coastal Research* in press.

Froelich. P. N. 1988 Kinetic control of dissolved phosphate in natural rivers and estuaries: A primer on the phosphate buffer mechanism *Limnology and Oceanography* **33**, 649-668.

Garbisch. E. 1994 The results of muskrat feeding on cattails in a tidal freshwater wetland *Wetlands Journal* **6**, 14-15.

Goodbred Jr. S. L. & Kuehl, S. A. 1998 Floodplain processes in the Bengal Basin and the storage of Ganges-Brahmaputra river sediment: An accretion study using ^{137}Cs and ^{210}Pb geochronology *Sedimentary Geology* **121**, 239-258.

Gornitz. V. & Lebedeff, S. 1987 Global sea level changes during the past century In *Sea level fluctuation and coastal evolution* (Nummedal, D., Pilkey, O. H., & Howard, J. D., eds). Society of Economic Paleontologists and Mineralogists Special Publication 41, Tulsa. Oklahoma, pp. 3-16.

Gornitz, V., Lebedeff, S. & Hansen, J. 1982 Global sea level trend in the past century *Science* **215**, 1611-1614.

He, Q.& Walling, E. 1996 Use of fallout Pb-210 measurements to investigate longer-term rates and patterns of overbank sediment deposition on the floodplains of lowland rivers *Earth Surface Processes and Landforms* **21**, 141-154.

Hedges, J. I. & Keil, R. G. 1995 Sedimentary organic matter preservation: an assessment and speculative synthesis *Marine Chemistry* **49**, 81-115.

Hedges, J. I. & Keil, R. G. 1999 Organic geochemical perspectives on estuarine processes: sorption reactions and consequences *Marine Chemistry* **65**, 55-65.

Henrichs, S.M. 1993 Early diagenesis of organic matter: The dynamics (rates) of cycling of organic compounds In *Organic Geochemistry: Principles and Applications* (Engel, M. H. & Macko, S. A., eds) Plenum Press, New York, pp. 101-117.

Holdahl, S. R. & Morrison, N. L. 1974 Regional investigations of vertical crustal movements in the U.S., using precise relevelings and mareograph data *Tectonophysics* **23**, 373-390.

Kearney, M. S., Stevenson, J. C., & Ward, L. G. 1994 Spatial and Temporal Changes in Marsh Vertical Accretion Rates at Monie Bay: Implications for Sea-Level Rise. *Journal of Coastal Research* **10**, 1010-1020.

108

Khan, H. & Brush, G. S. 1994 Nutrient and metal accumulation in a freshwater tidal marsh. *Estuaries* **9**, 310-319.

Ledwin, J. M. 1988 *Sedimentation and its role in the nutrient dynamics of a tidal freshwater marsh* M.A. Thesis, College of William and Mary, Virginia Institute of Marine Science, Gloucester Point.

Leonard, L. A. & Luther, M. E. 1995 Flow hydrodynamics in tidal marsh canopies *Limnology and Oceanography* **40**, 1474-1484.

Leonard, L. A. 1997 Controls of sediment transport and deposition in an incised mainland marsh basin, southeastern North Carolina *Wetlands* **17**, 263-274.

Leonard, L. A., Hine, A. C. & Luther, M. E. 1995 Surficial sediment transport and deposition processes in a *Juncus roemerianus* marsh, west-central Florida *Journal of Coastal Research* **11**, 322-336.

McKee, B. A., Nittrouer, C. A., & DeMaster, D. J. 1983 Concepts of sediment deposition and accumulation applied to the continental shelf near the mouth of the Yangtze River *Geology* **11**, 631-633.

Morris, J. T. & Bowden, W. B. 1986 A mechanistic, numerical model of sedimentation, mineralization, and decomposition for marsh sediments *Soil Science Society of America Journal* **50**, 96-105.

Neubauer, S. C., Miller, W. D. & Anderson, I. C. 2000. Carbon cycling in a tidal freshwater marsh ecosystem: A carbon gas flux study. *Marine Ecology Progress Series.* **199**: 13-30.

Odum, W. E., Smith III, T. J., Hoover, J. K. & McIvor, C. C. 1984 *The ecology of tidal freshwater marshes of the United States east coast: a community profile* United States Department of the Interior, Fish and Wildlife Service, FWS/OBS-83/17.

Olsen, C. R., Cutshall, N. H. & Larsen, I. L. 1982 Pollutant-particle associations and dynamics in coastal marine environments: A review *Marine Chemistry* **11**, 501-533.

Olsen, C. R., Larsen, I. L., Lowry, P. D., Cutshall, N. H. & Nichols, M.M. 1986 Geochemistry and deposition of ^{7}Be in river-estuarine and coastal waters. *Journal of Geophysical Research* **91**, 896- 908.

Orson, R. A., Simpson, R. L. & Good, R. E. 1990 Rates of sediment accumulation in a tidal freshwater marsh *Journal of Sedimentary Petrology* **60**, 859-869.

109

Orson, R. A., Simpson, R. L. & Good, R. E. 1992 The paleoecological development of a late- Holocene, tidal freshwater marsh of the upper Delaware River estuary *Estuaries* **15**, 130-146.

Pasternack, G. B. & Brush, G. S. 1998 Sedimentation cycles in a river-mouth tidal freshwater marsh *Estuaries* **21**, 407-415.

Perry III, J. E. & Hershner, C. 1999 Temporal changes in the vegetation pattern in a tidal freshwater marsh *Wetlands* **19**, 90-99.

Perry III, J. E. 1991 *Analysis of vegetation patterns in a tidal freshwater marsh* Ph.D. dissertation, College of William and Mary, Virginia Institute of Marine Science, Gloucester Point.

Reed, D. J. 1990 The impact of sea-level rise on coastal salt marshes *Progress in Physical Geography* **14**, 465-481.

Russell, I. J., Choquette, C. E., Fang, S. L., Dundulis, W. P., Pao, A. A. & Pszenny. A. A. P. 1981 Forest vegetation as a sink for atmospheric particulates: Quantitative studies in rain and dry deposition *Journal of Geophysical Research* **86**, 5247-5363.

Shi, Z., Pethick, J. S., Burd, F. & Murphy, B. 1996 Velocity profiles in a salt marsh canopy *Geo- Marine Letters* **16**, 319-323.

Silberhorn, G. M. & Zacherle, A. W. 1987 *King William County and Town of West Point Tidal Marsh Inventory* Special Report No. 289 in Applied Marine Science and Ocean Engineering. Virginia Institute of Marine Science, Gloucester Point, Virginia.

Skoog, D. A. & West, D.M. 1963 *Fundamentals of Analytical Chemistry*, 3rd ed. Holt, Rinehart and Winston, New York, pp. 71-78.

Stevenson, J. C., Ward, L. G. & Kearney, M. S. 1988 Sediment transport and trapping in marsh systems: implications of tidal flux studies *Marine Geology* **80**, 37-59.

Stuiver, M., Reimer, P. J., Bard, E., Beck, J. W., Burr, G. S., Hughen, K. A., Kromer, B., McCormac, G., van der Plicht, J. & Spurk, M. 1998 INTCAL98 Radiocarbon Age Calibration, 24000 – 0 Cal BP *Radiocarbon* **40**, 1041-1083.

Walling, D. E., Quine, T. A. & He, Q. 1992 Investigating contemporary rates of floodplain sedimentation. In *Lowland floodplain rivers: Geomorphological perspectives* (Carling, P. A. & Petts, G. E., eds), John Wiley and Sons, New York, pp. 165-184.

SECTION III

Tidal Freshwater Marsh Dissolved Inorganic Carbon Dynamics: Concentration, Isotopic

Composition and Evidence for Export[†]

[†] To be submitted to *Limnology and Oceanography* with Scott C. Neubauer, Iris Cofman

Anderson and Stephen A. Macko as authors.

ABSTRACT

The cycling of dissolved inorganic carbon (DIC) and the role of tidal marshes in estuarine DIC dynamics were studied in a Virginia tidal freshwater marsh. Seasonally, the concentration and isotopic composition of DIC were measured over diurnal cycles in a marsh creek and at the junction of the creek with the adjacent Pamunkey River. In the creek. DIC concentrations at high tide were controlled by the same processes affecting estuarine DIC gradients. At low tide. DIC concentrations were 1.5 to 5-fold enriched versus high tide concentrations. indicating an input of DIC from the marsh. Similar patterns (although dampened in magnitude) were observed at the creek mouth, suggesting that DIC was ultimately exported from the marsh. A ^{13}C isotope mass balance indicated a significant input of DIC from marsh porewater. Additional DIC sources suggested by the $\delta^{13}C_{DIC}$ data included water column respiration and the decomposition of marsh autotrophs. A model linking DIC concentrations with tidal water transport through the marsh showed that inputs of DIC from the marsh to the water column occurred throughout the tidal cycle. When extrapolated to an estuary-wide scale, marsh DIC export could explain a significant portion (85 ± 30%) of CO_2 supersaturation and excess DIC production in the tidal York and Pamunkey Rivers.

112

INTRODUCTION

One approach to understanding the cycling of organic carbon within ecosystems is through measurements of total system metabolism as the production and removal of organic matter are intimately linked to DIC (dissolved inorganic carbon) and O_2 cycling. Recent studies on estuarine CO_2 and DIC dynamics have shown that estuaries are generally supersaturated with respect to CO_2 and exhibit high rates of net heterotrophy (i.e. respiration > photosynthesis; Smith and Hollibaugh 1993; Cai and Wang 1998; Frankignoulle et al. 1998; Gatusso et al. 1998; Raymond et al. in press) although the main stem of Chesapeake Bay appears to be net autotrophic (Kemp et al. 1997). Sources of CO_2 and DIC to estuarine waters include water column and benthic respiration, riverine and groundwater inputs, photodegradation of dissolved organic matter, and inputs from intertidal marshes (Hopkinson and Vallino 1995; Kemp et al. 1997; Cai and Wang 1998). Accurate quantification of rates of net heterotrophy requires that one account for DIC produced within the estuary through *in situ* organic matter decomposition as well as DIC which is produced in the watershed (e.g. in intertidal wetlands or groundwater) and subsequently transported into the estuary. Thus, CO_2 supersaturation, by itself, is insufficient evidence for declaring the trophic status (e.g. net autotrophy or heterotrophy) of an estuary or other open ecosystem. Although the total area of estuaries is globally small, the biogeochemical cycling of carbon in these systems may be regionally significant (e.g. Smith and Hollibaugh 1993; Frankignoulle et al. 1998; Gattuso et al. 1998) so a more robust understanding of the sources, cycling and fates of DIC in estuarine waters is required.

113

Over the past 40 years, the fluxes of particulate and dissolved organic carbon (POC and DOC) and inorganic nutrients between intertidal marshes and estuarine waters have been studied, primarily to determine if the export of these materials could explain high rates of primary and secondary production in estuarine waters (see reviews by Nixon 1980; Childers 1994; Dame 1994). Although there is no consensus on the magnitude or direction of marsh–estuary organic carbon fluxes, the outwelling of DOC and POC from marshes followed by remineralization within the estuary is one mechanism by which marshes could support rates of net estuarine heterotrophy. In addition to marsh-derived organic materials supporting net heterotrophy in the estuary, there is a high potential for DIC transport from intertidal marshes to the estuary. This direct export of marsh-produced DIC has largely been ignored. The DIC may be added to waters overlying the marsh at high tide from plant decomposition, sediment metabolism and the upward diffusion of marsh porewater. Potential inputs at low tide include drainage of marsh porewater into tidal creeks and DIC fluxes from subtidal creek sediments. In order to accurately quantify the total DIC transport from a marsh, export during both high and low tides must be considered.

Several recent studies have suggested that there must be a significant marsh source of DIC to estuarine waters in order to balance measured levels of CO_2 supersaturation (Cai and Wang 1998; Cai et al. 1999; Raymond et al. in press). In the present study, hourly measurements of DIC concentration were made in a tidal creek draining a tidal freshwater marsh over diurnal cycles. Simultaneous measurements were made at the

114

mouth of the tidal creek to determine if DIC added to the creek was subsequently exported to the adjacent river. Marsh porewater DIC concentrations were measured to determine if drainage of porewater into the creek during low tide could explain the observed temporal patterns in DIC concentration. The stable isotopic compositions of creek and porewater DIC ($\delta^{13}C$ and $\delta^{18}O$) were used as additional means of identifying the source(s) of DIC added to the marsh creek. To determine seasonal differences in marsh DIC cycling, data were collected during the period of maximum marsh biomass (June), in late summer when rates of senescence and decomposition were high (August), and in November when rates of plant productivity and marsh respiration were low. Finally, the observed tidal and seasonal changes in DIC concentration were combined with estimates of tidal water transport through marsh creeks to quantify the annual export of DIC from the marsh.

MATERIALS AND METHODS

Study Site: Sweet Hall marsh is a 401 ha tidal freshwater marsh located on the Pamunkey River, approximately 69 km (by river) from the mouth of the York River, Virginia. The marsh is a site within the Chesapeake Bay National Estuarine Research Reserve system in Virginia (CB-NERRVA) and is seasonally dominated by the macrophytes *Peltandra virginica*, *Pontederia cordata*, and *Zizania aquatica* (Doumlele 1981; Perry 1991). At Sweet Hall, the Pamunkey River is microtidal, with a mean tidal range of 70 cm (neap tide) to 90 cm (spring tide). Historical records indicate that the long-term average salinity at Sweet Hall is 0.5 ppt (Brooks 1983). However, during this

115

study (1999), salinity ranged from 0.0 to 15.9 ppt (average 2.8 ppt; CB-NERRVA unpublished data) with the highest salinities in late August and early September following a dry summer. Pamunkey River discharge rates during May to August 1999 were the lowest recorded over the last 30 years (USGS 2000).

Diurnal Tidal Sampling: Studies examining tidal exchanges of DIC between the marsh, creek, and river were conducted in June, August, and November 1999. All sampling dates were within 2 days of spring tide. Water samples were collected from a small tidal creek (Hill's Ditch) draining Sweet Hall marsh (hereafter referred to as the "creek" site), and at the junction of this creek with the Pamunkey River ("mouth" site; Fig. 1). Fifty ml water samples were collected hourly using polypropylene syringes and immediately filtered for DIC analyses as described below. A YSI 6000 datasonde (YSI, Inc., Yellow Springs, Ohio) recorded water depth, salinity, pH, temperature, and dissolved oxygen at 15 minute intervals. At the creek site, the water intake and YSI datasonde were located 10 to 15 cm above the creek bed. The intake at the mouth site was suspended from a floating platform and sampled 20 to 30 cm below the water surface (~5 to 70 cm above the sediment surface, depending on tidal stage).

Water samples for DIC analysis were filtered (0.45 μM Gelman Supor Acrodiscs) into 12.8 ml gas tight Hungate tubes, stored on ice in the field, and refrigerated until analysis. Sample DIC concentrations were measured within 2 days of collection. Laboratory experiments over a range of DIC concentrations (0.5 to 7.0 mM) showed no significant storage effects over 12 days (t-test, $\alpha = 0.05$; unpublished data). Fifty μl

116
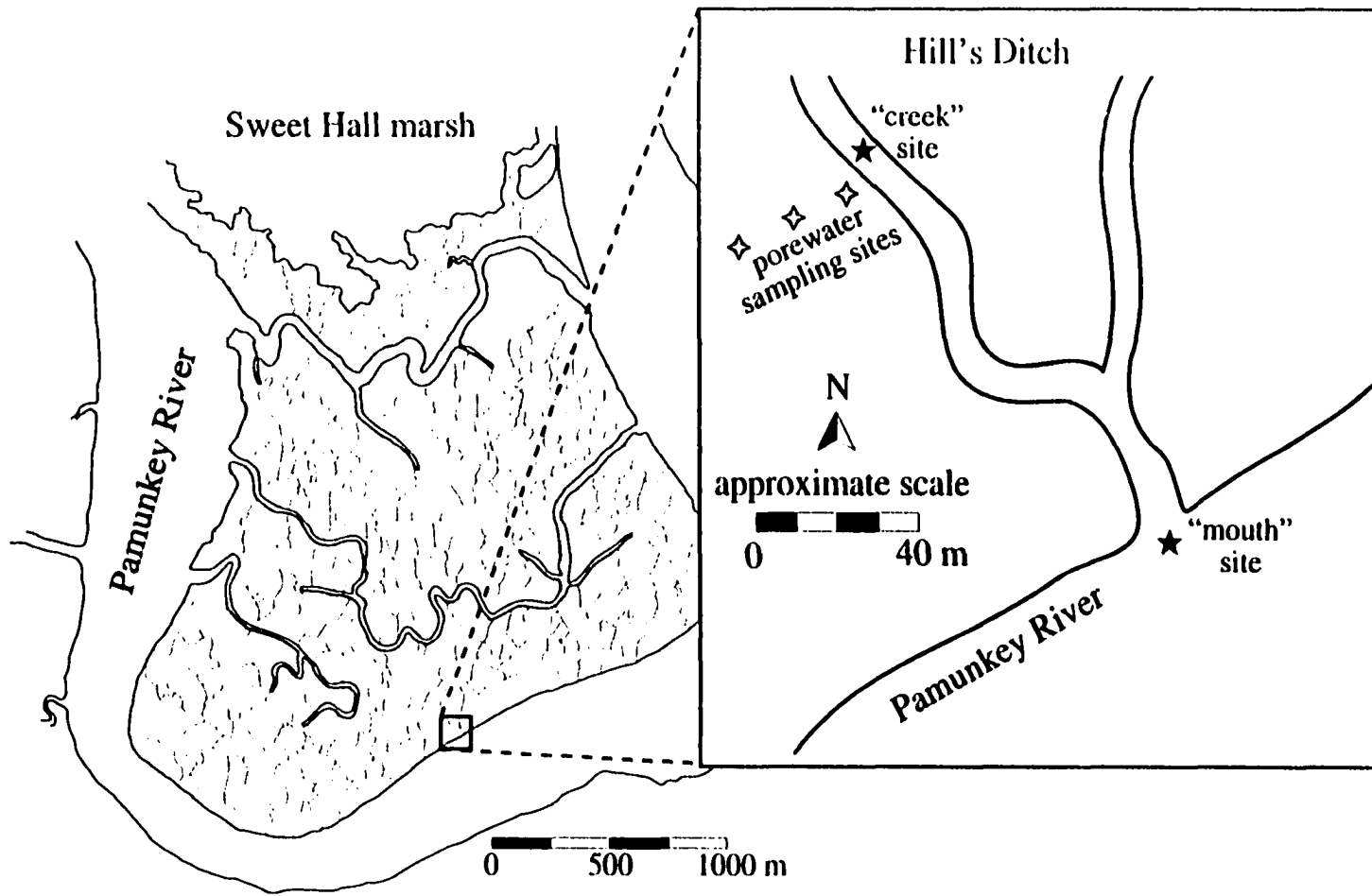
Figure 1: Map of Sweet Hall marsh showing location of study site. Blow-up shows location of creek and mouth water sampling sites as well as porewater sippers within the marsh

samples were injected into a vessel filled with 25 ml of 0.05 M H_2SO_4 that was continuously sparged with CO_2-free N_2 into a LI-COR 6252 infrared gas analyzer (LI-COR Inc., Lincoln, NE). Calibrations were performed routinely by injecting a series of Na_2CO_3 standards (0.5 to 10 mM). Median sample precision for 3 to 5 replicate standard injections was 0.01 mM.

For DIC isotopic analyses, water samples were acidified under vacuum by injection of 1 ml 100% H_3PO_4 and the resultant CO_2 was cryogenically purified and trapped on a vacuum line using an ethanol/dry ice slush and liquid N_2. Purified samples were analyzed for $\delta^{13}C$ and $\delta^{18}O$ on a Prism isotope ratio mass spectrometer (Micromass, Inc., Manchester, UK). Reproducibility of Na_2CO_3 standards was better than 0.5‰ for $\delta^{13}C$ and $\delta^{18}O$. A high correlation between the mass spectrometer ion signal and DIC concentration indicated similar DIC recovery across a range of sample concentrations and therefore no preferential fractionation of larger or smaller samples (Fig. 2).

Porewater Sampling: Marsh porewater was sampled on the same dates as water column samples using porewater samplers ("sippers") that were installed in the marsh in February 1999. Clusters of three sippers were located at 1, 15, and 30 m along a transect extending from creekbank (0 m) toward the marsh interior (30 m; Fig. 1). Each sipper had a 5 cm sampling window of porous sintered plastic centered around a depth of 5, 15, or 25 cm. Prior to sampling, sippers were purged of water and filled with argon gas to maintain anaerobic conditions. Each sipper was then evacuated to a vacuum of 50 to 60 cm Hg and allowed to refill for 4 to 5 hours before sampling. Water was collected from sippers

118
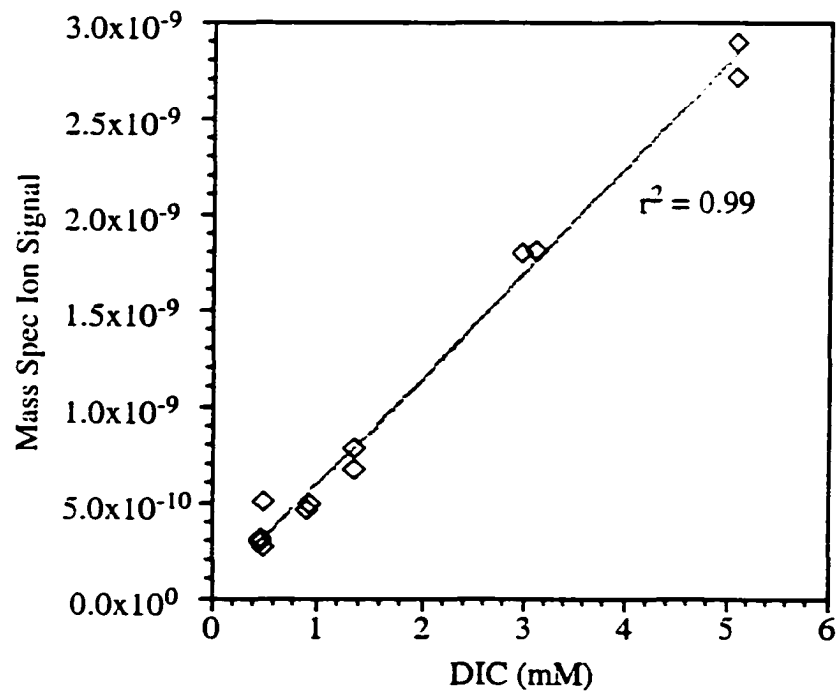
Figure 2: Relationship between DIC concentration and mass spectrometer signal strength indicating similar DIC recovery efficiency (and therefore no preferential fractionation) across a range of Na_2CO_3 DIC standards

119

within 1 hour of low and high tides using polypropylene syringes and filtered for DIC

analysis as described above. In spite of the relatively high vacuum and long recharge

times, there were occasions when there was not enough water for DIC analyses.

RESULTS AND DISCUSSION

Water Column Conditions: The semi-diurnal tides at Sweet Hall create a dynamic

environment with large variations in water column conditions (e.g. depth, salinity,

dissolved oxygen). During the sampling dates, the tidal range varied between 0.55 and

0.83 m (Fig. 3). Daily trends in water temperature were determined by the day-night

cycle rather than by tidal effects. There was a wide variation in salinity between

sampling dates (June: 1.5 to 4.9; Aug 6.1 to 8.9; Nov 0.3 to 1.1 ppt) as well as over

individual tidal cycles (Fig. 3). In June, the salinity at the mouth site was greater than at

the creek site by an average of 1.2 ppt; there were no consistent differences between sites

in August and November. Water column pH and dissolved oxygen followed similar tidal

patterns with lowest pH and dissolved oxygen (DO) concentrations near low tide (Fig. 3).

The pH at the creek site was generally lower than at the mouth site, suggesting an input

of acidic water within the marsh–creek system. Measured DO concentrations were

typically lower than the predicted saturation values (calculated from temperature and

salinity data; Millero and Sohn 1992).

120
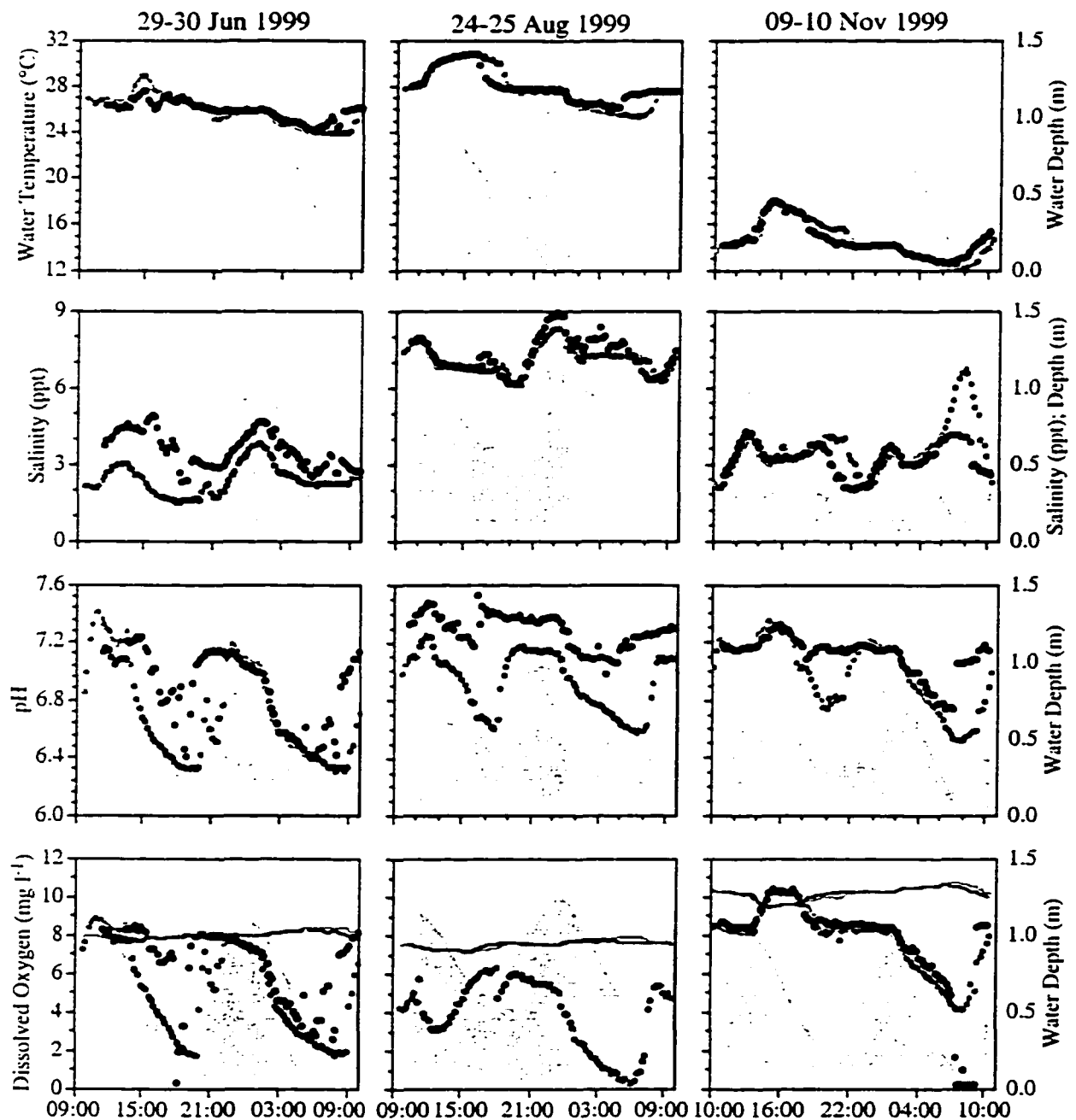
Figure 3: Water column conditions at the creek and mouth sites during diurnal samplings. Gray symbols represent creek data; black symbols indicate the mouth site. On the salinity panels, June and August data are on the same scale (0 to 9 ppt) while the November data are on a 0 to 1.5 ppt scale. Solid lines in the dissolved oxygen panels indicate O_2 saturation values calculated from temperature and salinity data. Gray shading indicates water depth.

121

DIC Concentrations

Water Column DIC Concentrations: Within the water column, there were large

variations in DIC concentrations over the tidal and seasonal time scales (Fig. 4). Near

high tides, DIC concentrations were similar at both creek and mouth sites (June: ~0.5

mM; Aug: ~1.1 mM; Nov: ~0.5 mM). These high tide concentrations were within ± 0.05

mM of those calculated from DIC versus salinity regression equations for the York and

Pamunkey Rivers (Raymond et al. in press; exception: one point in August was

overestimated by 0.10 mM). This suggests that the DIC concentrations in the marsh tidal

creek at high tide were controlled by the same processes that affect estuarine DIC

gradients in the York and Pamunkey Rivers. In part, estuarine DIC concentrations are

influenced by the mixing of high DIC ocean water with low DIC freshwater, the spatial

patterns in estuarine production and respiration, the retention of DIC within the system

due to conversion of atmosphere-exchangeable CO_2 to non-volatile HCO_3^- down-estuary,

and an increase in water residence time (which allows DIC to accumulate) due to the

broadening and deepening of the saline end of funnel-shaped estuaries (e.g. Spiker and

Schemel 1979; Coffin et al. 1994; Cai and Wang 1998; Raymond et al. in press)

At both the creek and mouth sites, DIC concentrations during ebb tide increased

steadily (by 0.6 to 1.9 mM) before reaching a maximum approximately 1 hour before low

tide at the mouth site and slightly after low tide in the creek (Fig. 4). Maximum

concentrations at the creek site were always greater than at the mouth site. Because these

low tide concentrations were up to 1.9 mM greater than predicted by the DIC versus

salinity regression equations of Raymond et al. (in press), we suggest that processes

122
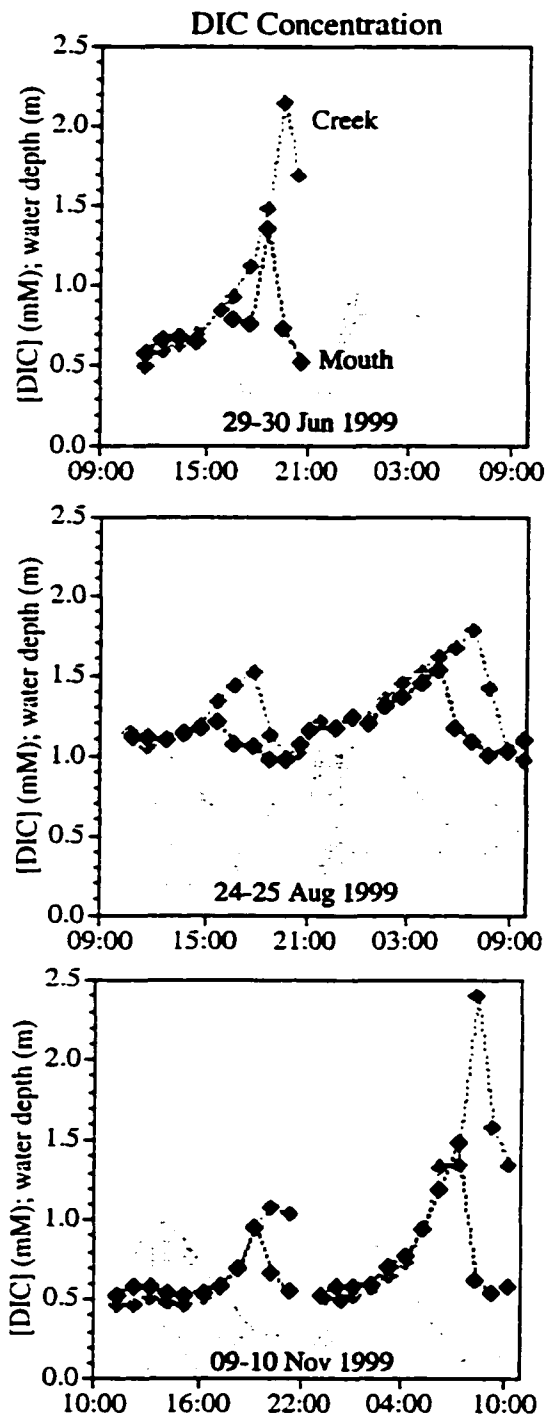
Figure 4: Diurnal profiles of DIC concentration. Sampling in June 1999 was cut short due to severe weather. Gray symbols represent creek data; black symbols indicate the mouth site. Gray shading indicates water depth.

123

occurring within the marsh–tidal creek system had a strong effect on DIC concentrations at low tide. Within marsh tidal creeks, DIC concentrations can be affected by *in situ* autotrophic and heterotrophic activity, the mixing of creek water with other end members (e.g. river water, marsh porewater, groundwater), and CO_2 exchange with the atmosphere. Assuming an atmospheric pCO_2 of 360 ppmv, water column CO_2 concentrations during this study (800 to >20,000 ppmv; calculated from measured salinity, temperature and pH data; Park 1969; Weiss 1974; Millero 1995) were 2 to 69 times greater than predicted saturation values, suggesting that the creek was a source of CO_2 to the atmosphere. To estimate inputs of DIC from water column and subtidal sediment respiration, changes in dissolved oxygen measured over diurnal cycles in the tidal creek (Fig. 3) were converted to carbon production rates assuming a respiratory quotient of 1.0. Although large decreases in dissolved oxygen near low tide corresponded with peaks in DIC concentration, respiration in the water column and subtidal creek sediments could explain less than 0.2 mM of the observed 0.6 to 1.9 mM DIC enrichment at low tide. Because creek and mouth DIC concentrations were always supersaturated with respect to the atmosphere and could not be completely explained by respiration within the creek, there must have been an allochthonous source(s) of high DIC water that was mixing with the creek and river waters.

Porewater DIC Concentrations: With the exception of the shallow creekbank sipper in June and November, all porewater DIC concentrations (1.14 to 6.73 mM) were greater than those measured in the creek or at the mouth (Table 1). On the basis of concentration data, inputs of marsh porewater to the creek may explain the tidal patterns in water

124

Table 1: Marsh porewater DIC concentrations and isotopic signatures. Samples were collected within 1 hr of low tide on each sampling date along a transect extending from creekbank (0 m) to the marsh interior (30 m; Fig. 1).

Distance (m)	Depth (cm)	29 June 1999 [DIC] (mM)	$^{13}C_{DIC}$ (‰)	$^{18}O_{DIC}$ (‰)	24 August 1999 [DIC] (mM)	$^{13}C_{DIC}$ (‰)	$^{18}O_{DIC}$ (‰)	09 November 1999 [DIC] (mM)	$^{13}C_{DIC}$ (‰)	$^{18}O_{DIC}$ (‰)
1	5	1.14	−17.71	38.54	2.43	−15.26	36.84	2.10	(no isotopes)	
1	15	3.11	−14.64	35.71	4.86	(no isotopes)		3.66	−17.89	36.81
1	25	(no sample)			2.15	−11.18	36.84	(no sample)		
15	5	2.70	(no isotopes)		5.56	(no isotopes)		3.65	−6.89	36.95
15	15	4.66	−13.38	41.34	6.73	(no isotopes)		5.45	(no isotopes)	
15	25	4.68	−11.86	33.99	6.60	−7.36	36.94	4.58	−6.37	37.44
30	5	3.22	(no isotopes)		4.69	−15.73	38.46	2.47	−14.16	36.08
30	15	3.99	−16.12	38.47	3.52	−12.40	36.85	3.68	(no isotopes)	
30	25	4.22	(no isotopes)		2.75	−8.34	36.73	3.09	−10.09	38.28

column DIC concentration. The DIC concentrations were generally higher below 5 cm depth; this was likely due to water residence time within marsh sediments. Using a vertical infiltration rate for Sweet Hall marsh of 0.15 to 2.77 L m^{-2} tide^{-1} (water column to marsh sediments; Reay 1989), an average dry sediment bulk density of 0.408 g cm^{-3} (this report, section II), and an average sediment water content of 67% by mass (SCN, unpublished data), it takes 47 to >800 days to completely replace all porewater to a depth of 30 cm. Thus, while shallow (5 cm) porewater can exchange readily with overlying water at high tide, deeper porewater turns over more slowly; this allows DIC produced by sediment heterotrophic processes to accumulate in deeper sediments.

Composition of DIC (Carbonate Equilibrium): Carbon dioxide (and CH$_4$ in anaerobic sediments) are end products of organic carbon metabolism. With respect to the atmosphere, aquatic or water-saturated systems may represent a carbon source or sink. Carbon dioxide can be lost by evasion to the atmosphere or it can be converted to HCO$_3^-$ or CO$_3^{2-}$ which represent longer-term, non-atmosphere-exchangeable sinks for carbon. In order to determine if the observed low tide peak in DIC represents an atmospheric source (CO$_2$) or an estuarine sink (HCO$_3^-$ or CO$_3^{2-}$) for carbon, measured pH and DIC concentrations were combined with equations from Park (1969) to calculate DIC partitioning between carbonic acid (H$_2$CO$_3$, primarily as hydrated molecular CO$_2$), bicarbonate (HCO$_3^-$) and carbonate (CO$_3^{2-}$). The observed pH decrease around low tide (Fig. 3) caused the fraction of CO$_2$ in the total DIC pool to increase relative to bicarbonate and carbonate, with the highest proportion of CO$_2$ (up to 38%) occurring when DIC concentrations were greatest (Fig. 5). At all sampling points, HCO$_3^-$

126
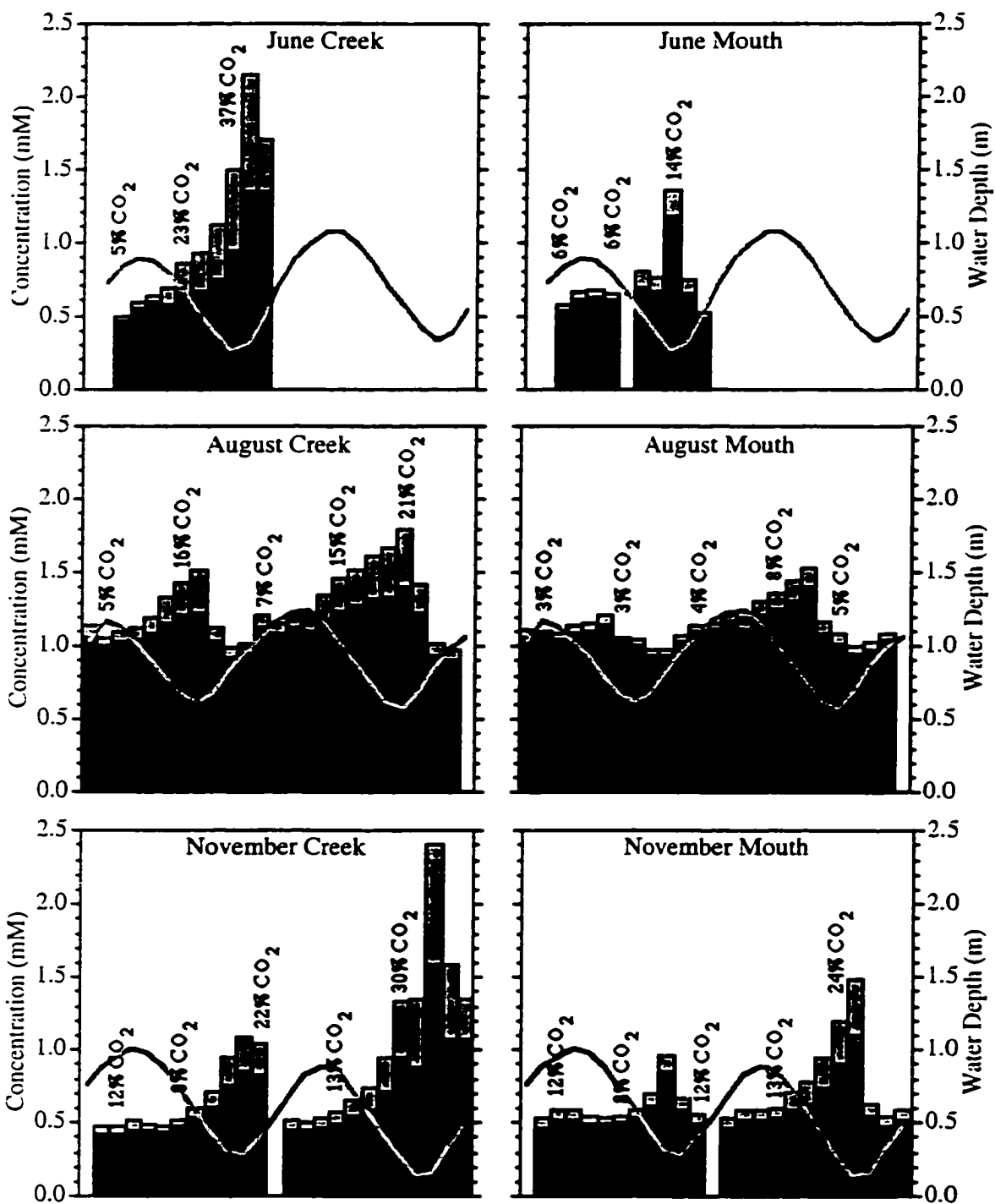
Figure 5: Calculated distribution of carbonate species (CO_2, HCO_3^-) based on pH,

salinity, and temperature. Concentrations of CO_2 indicated by light gray bars, HCO_3^- by

darker gray bars, total DIC is the sum of the two bars (CO_3^{2-} concentrations were too low

to show up on figure). The light gray line represents water depth (right y-axis).

127

comprised the bulk (62 to 94%) of the total DIC pool, while the proportion of CO_3^{2-} was

consistently <2%. During the low tide peak in DIC, concentrations (mM) of both CO_2

and HCO_3^- increased (Fig. 5). Thus, while the marsh was a source of CO_2 to tidal waters,

HCO_3^- was also generated which indicates that there was a source of alkalinity within the

marsh–creek system to consume H^+ (i.e. raise pH) and convert CO_2 to HCO_3^-. While

sulfate reduction has been proposed as a significant source of alkalinity in estuarine

systems (Smith and Hollibaugh 1997; Cai and Wang 1998; Raymond et al. in press), its

significance is lessened in freshwater marshes (except during transient salinity increases)

due to the decreased availability of seawater sulfate. Other microbial reactions which can

generate alkalinity include denitrification, iron and manganese reduction, and

methanogenesis.

Stable Isotopic Data: The quality of the $\delta^{13}C_{DIC}$ isotopic data was evaluated using $\delta^{18}O$

signatures for the same samples. Due to latitudinal gradients in the $\delta^{18}O$ content of

precipitation (Fairbanks 1982; Lajtha and Marshall 1994, Hendricks et al. 2000), $\delta^{18}O_{H_2O}$

values for freshwater rivers along the Atlantic coast of North America vary from -25 to

-20‰ for high latitude rivers to > -5‰ in the southeast (Dansgaard 1964; Fairbanks

1982). For mid-Atlantic rivers, $\delta^{18}O_{H_2O}$ values typically range from -10 to -5‰ (e.g.

Torgersen 1979; Fairbanks 1982). Thus, values that lie outside of these typical ranges

should be viewed with caution. In this study, we measured $\delta^{18}O_{DIC}$ values in samples that

had been stored for at least 1 week. During this time, ^{18}O in DIC will equilibrate with ^{18}O

in water. Using the measured $\delta^{18}O_{DIC}$ values and a temperature dependent fractionation

factor between $\delta^{18}O_{CO_2}$ and $\delta^{18}O_{H_2O}$ ($\alpha = 1.044$ at storage temperature of $8.5°C$: calculated from Friedman and O'Neil 1977), calculated $\delta^{18}O_{H_2O}$ values ranged from -23.2 to $-2.3‰$. While heavy $\delta^{18}O_{H_2O}$ values can be explained by preferential evaporation of ^{16}O, at this time we know of no plausible mechanisms to explain the highly depleted $\delta^{18}O_{H_2O}$ values observed in this study. Therefore when $\delta^{18}O_{H_2O}$ was less than $-10‰$, $^{13}C_{DIC}$ and $^{18}O_{DIC}$ values were discarded due to the possibility of fractionation during sample processing. The full dataset, including questionable isotopic data, is presented in Appendix 1.

Temporal variability: At the creek and mouth sites, the isotopic concentration of DIC varied both seasonally and over the tidal cycle (Fig. 6). In June, $\delta^{13}C_{DIC}$ values were lighter in the creek than at the mouth site by an average of $2‰$. The lightest values at both sites were measured near low tide, roughly coincident with the highest DIC concentrations (compare Fig. 6 with Fig. 4). In contrast, the opposite pattern was observed at the creek site in November; $\delta^{13}C_{DIC}$ values were generally heavier near low tide. There were no distinct tidal patterns in $\delta^{13}C_{DIC}$ in August at the creek or mouth sites. When averaged across all data points within a month, $\delta^{13}C_{DIC}$ values at the creek site were not significantly different from June ($-13.8 \pm 1.3‰$) to August ($-14.3 \pm 0.5‰$) to November ($-13.1 \pm 0.9‰$; ANOVA, p = 0.185). At the mouth site, August $\delta^{13}C_{DIC}$ values ($-14.7 \pm 0.6‰$) were lighter than in June ($-11.9 \pm 0.6‰$; ANOVA, p = 0.010; Tukey's HSD, p = 0.014); neither month was significantly different from November ($-13.7 \pm 1.2‰$; Tukey's HSD, p > 0.05).

129
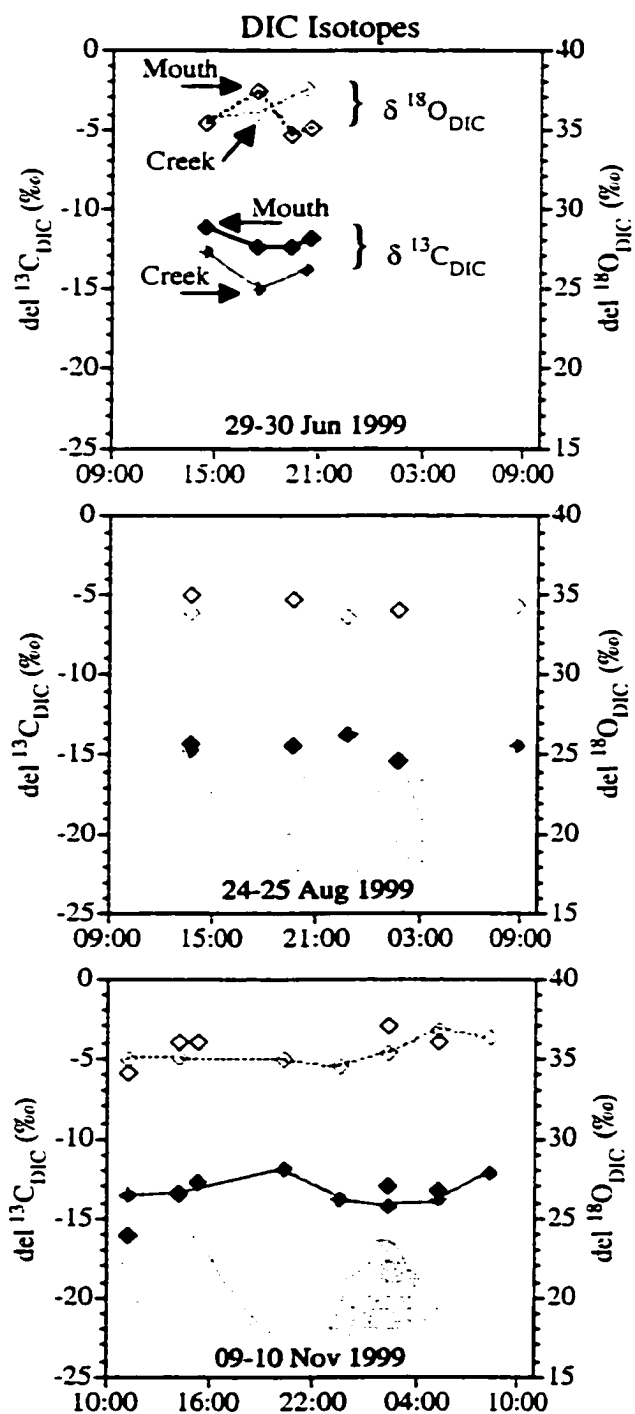
Figure 6: Isotopic composition of water column DIC: $\delta^{13}C_{DIC}$ (left y-axis; filled symbols) and $\delta^{18}O_{DIC}$ (right y-axis; open symbols). Sampling in June 1999 was cut short due to severe weather. Gray symbols represent creek data; black symbols indicate the mouth site. Shading indicates water depth.

130

<u>Isotopic Mixing Model</u>: Tidal changes in DIC concentration in all months suggested a marsh input of DIC to the tidal creek. To identify possible sources of this added DIC, an isotopic mixing model was used to calculate the isotopic composition of marsh-derived DIC ($\delta^{13}C_{marsh}$):

$$\delta^{13}C_{meas} \times [DIC]_{meas} = \left(\delta^{13}C_{river} \times [DIC]_{river}\right) + \left(\delta^{13}C_{marsh} \times [DIC]_{marsh}\right) \qquad (1)$$

where $\delta^{13}C_{meas}$ and $[DIC]_{meas}$ were measured in the marsh creek. The isotopic composition of riverine DIC ($\delta^{13}C_{river}$) was estimated seasonally as the average $\delta^{13}C_{DIC}$ value for the mouth site at high tide. In August, there were no $\delta^{13}C_{DIC}$ values from the mouth site at high tide so the mixing model was not used to calculate $\delta^{13}C_{marsh}$. The $[DIC_{river}]$ values were calculated from York and Pamunkey River DIC versus salinity regression equations from Raymond et al. (in press). The concentration of DIC added by the marsh ($[DIC]_{marsh}$) was calculated by difference:

$$[DIC]_{meas} = [DIC]_{marsh} + [DIC]_{river}. \qquad (2)$$

The $[DIC_{marsh}]$ term includes all DIC added within the marsh–tidal creek system while $[DIC_{river}]$ consists of DIC produced in the Pamunkey River (water column or subtidal sediments) or advected from upstream.

Estimated values for riverine DIC (June: -11.1‰; November: -13.2‰; Table 2) were similar to $\delta^{13}C_{DIC}$ values (-14.6 to -5.7‰) measured by Raymond (1999) in the low salinity (< 7 ppt) region of the York and Pamunkey Rivers. Using the isotopic mixing model, estimates of $\delta^{13}C_{marsh}$ for June ranged from -18.7 to -15.0‰ (Table 2). In November, the isotopic composition of marsh-derived DIC varied over the tidal cycle;

131

Table 2: Isotopic composition of marsh-added DIC ($\delta^{13}C_{marsh}$). Calculations were not made in August due to a lack of data for the estimation of the isotopic composition of riverine DIC ($\delta^{13}C_{river}$).

Month	$\delta^{13}C_{river}$ (‰)[a]	$\delta^{13}C_{marsh}$ (‰)[b]
June	-11.1	-18.7 to -15.0 (all tide stages)
November	-13.2	-11.7 to -10.8 (low tide only)
November	-13.2	-24.3 to -14.5 (other tide stages)

[a] Estimated as $\delta^{13}C_{DIC}$ from the mouth site at high tide.

[b] Calculated from the isotopic mixing model, equation 1.

132

DIC added near low water was -11.7 to -10.8‰ while that added during other stages of the tide ranged from -24.3 to -14.5‰ ($\bar{x}$ = 20.2‰). The ranges for added DIC in each month overlapped the values for porewater $\delta^{13}C_{DIC}$ for the same months (June: -17.7 to -11.9‰; November: -17.9 to -6.4‰; Table 1), suggesting that some of the DIC added to the creek may have originated in marsh porewaters and entered the tidal creek through drainage at low tide or diffusive fluxes at high tide. In porewater, the lightest porewater $\delta^{13}C_{DIC}$ values for all months were generally coincident with the lowest DIC concentrations and more shallow depths. The heavy porewater $^{13}C_{DIC}$ values in some samples may have been due to higher rates of methanogenesis in deeper sediments which produced isotopically light CH_4 ($\delta^{13}C$ = -57 to -58‰; Chanton et al. 1992; Chanton and Whiting 1996) and heavier residual CO_2. In both June and November, some calculated $\delta^{13}C_{marsh}$ values were lighter than measured porewater $\delta^{13}C_{DIC}$ values, indicating an additional source(s) of DIC to the creek.

Sources of Marsh-Derived DIC: Given a system controlled by the mixing of 2 end members with differing DIC concentrations and isotopic compositions, a plot of 1/[DIC] vs. $\delta^{13}C_{DIC}$ will be linear (after Faure 1986; Mariotti et al. 1988; Hellings et al. 2000). For all June data, as well as combined June and August samples, significant linear relationships (p < 0.04) were observed between $\delta^{13}C_{DIC}$ and 1/[DIC] (Figure 7). For August (p = 0.48) and November (p = 0.07) data, the slope of this relationship was not significantly different from zero. Given a significant $\delta^{13}C_{DIC}$ versus 1/[DIC] regression, the y-intercept provides an estimate of the isotopic value of DIC added by the marsh (Grossman et al. 1989; Nascimento et al. 1997; Hellings et al. 2000). In June, the y-

133
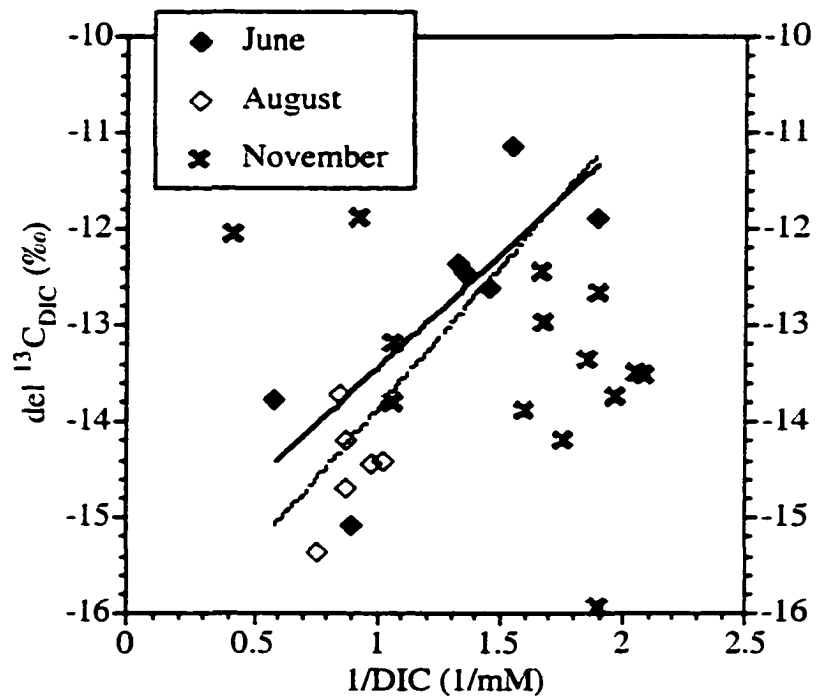
Figure 7: Plot of $\delta^{13}C_{DIC}$ versus 1/[DIC] for diurnal water column samples (creek and

mouth sites). A linear relationship between these parameters indicates mixing between

two distinct sources. The solid line is fit to June data; dashed line is fit to combined June

and August data.

134

intercept was $-15.8‰$ (95th percentiles of -18.7 to $-12.9‰$); this is similar to the range of -18.7 to $-15.0‰$ for $\delta^{13}C_{marsh}$ calculated from the mixing model (Table 2). In all months, the regression coefficients (r^2) for the $1/[DIC]$ versus $\delta^{13}C_{DIC}$ relationships were low (Jun: $r^2 = 0.62$; Jun + Aug: $r^2 = 0.69$; Nov: $r^2 = 0.24$), indicating that other factors, in addition to simple mixing between marsh porewater and river water, affected DIC concentration and isotopic composition. These might include *in situ* changes in DIC (i.e. water column photosynthesis and respiration) or mixing between more than 2 sources. In this case, the y-intercept on a plot of $\delta^{13}C_{DIC}$ versus $1/[DIC]$ represents a composite $\delta^{13}C_{DIC}$ value for the multiple sources (Hellings et al. 2000)

Potential sources of DIC from the marsh–creek system include CO_2 and DIC produced by sediment metabolism and plant decomposition when the marsh is flooded, inputs of marsh and subtidal creek porewater, and the decomposition of marsh derived particulate or dissolved organic matter within the water column. As previously discussed, the isotopic mass balance model periodically predicted inputs of DIC that were isotopically lighter than measured porewater values. Unless there was a change in the porewater $^{13}C_{DIC}$ signature, perhaps due to the oxidation of light porewater CH_4 during transport from anoxic porewater to the aerobic creek, there must be additional sources of DIC to the water column. Based on diurnal patterns in dissolved oxygen concentrations, respiration within the water column and subtidal creek sediments could not explain the entire DIC enrichment. However, the decomposition of water column particulates ($\delta^{13}C$ = -29 to $-21‰$) or dissolved organic carbon ($\delta^{13}C$ = -33 to $-23‰$; this report section IV) would result in inputs of isotopically depleted DIC to the water column. An additional

135

source of depleted DIC is the decomposition of marsh macrophyte and sediment microalgal biomass ($\delta^{13}C$ = -29 to -23‰; this report section IV) when the marsh surface is flooded. For example, Keough et al. (1998) calculated that CO_2 from the decomposition of plant biomass in a Michigan freshwater wetland could explain approximately 25% of the DIC ($\delta^{13}C_{DIC}$ = -13 to -10‰) in that system.

Total Marsh DIC Flux: Previous studies that have examined estuarine DIC dynamics have suggested a tidal marsh source of DIC in order to explain observed DIC and pCO_2 supersaturation (e.g. Cai and Wang 1998; Cai et al. 1999; Raymond et al., in press). The consistent peaks in DIC concentration at low tide and tidal changes in the isotopic composition of DIC support the idea that the marsh was a source of DIC to marsh creek waters. Because the concentration and isotopic trends were similar at the creek mouth (but somewhat less in magnitude), we suggest that the DIC added by the marsh was ultimately exported to the adjacent river. To quantify this export and place our data in a larger ecological context, we extrapolated our DIC profiles from a single tidal creek to an estimate of whole marsh DIC flux to the estuary.

DIC Export Calculations: In the absence of marsh DIC inputs, the concentration of DIC in water within the marsh and creeks can be estimated using York and Pamunkey River DIC versus salinity regressions presented in Raymond et al. (in press). Due to changes in salinity (Figure 3), calculated DIC values varied by 0.1 to 0.2 mM over the tidal cycle. Any DIC in excess of that predicted by the regression equations represents an input of DIC from the marsh due to respiration, diffusive fluxes of porewater DIC from the marsh

136

and subtidal creek sediments during flooding, and drainage of porewater DIC during low tide. This DIC enrichment due to marsh input (DIC_{marsh}) for each hourly sampling point was calculated as the difference between measured DIC concentrations and concentrations predicted by Raymond et al. (in press; equation 2). Periodically, measured concentrations were less than calculated values (generally by <0.05 mM); on these occasions we assumed that $[DIC]_{marsh}$ was zero and within the prediction error of the DIC versus salinity regressions.

At Sweet Hall, water is confined to the tidal creeks at low tide but the entire marsh is flooded to 20 to 40 cm at high tide. Measured water column depth data (relative to marsh elevation) were used to determine when flooding of the marsh surface began (i.e. "creek-full depth"). To account for spatial variations in marsh elevation and temporal changes in tidal range (e.g. over spring-neap tidal cycles), we varied this depth by ±10 cm to calculate a range of DIC export. Using a computer graphics package (Canvas 5.0; Deneba Systems, Miami FL), the total length of all creeks on a digitized USGS topographic map of Sweet Hall marsh (Terraserver 2000) was estimated as 48 km. Several deep (>2 m) and broad (>30 m) tidal channels that bisect the marsh were not included in this estimate. Based on the resolution of an individual pixel on the digitized map (4 x 4 m), we assumed that all creeks were 4 m wide. When water depth was below the creek-full depth, the total volume of water in all tidal creeks at Sweet Hall was calculated using measured water depths and estimates of creek width and length:

$$\text{If } D_{meas} \leq D_{full}, \quad V = [D_{meas} \times L \times W], \tag{3}$$

137

where D_{meas} is measured water depth (m), D_{full} is the creek-full depth (m), V is water volume (m^3); L is total creek length (4.8 x 10^4 m), and W is creek width (4 m). When measured water depth was greater than the creek-full depth, the total volume of water in the marsh was calculated as sum of water in the marsh creeks and that overlying the marsh:

$$\text{If } D_{meas} > D_{full}, \quad V = [D_{full} \times L \times W] + [(D_{meas} - D_{full}) \times A], \qquad (4)$$

where A is the total area of Sweet Hall marsh (4 x 10^6 m^2; Silberhorn and Zacherle 1987).

Rates of DIC export were calculated during ebb tide when there was a hydrological export of water, and therefore DIC, from the marsh. For each set of adjacent hourly time points during ebb tide ($t_{(i)}$ and $t_{(i+1)}$), the average DIC enrichment (DIC_{marsh}; mM) was multiplied by the change in volume (V; liters) to calculate hourly DIC export (DIC_{export}; mmol hr^{-1}):

$$DIC_{export} = \left[\frac{DIC_{marsh, t(i)} + DIC_{marsh, t(i+1)}}{2} \right] \times \left(V_{t(i)} - V_{t(i+1)} \right). \qquad (5)$$

Marsh DIC fluxes were summed over the entire ebb tide and divided by the total marsh area (401 ha) to calculate the average flux per m^2 of marsh area per ebb tide. When extrapolated to seasonal time scales, calculated DIC export rates were similar in June (1.2 to 4.4 mol C m^{-2} month^{-1}) and August (1.1 to 3.1 mol C m^{-2} month^{-1}), and lower in November (0.6 to 1.5 mol C m^{-2} month^{-1}; Table 3). Similar seasonal trends were seen in marsh community respiration (marsh to atmosphere CO_2 + CH_4 gas fluxes; Neubauer et al. 2000) and are presumably related to seasonal temperature variability as well as the supply of organic matter. Marsh macrophyte vegetation begins to die in mid-summer as temperatures increase; this die-off continues rapidly through approximately October. To

138

Table 3: Calculation of DIC export from Sweet Hall marsh based on changes in DIC

enrichment and water volume during ebb tide. Export rates are summarized on monthly,

seasonal, and annual time scales.

DIC Export (mol C m^{-2} month^{-1})		
Date	Range[a]	Average
29 to 30 Jun 1999	1.2 to 4.4	2.7 ± 1.6
24 to 25 Aug 1999	1.1 to 3.1	2.0 ± 1.0
09 to 10 Nov 1999	0.6 to 1.5	1.0 ± 0.4

DIC Export (mol C m^{-2} season^{-1})		
Season	Range	Average
"growth" (Mar to Jul)	6.1 to 21.9	13.4 ± 7.6
"senescence" (Aug to Oct)	3.3 to 9.4	6.1 ± 3.1
"winter" (Nov to Feb)	2.4 to 5.8	4.0 ± 1.7
Annual (mol m^{-2} y^{-1})	11.8 to 37.1	23.5 ± 8.3

[a] To account for spatial variations in marsh elevation and temporal changes in tidal

range, the creek-full depth (D_{full}) was varied by ±10 cm. The range and average DIC

export rates (±SD; n = 3) are provided for model output over the range in D_{full}.

139

convert DIC export rates from discrete months to an annual rate, seasons were classified as periods of macrophyte "growth" (Mar to Jul), "senescence" (Aug to Oct) and "winter" (Nov to Feb; after Neubauer et al. 2000). When calculated for the entire year, marsh DIC export ranged from 11.8 to 37.1 mol C $m^{-2} y^{-1}$ ($\bar{x}$ = 23.5 ± 8.3 mol C $m^{-2} y^{-1}$; Table 3).

DIC Export Mechanisms: Although there are numerous DIC sources within the marsh, our calculations thus far have not distinguished DIC inputs when the marsh is flooded (e.g. upward diffusion of sediment porewater and the decomposition of plants and detritus) from processes occurring within the creek basin (e.g. porewater drainage, fluxes from subtidal sediments). At Sweet Hall, CO_2 fluxes from the marsh surface to overlying water (corrected for water column respiration) in September 1997 averaged 3.45 mmol C $m^{-2} h^{-1}$ (n = 4; water depth 22 to 39 cm; Neubauer et al. 2000). With 2 high tides per 25 hrs and assuming flooding of the marsh surface for 6 hr per high tide, we estimated a DIC flux of 1.2 mol C m^{-2} from the submerged marsh surface for the month of September. Compared to whole marsh DIC export in August ($\bar{x}$ = 2.0 mol C m^{-2}; Table 3), the flux from the flooded marsh represented an average of 58% (1.2 mol C m^{-2} / 2.0 mol C m^{-2}) of the total DIC export. The remaining 42% of the DIC exported from the marsh was added to the marsh creeks when the surface of the marsh was exposed to air. Thus, while the surface area of tidal creeks is only ~5% of the total area of Sweet Hall marsh, inputs of DIC to these creeks may be quantitatively important. Although Cai and Wang (1998) suggested the possibility of significant advective (drainage) DIC losses based on high porewater DIC concentrations, this route of carbon loss from intertidal marshes has been largely ignored. We suggest that previous estimates which have considered only

140

respiratory and diffusive DIC fluxes during periods of marsh submergence may have substantially underestimated the total marsh DIC export.

DIC Export and Estuarine Net Heterotrophy: In the York and Pamunkey Rivers (Virginia), Raymond et al. (in press) calculated that net heterotrophy (based on CO_2 evasion and DIC export rates) averaged ~8.3 mol C m^{-2} of river surface y^{-1}. While we agree with Raymond et al. that this system was net heterotrophic, our data suggest that the observed "net heterotrophy" resulted both from *in situ* respiration of labile DOC as well as DIC transported into the river from tidal marshes. Based on incubation experiments, Raymond (1999) calculated that bacterial respiration of DOC could account for $20 \pm 12\%$ of CO_2 evasion in the tidal freshwater Pamunkey River and suggested that the remaining 80% was due to respiration within river bottom sediments, remineralization of particulate organic carbon, or inputs of DIC from tidal marshes. To determine the contribution of tidal marshes to the excess DIC pool in the York and Pamunkey Rivers (i.e. Raymond et al's net heterotrophy), we scaled our estimates of DIC flux from Sweet Hall marsh to the total area of tidal marshes in the estuary. Our subsequent calculations and those of Raymond et al. included the Pamunkey River (which contributes ~70% of the flow to the York River) and the York River itself; the Mattaponi River was not included in DIC production or flux estimates.

Multiplying the rate of excess DIC production in the York River estuary (8.3 mol C m^{-2} y^{-1}; Raymond et al. in press) by the area of the tidal York and Pamunkey Rivers (1.8×10^8 m^2), we calculated that there must be an input of 1.5×10^9 mol C y^{-1} to the York River

141

to account for the excess DIC pool. As previously mentioned, some of this DIC may be produced by organic matter respiration in the river itself. From an annual DIC export of 11.8 to 37.1 mol C m^{-2} of marsh area y^{-1} (this study, Table 3) and a total tidal marsh area along the York and Pamunkey Rivers of 5419.9 ha (calculated from Silberhorn 1974; Moore 1976; Doumlele 1979; Moore 1980; Priest et al. 1987; Silberhorn and Zacherle 1987), the total export of DIC from tidal marshes could account for 1.3×10^9 ($\pm 0.4 \times 10^9$) mol C y^{-1}, or $85 \pm 30\%$ of the carbon required to support the annual excess DIC production reported by Raymond et al. (in press). Sources of the remaining fraction of carbon to support excess DIC production in the estuary could include water column or sediment metabolism of allochthonous DOC and POC and groundwater inputs to the river.

Our annual flux estimates were based on DIC measurements during three months (June, August, and November) while rates of estuarine heterotrophy (and excess DIC production) are driven by a suite of interacting biological, chemical, and physical factors and are therefore temporally and spatially variable. In the York River estuary, Raymond et al. (in press) measured the highest rates of excess DIC production in the low salinity regions of the estuary during the summer and autumn (June to October). Therefore, if tidal marshes are driving the production of excess DIC in the York River, there should be evidence of greater marsh DIC export during the summer versus the winter as well as a larger DIC input to the freshwater reaches of the estuary. Because DIC flux estimates (Table 3) and CO_2 gas flux measurements from the marsh surface (Neubauer et al. 2000) reproduce the seasonal patterns of excess DIC in the York River, there appears to be

142

temporal coupling between processes occurring within tidal marshes and estuarine DIC

dynamics. Also, the ratio of marsh to open water is greater in the Pamunkey River (1.34)

than the York River (0.22) which suggests that the relative influence of marshes as DIC

sources will be greater in the low salinity reaches of the system. This calculation exercise

confirms the suggestions of Cai and Wang (1998), Cai et al. (1999) and Raymond et al.

(in press) that tidal marshes are significant contributors of DIC to estuarine waters and

can explain a substantial portion of CO_2 supersaturation and excess DIC production

within these systems.

143

LITERATURE CITED

Brooks TJ 1983. *Pamunkey River slack water data report: Temperature, salinity, dissolved oxygen 1970-1980* Virginia Institute of Marine Science Data Report 20.

Cai W-J, Wang Y 1998. The chemistry, fluxes, and sources of carbon dioxide in the estuarine waters of the Satilla and Althamaha Rivers, Georgia. *Limnol. Oceanogr.* 43(4): 657-668.

Cai W-J, Pomeroy LR, Moran MA, Wang Y 1999. Oxygen and carbon dioxide mass balance for the estuarine-intertidal marsh complex of five rivers in the southeastern U.S. *Limnol. Oceanogr.* 44(3): 639-649.

Chanton JP, Whiting GJ, Showers WJ, Crill P M 1992. Methane flux from *Peltandra virginica*: stable isotope tracing and chamber effects. *Global Biogeochem Cycles* 6(1):15-31.

Chanton JP, Whiting GJ 1996. Methane stable isotopic distributions as indicators of gas transport mechanisms in emergent aquatic plants. *Aquatic Botany.* 54: 227-236.

Childers DL 1994. Fifteen years of marsh flumes: A review of marsh-water column interactions in southeastern USA estuaries. in Mitsch WJ (ed). *Global wetlands: Old World and New.* Elsevier: New York. pp. 277-293.

Coffin RB, Cifuentes LA, Elderidge PM 1994. The use of stable carbon isotopes to study microbial processes in estuaries. in Lajtha K, Michener RH (eds). *Stable isotopes in ecology and environmental science.* Blackwell: Oxford. pp. 222-240.

Dansgaard W 1964. Stable isotopes in precipitation. *Tellus.* 16: 436-468.

Dame RF 1994. The net flux of materials between marsh-estuarine systems and the sea: The Atlantic coast of the United States. in Mitsch WJ (ed). *Global wetlands: Old World and New.* Elsevier: New York. pp. 277-293.

Doumlele DG 1979. *New Kent County Tidal Marsh Inventory* Special Report No. 208 in Applied Marine Science and Ocean Engineering. Virginia Institute of Marine Science, Gloucester Point, Virginia.

Doumlele DG 1981. Primary production and seasonal aspects of emergent plants in a tidal freshwater marsh. *Estuaries* 4(2): 139-142.

144

Fairbanks RG 1982. The origin of continental shelf and slope water in the New York

    Bight and Gulf of Maine: Evidence from $H_2^{18}O/H_2^{16}O$ ratio measurements. *J.*

    Geophys. Res. 87(C8): 5796-5808.

Faure G 1986. Isotope systematics of two component mixtures. In Faure G (ed)

    Principles of Isotope Geology. John Wiley and Sons: New York. pp. 141-153.

Friedman I, O'Neil JR 1977. Compilation of stable isotopic fractionation factors of

    geochemical interest. In Fleischer M. (ed) *Data of Geochemistry,* 6th ed. chapter KK.

    United States Department of the Interior, Geological Survey Professional Paper 440-

    KK.

Frankignoulle M, Abril G, Borges A, Bourge I, Canon C, Delille B, Libert E, Theate J-M

    1998. Carbon dioxide emission from European estuaries. *Science.* 282: 434-436.

Gattuso J-P, Frankignoulle M, Wollast R 1998. Carbon and carbonate metabolism in

    coastal ecosystems. *Ann. Rev. Ecol. Syst.* 29: 405-434.

Grossman E, Coffman BK, Fritz SJ, Wada H 1989. Bacterial production of mathane and

    its influence on ground-water chemistry in east-central Texas aquifers. *Geology.* 17:

    495-499.

Hellings L, van den Driessche K, Baeyens W, Keppens E, DeHairs F 2000. Origin and

    fate of dissolved inorganic carbon in interstitial waters of two freshwater intertidal

    areas: A case study of the Scheldt Estuary, Belgium. *Biogeochem.* 51: 141-160.

Hendricks MB, DePaolo DJ, Cohen RC 2000. Space and time variation of $\delta^{18}O$ and δD in

    precipitation: Can paleotemperature be estimated from ice cores? *Global*

    Biogeochem. Cycles. 14(3): 851-861.

Hopkinson CS, Vallino JJ 1995. The relationships between man's activities in watersheds

    and estuaries: A model of runoff effects on patterns of estuarine community

    metabolism. *Estuaries.* 18: 598-621.

Keough JR, Hagley CA, Ruzycki E, Sierszen M 1998. $\delta^{13}C$ composition of primary

    producers and role of detritus in a freshwater coastal ecosystem. *Limnol. Oceanogr.*

    43(4): 734-740.

Lajtha K, Marshall JD 1994. Sources of variation in the stable isotopic composition of

    plants. in Lajtha K, Michener RH (eds). *Stable isotopes in ecology and*

    environmental science. Blackwell: Oxford. pp. 222-240.

Kemp WM, Smith E, Marvin-Dipasquale M, Boynton WR 1997. Organic carbon balance and net ecosystem metabolism in Chesapeake Bay. *Mar. Ecol. Prog. Ser.* 150: 229-248.

Mariotti A, Landreau A, Simon B 1988. ^{15}N isotope biogeochemistry and natural denitrification process in groundwater: Application to the chalk aquifer of northern France. *Geochim. Cosmochim. Acta.* 52: 1869-1878.

Millero FJ 1995. Thermodynamics of the carbon dioxide system in the oceans. *Geochim Cosmochim. Acta.* 59(4): 661-677.

Millero FJ, Sohn ML 1991. *Chemical Oceanography.* CRC Press: Boca Raton. 531 pg.

Moore KA 1976. *Gloucester County Tidal Marsh Inventory* Special Report No. 64 in Applied Marine Science and Ocean Engineering. Virginia Institute of Marine Science, Gloucester Point, Virginia.

Moore KA 1980. *James City County Tidal Marsh Inventory* Special Report No. 188 in Applied Marine Science and Ocean Engineering. Virginia Institute of Marine Science, Gloucester Point, Virginia.

Nascimento C, Atekwana EA, Krishnamurthy RV 1997. Concentrations and isotope ratios of dissolved inorganic carbon in denitrifying environments. *Geophys. Res. Lett.* 24(12): 1511-1514.

Neubauer SC, Miller WD, Anderson IC 2000. Carbon cycling in a tidal freshwater marsh ecosystem: A carbon gas flux study. *Mar. Ecol. Prog. Ser.* 199:13-30.

Nixon SW 1980. "Between Coastal Marshes and Coastal Waters - A Review of Twenty Years of Speculation and Research in the Role of Salt Marshes in Estuarine Productivity and Water Chemistry." in Hamilton P, McDonald KB (eds). *Estuarine and Wetland Processes with Emphasis on Modelling.* Plenum Press: New York. pp. 437-525.

Park PK 1969. Oceanic CO_2 system: An evaluation of ten methods of investigation. *Limnol. Oceanogr.* 14(2): 179-186.

Perry III JE 1991. *Analysis of vegetation patterns in a tidal freshwater marsh.* PhD dissertation, College of William and Mary, Virginia Institute of Marine Science, Gloucester Point.

Priest III WI. Silberhorn GM, Zacherle AW 1987. *King and Queen County Tidal Marsh Inventory* Special Report No. 291 in Applied Marine Science and Ocean Engineering. Virginia Institute of Marine Science, Gloucester Point, Virginia.

Raymond PA 1999. *Carbon cycling in the York River estuary: An isotopic and mass balance approach using natural ^{14}C and ^{13}C isotopes.* PhD dissertation, College of William and Mary, Virginia Institute of Marine Science, Gloucester Point.

Raymond PA, Bauer JE, Cole JJ in press. Atmospheric CO_2 evasion, dissolved inorganic carbon production, and net heterotrophy in the York River estuary. *Limnol. Oceanogr.*

Reay WG 1989. *A geohydrological approach to subsurface hydrodynamics and nutrient exchange within an extensive tidal freshwater wetland.* MS Thesis, College of William and Mary, Virginia Institute of Marine Science, Gloucester Point.

Silberhorn GM 1974. *York County and Town of Poquoson Tidal Marsh Inventory* Special Report No. 53 in Applied Marine Science and Ocean Engineering. Virginia Institute of Marine Science, Gloucester Point, Virginia.

Silberhorn GM, Zacherle AW 1987. *King William County and Town of West Point Tidal Marsh Inventory* Special Report No. 289 in Applied Marine Science and Ocean Engineering. Virginia Institute of Marine Science, Gloucester Point, Virginia.

Smith SV, Hollibaugh JT 1993. Coastal metabolism and the oceanic organic carbon balance. *Rev. Geophys.* 31: 75-89.

Smith SV, Hollibaugh JT 1997. Annual cycle and interannual variability of ecosystem metabolism in a temperate climate embayment. *Ecol. Monogr.* 67(4): 509-533.

Spiker EC, Schemel LE 1979. Distribution and stable isotope composition of carbon in San Francisco Bay. in *San Francisco Bay: the urbanized estuary.* Proceedings of the 58th Annual meeting of the Pacific Division/American Association for the Advancement of Science, San Francisco, June 12-16 1977, pp 195-212.

Terraserver 2000. Microsoft Terraserver digitized USGS topographic maps; New Kent VA quadrangle, 1:24,000 scale. (accessed 03 Jun 2000); available at http://terraserver.microsoft.com.

Torgersen T 1979. Isotopic composition of river runoff on the U.S. east coast: Evaluation of stable isotope versus salinity plots for coastal water mass identification. *J. Geophys Res.* 84(C7): 3773-3775.

USGS 2000. Water resources for the United States; discharge data for the Pamunkey River near Hanover VA; station no. 01673000. United States Geological Survey, Washington D.C. (accessed 14 Jun 2000); available at http://water.usgs.gov.

Weiss RF 1974. Carbon dioxide in water and seawater: The solubility of a non-ideal gas. *Mar. Chem.* 2: 203-215.

Appendix 1: Compilation of DIC concentration and isotope data by date, time, and location. Concentration and $\delta^{13}C_{DIC}$ and $\delta^{18}O_{DIC}$ were measured; $\delta^{18}O_{H_2O}$ was calculated using equations in Friedman and O'Neil 1977 ($\alpha = 1.044$ at 8.5°C). The $\delta^{18}O_{H_2O}$ values were used to evaluate the isotope data: for mid-Atlantic freshwaters, $\delta^{18}O_{H_2O}$ is typically -5 to -10‰ (Torgersen 1979; Fairbanks 1982). Therefore, isotope data associated with samples with $\delta^{18}O_{H_2O} < -10‰$ were not included in the main body of the dissertation; DIC concentration data were included for all samples. Porewater sample are designated as "pore a-b" where a is the distance from the creekbank (m) and b is the depth of the screened interval (cm).

Location	Date	(EST) Time	(mM) DIC	(‰) $\delta^{13}C_{DIC}$	(‰) $\delta^{18}O_{DIC}$	(‰) $\delta^{18}O_{H_2O}$	Isotopes included?	Comments
creek	06/29/99	11:30	0.50	-11.9	32.2	-11.5	N	low $\delta^{18}O$
creek	06/29/99	12:30	0.60	–	–	–	–	–
creek	06/29/99	13:30	0.64	–	–	–	–	–
creek	06/29/99	14:30	0.69	-12.6	35.7	-8.0	Y	normal
creek	06/29/99	15:30	0.85	–	–	–	–	–
creek	06/29/99	16:30	0.93	–	–	–	–	–
creek	06/29/99	17:30	1.12	-15.1	36.1	-7.5	Y	normal
creek	06/29/99	18:30	1.49	–	–	–	–	–
creek	06/29/99	19:30	2.15	–	–	–	–	–
creek	06/29/99	20:30	1.70	-13.8	37.6	-6.0	Y	normal
mouth	06/29/99	11:30	0.58	14.3	76.8	–	N	air in sample
mouth	06/29/99	12:30	0.67	–	–	–	–	–
mouth	06/29/99	13:30	0.68	–	–	–	–	–

mouth	06/29/99	14:30	0.65	-11.1	35.4	-8.2	Y	normal
mouth	06/29/99	15:30	–	–	–	–	–	no sample
mouth	06/29/99	16:30	0.80	–	–	–	–	–
mouth	06/29/99	17:30	0.76	-12.3	37.5	-6.2	Y	normal
mouth	06/29/99	18:30	1.36	–	–	–	–	–
mouth	06/29/99	19:30	0.74	-12.4	34.8	-8.9	Y	normal
mouth	06/29/99	20:30	0.53	-11.9	35.2	-8.5	Y	normal
pore 1-5	06/29/99	low tide	1.14	-17.7	38.5	-5.1	Y	normal
pore 1-15	06/29/99	low tide	3.11	-14.6	35.7	-7.9	Y	normal
pore 1-25	06/29/99	low tide	–	–	–	–	–	no sample
pore 15-5	06/29/99	low tide	2.70	–	–	–	–	sample too small
pore 15-15	06/29/99	low tide	4.66	-13.4	41.3	-2.3	Y	normal
pore 15-25	06/29/99	low tide	4.68	-11.9	34.0	-9.7	Y	normal
pore 30-5	06/29/99	low tide	3.22	–	–	–	–	sample too small
pore 30-15	06/29/99	low tide	3.99	-16.1	38.5	-5.2	Y	normal
pore 30-25	06/29/99	low tide	4.22	–	–	–	–	–
creek	08/24/99	10:45	1.15	-19.5	28.7	-15.0	N	low $\delta^{18}O$
creek	08/24/99	11:45	1.07	–	–	–	–	–
creek	08/24/99	12:45	1.11	–	–	–	–	–
creek	08/24/99	13:45	1.14	-14.7	33.9	-9.8	Y	normal
creek	08/24/99	14:45	1.20	–	–	–	–	–
creek	08/24/99	15:45	1.34	–	–	–	–	–
creek	08/24/99	16:45	1.44	-21.1	22.5	-21.1	N	low $\delta^{18}O$

								δ¹⁸O suspect
creek	08/24/99	17:45	1.52	—	—	—	—	—
creek	08/24/99	18:45	1.13	—	—	—	—	—
creek	08/24/99	19:45	0.99	-30.7	6.8	-36.9	N	δ¹⁸O suspect
creek	08/24/99	20:45	1.02	—	—	—	—	—
creek	08/24/99	21:45	1.22	—	—	—	—	—
creek	08/24/99	22:45	1.17	-13.7	33.7	-10.0	Y	normal
creek	08/24/99	23:45	1.23	—	—	—	—	—
creek	08/25/99	00:45	1.23	—	—	—	—	—
creek	08/25/99	01:45	1.36	-16.7	32.8	-10.9	N	low δ¹⁸O
creek	08/25/99	02:45	1.46	—	—	—	—	—
creek	08/25/99	03:45	1.52	—	—	—	—	—
creek	08/25/99	04:45	1.62	-24.7	20.5	-23.2	N	low δ¹⁸O
creek	08/25/99	05:45	1.67	—	—	—	—	—
creek	08/25/99	06:45	1.79	-20.6	27.5	-16.2	N	low δ¹⁸O
creek	08/25/99	07:45	1.42	-17.2	32.3	-11.4	N	low δ¹⁸O
creek	08/25/99	08:45	1.02	-14.5	34.4	-9.3	Y	normal
creek	08/25/99	09:45	0.98	—	—	—	—	—
mouth	08/24/99	10:45	1.12	—	—	—	N	too small
mouth	08/24/99	11:45	1.12	—	—	—	—	—
mouth	08/24/99	12:45	1.10	—	—	—	—	—
mouth	08/24/99	13:45	1.15	-14.2	35.1	-8.6	Y	normal
mouth	08/24/99	14:45	1.17	—	—	—	—	—
mouth	08/24/99	15:45	1.22	—	—	—	—	—

mouth	08/24/99	16:45	1.08	-18.0	27.7	-15.9	N	low δ¹⁸O
mouth	08/24/99	17:45	1.06	–	–	–	–	–
mouth	08/24/99	18:45	0.98	–	–	–	–	–
mouth	08/24/99	19:45	0.98	-14.4	34.7	-8.9	Y	normal
mouth	08/24/99	20:45	1.08	–	–	–	–	–
mouth	08/24/99	21:45	1.16	–	–	–	–	–
mouth	08/24/99	22:45	1.17	–	–	–	–	too small
mouth	08/24/99	23:45	1.24	–	–	–	–	–
mouth	08/25/99	00:45	1.20	–	–	–	–	–
mouth	08/25/99	01:45	1.32	-15.4	34.1	-9.5	Y	normal
mouth	08/25/99	02:45	1.37	–	–	–	–	–
mouth	08/25/99	03:45	1.45	–	–	–	–	–
mouth	08/25/99	04:45	1.54	-18.4	31.3	-12.3	N	low δ¹⁸O
mouth	08/25/99	05:45	1.17	–	–	–	–	–
mouth	08/25/99	06:45	1.09	–	–	–	–	–
mouth	08/25/99	07:45	1.01	-14.9	31.9	-11.8	N	low δ¹⁸O
mouth	08/25/99	08:45	1.04	–	–	–	–	–
mouth	08/25/99	09:45	1.10	–	–	–	–	–
pore 1-5	08/24/99	low tide	2.43	-15.3	36.8	-6.8	Y	normal
pore 1-15	08/24/99	low tide	4.86	–	–	–	–	–
pore 1-25	08/24/99	low tide	2.15	-11.2	36.8	-6.8	Y	normal
pore 15-5	08/24/99	low tide	5.56	-13.6	30.9	-12.8	N	low δ¹⁸O
pore 15-15	08/24/99	low tide	6.73	-12.7	38.4	-5.3	N	air in sample
pore 15-25	08/24/99	low tide	6.60	-7.4	36.9	-6.7	Y	normal

pore 30-5	08/24/99	low tide	4.69	-15.7	38.5	-5.2	Y	normal
pore 30-15	08/24/99	low tide	3.52	-12.4	36.9	-6.8	Y	normal
pore 30-25	08/24/99	low tide	2.75	-8.3	36.7	-6.9	Y	normal
creek	11/09/99	11:15	0.48	-13.5	35.0	-8.6	Y	normal
creek	11/09/99	12:15	0.48	-	-	-	-	-
creek	11/09/99	13:15	0.51	-	-	-	-	-
creek	11/09/99	14:15	0.49	-13.5	35.1	-8.6	Y	normal
creek	11/09/99	15:15	0.47	-	-	-	-	-
creek	11/09/99	16:15	0.51	-	-	-	-	-
creek	11/09/99	17:15	0.60	-12.4	34.7	-8.9	Y	normal
creek	11/09/99	18:15	0.71	-	-	-	-	-
creek	11/09/99	19:15	0.95	-	-	-	-	-
creek	11/09/99	20:15	1.09	-11.9	35.0	-8.6	Y	normal
creek	11/09/99	21:15	1.04	-	-	-	-	-
creek	11/09/99	22:15	-	-	-	-	-	no sample
creek	11/09/99	23:15	0.51	-13.7	34.5	-9.1	Y	normal
creek	11/10/99	00:15	0.50	-	-	-	-	-
creek	11/10/99	01:15	0.53	-	-	-	-	-
creek	11/10/99	02:15	0.57	-14.2	35.4	-8.3	Y	normal
creek	11/10/99	03:15	0.66	-	-	-	-	-
creek	11/10/99	04:15	0.74	-	-	-	-	-
creek	11/10/99	05:15	0.94	-13.8	36.8	-6.8	Y	normal
creek	11/10/99	06:15	1.34	-	-	-	-	-

creek	11/10/99	07:15	1.35	–	–	–	–	–
creek	11/10/99	08:15	2.40	-12.0	36.4	-7.2	Y	normal
creek	11/10/99	09:15	1.59	–	–	–	–	–
creek	11/10/99	10:15	1.35	–	–	–	–	–
mouth	11/09/99	11:15	0.53	-15.9	34.1	-9.5	Y	normal
mouth	11/09/99	12:15	0.58	–	–	–	–	–
mouth	11/09/99	13:15	0.58	–	–	–	–	–
mouth	11/09/99	14:15	0.54	-13.4	36.0	-7.6	Y	normal
mouth	11/09/99	15:15	0.53	-12.6	36.1	-7.6	Y	normal
mouth	11/09/99	16:15	0.55	–	–	–	–	–
mouth	11/09/99	17:15	0.59	-16.7	26.1	-17.5	N	very small size
mouth	11/09/99	18:15	0.70	–	–	–	–	–
mouth	11/09/99	19:15	0.96	–	–	–	–	–
mouth	11/09/99	20:15	0.67	-14.1	34.2	-9.5	N	air in sample
mouth	11/09/99	21:15	0.56	–	–	–	–	–
mouth	11/09/99	22:15	–	–	–	–	–	no sample
mouth	11/09/99	23:15	0.53	-13.8	32.7	-10.9	N	low $\delta^{18}O$
mouth	11/10/99	00:15	0.59	–	–	–	–	–
mouth	11/10/99	01:15	0.58	–	–	–	–	–
mouth	11/10/99	02:15	0.60	-13.0	37.0	-6.6	Y	normal
mouth	11/10/99	03:15	0.71	–	–	–	–	–
mouth	11/10/99	04:15	0.78	–	–	–	–	–
mouth	11/10/99	05:15	0.94	-13.2	36.1	-7.5	Y	normal
mouth	11/10/99	06:15	1.19	–	–	–	–	–

	Date	Time/Tide						
mouth	11/10/99	07:15	1.49	–	–	–	–	–
mouth	11/10/99	08:15	0.63	-13.9	35.3	-8.4	Y	normal
mouth	11/10/99	09:15	0.55	–	–	–	–	–
mouth	11/10/99	10:15	0.58	–	–	–	–	–
pore 1-5	11/09/99	low tide	2.10	-22.1	27.1	-16.5	N	low $\delta^{18}O$
pore 1-15	11/09/99	low tide	3.66	-17.9	36.8	-6.8	Y	normal
pore 1-25	11/09/99	low tide	–	–	–	–	–	no sample
pore 15-5	11/09/99	low tide	3.65	-6.9	37.0	-6.7	Y	normal
pore 15-15	11/09/99	low tide	5.45	-8.2	34.7	-9.0	N	air in sample
pore 15-25	11/09/99	low tide	4.58	-6.4	37.4	-6.2	Y	normal
pore 30-5	11/09/99	low tide	2.47	-14.2	36.1	-7.6	Y	normal
pore 30-15	11/09/99	low tide	3.68	-15.8	32.4	-11.3	N	air in sample
pore 30-25	11/09/99	low tide	3.09	-10.1	38.3	-5.4	Y	normal

SECTION IV

Carbon and Nitrogen Sources in a Tidal Freshwater Marsh Creek: A Stable Isotope Mass

Balance Approach[†]

ABSTRACT

Measurements of the concentration and isotopic composition (^{13}C and ^{15}N) of

dissolved and particulate matter were used to determine carbon and nitrogen sources

within a tidal freshwater marsh creek. Over diurnal cycles in early and late summer (June

and August) and at the end of the growing season (November), water samples were

collected from a marsh tidal creek and at the mouth of the creek. Concurrently, shallow

marsh porewater was collected at low tide. Seasonally, marsh macrophytes and benthic

microalgae were collected as potential sources of marsh-derived organic matter. Over

tidal cycles. there was no evidence of a net flux of dissolved or particulate organic carbon

(DOC, POC) or total dissolved or particulate nitrogen (TDN, PN) between the marsh,

tidal creek and adjacent river. The ^{15}N data for dissolved and particulate matter were

equivocal due to small sample masses. Preliminary interpretation of the limited data set

indicate possible seasonal shifts in the $\delta^{15}N_{PN}$ signatures due to water column diagenesis.

An isotopic mass balance model combined with water column chlorophyll and POC data

suggested that the relative contribution of phytoplankton to the suspended POC pool

varied from 40 to 60% during summer (June and August) to <25% in November.

Similarly, the contribution of DOC exudates from creek phytoplankton to the water

column decreased over the same time period. In all months, the ^{13}C isotopic composition

of water column POC and DOC were reasonably well predicted by a mixture of

phytoplankton and marsh autotrophs; macrophytes and microalgae were indistinguishable

based on δ^{13}C signatures. Inputs of terrestrial POC and DOC were presumed to be

insignificant as the summer of this study was characterized by record low river discharge

157

rates: the importance of local (marsh, creek and riverine) versus watershed carbon

sources may be different during periods of higher flow.

-

158

INTRODUCTION

The naturally occurring stable isotopes of carbon and nitrogen (^{13}C and ^{15}N) have been used to trace organic matter flow within ecosystems (e.g. Haines 1976; Peterson and Howarth 1987; Sullivan and Moncreiff 1990; Deegan and Garritt 1997), to assess physical mixing between isotopically distinct end-members (e.g. Sweeney and Kaplan 1980; Macko 1983; Mariotti et al. 1984), and to determine rates and pathways of biogeochemical cycling (e.g. Mariotti et al. 1984; Cifuentes et al. 1988; 1989). In order to interpret stable isotope data, knowledge of the processes that can change isotope ratios is required. Physical mixing processes are conservative with respect to isotope ratios. Understanding the biogeochemical cycling of carbon and nitrogen isotopes is more difficult as there are fractionations associated with biosynthesis (e.g. photosynthesis, nutrient assimilation), catabolism (e.g. respiration, decomposition, remineralization), and oxidation-reduction reactions (e.g. nitrification, denitrification). For example, the fractionation of ^{13}C associated with photosynthesis depends on the photosynthetic mechanism (i.e. C_3 versus C_4 metabolism), the concentration and species of assimilated inorganic carbon (CO_2 versus HCO_3^-), temperature, water use efficiency, and nutrient supply (Fogel and Cifuentes 1993; Lajtha and Marshall 1994). Similarly, the fractionation of ^{15}N during nitrogen assimilation is affected by the concentration and species of inorganic nitrogen (NH_4^+ versus NO_3^-) and the uptake transport mechanism (i.e. active versus passive transport; summarized in Fogel and Cifuentes 1993). In general, biosynthetic, catabolic, and oxidation-reduction reactions result in the

159

preferential utilization of the lighter isotope (^{12}C or ^{14}N); thus while the product becomes lighter (^{13}C or ^{15}N depleted), the residual substrate becomes heavier (^{13}C or ^{15}N enriched).

Tidal marshes are sites of high rates of primary production (Whigham et al. 1978; Schubauer and Hopkinson 1984), organic matter decomposition (Odum and Heywood 1978; Benner et al. 1991; Neubauer et al. 2000) and active nitrogen cycling (Bowden 1984; Morris and Bowden 1986; Anderson et al. 1997; Hughes et al. 2000; Tobias et al. in press). In tidal salt marshes, there is a long history of stable isotope analysis (at natural abundance levels) to infer trophic relationships between marsh primary producers and consumers in the adjacent estuary (e.g. Haines 1976; Peterson and Howarth 1987; Sullivan and Moncreiff 1990), describe decomposition dynamics (e.g. Benner et al. 1987; Fogel et al. 1989; Currin et al. 1995), and trace nitrogen cycling in marsh sediments (e.g. Velinsky et al. 1991; Tobias et al. in press). In freshwater riverine systems, stable isotopes have been used to determine nutrient sources and food web dynamics in freshwater systems (Kline et al. 1990; Bilby et al. 1996; Deegan and Garritt 1997; Garman and Macko 1998; MacAvoy et al. 1998; 2000) and understand the cycling of dissolved organic and inorganic carbon (Peterson et al. 1994; Raymond 1999; Neubauer dissertation section III).

In this study, the stable isotope ratios ($\delta^{13}C$ and $\delta^{15}N$) of dissolved and suspended particulate matter were used to determine dominant carbon and nitrogen sources to a creek in a tidal freshwater marsh and determine if the marsh was a source of these materials to the adjacent river. Samples were collected from a tidal freshwater marsh

creek and at the mouth of the creek over diurnal cycles in the early and late summer (June and August) and at the end of the growing season (November). Seasonally, samples were collected from shallow marsh porewater at low tide. The ^{13}C and ^{15}N signatures of marsh primary producers (macrophytes and benthic microalgae) were measured as possible organic matter sources from the marsh itself. The stable isotope data were combined with bulk characterization of the particulate and dissolved pools (e.g. concentrations of chlorophyll a, particulate and dissolved organic carbon) and isotopic mixing models to determine the relative importance of phytoplankton versus other organic matter sources (e.g. marsh macrophytes and microalgae) within the marsh tidal creek system.

MATERIALS AND METHODS

Study Site: Sweet Hall marsh is a 401 ha tidal freshwater marsh located on the Pamunkey River, approximately 69 km (by river) from the mouth of the York River, Virginia (Fig. 1). Sweet Hall marsh is a site within the Chesapeake Bay National Estuarine Research Reserve system in Virginia (CB-NERRVA). The Pamunkey River watershed is predominately undeveloped (65% forested, 6% tidal + non-tidal wetlands), with 27% as grass and croplands and <2% urbanized (EPA 1996). At Sweet Hall, the Pamunkey River is microtidal, with a mean tidal range of 70 cm (neap tide) to 90 cm (spring tide). For this study, all sampling was conducted along the western branch of Hill's Ditch, a small tidal creek draining the southern end of the marsh (Fig. 1). The study site was dominated by the broadleaf macrophytes *Peltandra virginica* and

161
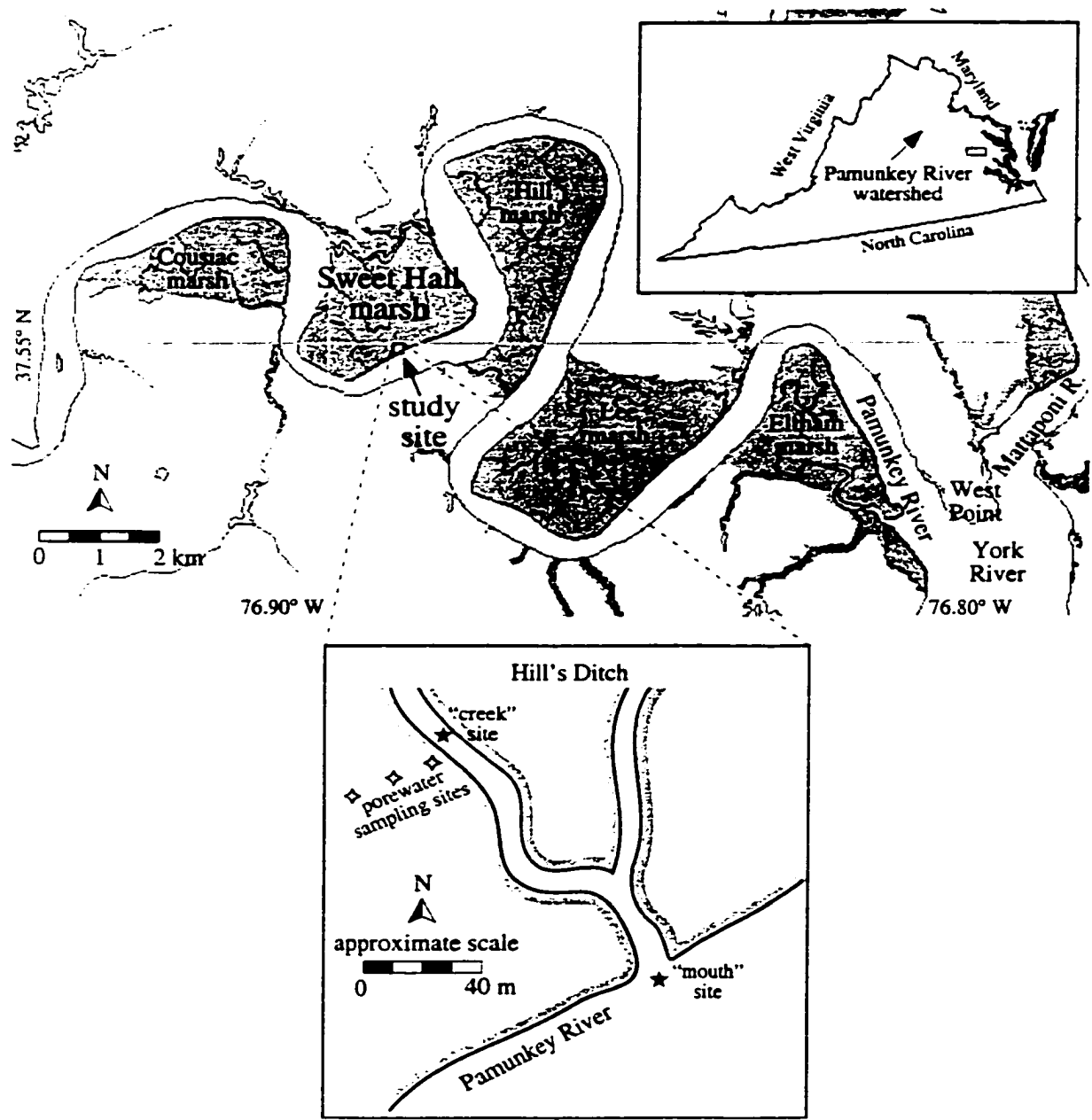
Figure 1: Map of lower Pamunkey River, Virginia showing location of Sweet Hall and other tidal marshes (shaded areas). Tidal marsh areas were redrawn from Doumlele (1979) and Silberhorn and Zacherle (1987). Inset shows location of Pamunkey watershed in Virginia while blow up shows sampling location within marsh. On blow up of study site, the creek width is exaggerated for clarity (actual creek width ~4 to 5 m).

162

Pontederia cordata through most of the summer while the grass *Zizania aquatica* was abundant late in the growing season.

Historical records indicate that the long-term average salinity at Sweet Hall was 0.5 ppt (Brooks 1983). However, during 1999, salinity ranged from 0.0 to 15.9 ppt (average 2.8 ppt; CB-NERRVA unpublished data) with the highest salinities in late August and early September following a dry summer. Pamunkey River discharge for all of 1999 (except in September) was lower than the 1970 to 1999 average, while rates from May to August were the lowest recorded during this 30 year period (Fig. 2; USGS 2000). In addition to affecting salinity, low discharge rates are likely to reduce the runoff of materials from the surrounding uplands and increase water residence time within the estuary which can have implications for organic matter cycling and retention within the system.

Diurnal Tidal Sampling: Studies examining tidal exchanges of dissolved organic carbon (DOC), total dissolved nitrogen (TDN), particulate organic matter (POM), and chlorophyll (chl *a*) between the marsh, creek, and river were conducted in June, August, and November 1999. All sampling dates were within 2 days of spring tide. Water samples were collected from a small tidal creek (Hill's Ditch) draining Sweet Hall marsh (hereafter referred to as the "creek" site), and at the junction of this creek with the Pamunkey River ("mouth" site; Fig. 1). Fifty ml water samples were collected at 2 h intervals for DOC and TDN analyses using polypropylene syringes and immediately filtered as described below. Simultaneously, automated water samplers (ISCO model

163
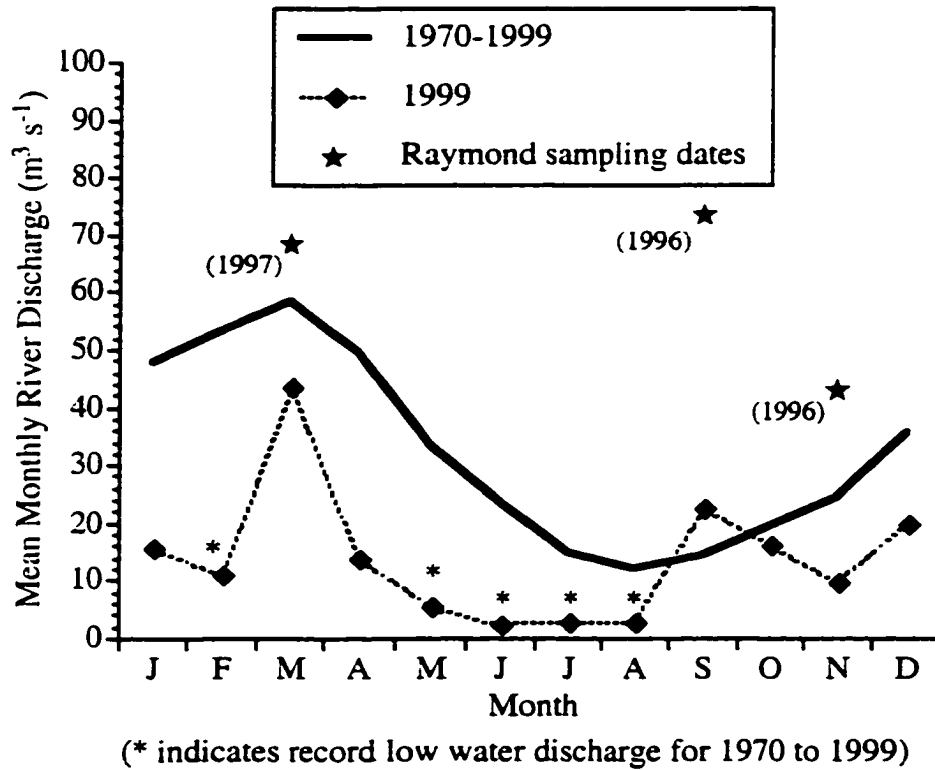
Figure 2: Water discharge rates for the Pamunkey River at Hanover, Virginia. During
1999 (this study) discharge rates were below the 1970 to 1999 average and were
frequently the lowest recorded monthly discharges during this 30 year period (indicated
by *). In contrast, Raymond (1999) studied Pamunkey River DOC dynamics during a
higher than average flow period.

6700, Lincoln, NE) collected samples for particulate matter and chl *a* analyses from both sites while a YSI 6000 datasonde (YSI, Inc., Yellow Springs, Ohio) recorded water depth, salinity, turbidity, pH, temperature, and dissolved oxygen at 15 minute intervals. At the creek site, the water intakes and YSI datasonde were located 10-15 cm above the creek bed, whereas the intakes at the creek mouth site were suspended from a floating platform and sampled 20 to 30 cm below the water surface (~5 to 70 cm above the sediment surface, depending on tidal stage).

Marsh porewater was sampled on the same dates using porewater samplers ("sippers") that had been installed in the marsh in February 1999. Clusters of three sippers were located at 1, 15, and 30 m along a transect extending from creekbank (0 m) toward the marsh interior (30 m; Fig. 1). Each sipper had a 5 cm sampling "window" of porous sintered plastic centered around a depth of 5, 15, or 25 cm. Prior to sampling, sippers were purged of water and filled with argon gas to maintain anaerobic conditions. Each sipper was then evacuated to a vacuum of 50 to 60 cm Hg and allowed to refill for 4 to 5 hours before sampling. Water was collected from sippers within 1 hour of low tide on each sampling date using polypropylene syringes and filtered prior to analyses as described below. In spite of the relatively high vacuum and long recharge times, there were occasions when there was not enough water for all analyses.

The DOC and TDN samples were filtered (0.45 μM Gelman Supor Acrodiscs) into duplicate 20 ml precombusted (5 hr @ 500°C) glass scintillation vials and stored frozen until analysis. One of each pair of vials was thawed and analyzed for DOC and dissolved

165

inorganic nitrogen (DIN; NH_4^+, NO_3^-, NO_2^-) concentrations. A Shimadzu 5000A TOC analyzer, calibrated with a range of 5 to 10 glucose standards, was used to measure DOC concentrations. The median precision for 3 replicate injections of each standard was ± 7.0 μM. Nutrients were measured spectrophotometrically (for NH_4^+) following the phenolhypochlorite method of Solorzano (1969) or on an Alpkem nutrient autoanalyzer (for NO_3^- and NO_2^-). The contents of the second scintillation vial were freeze-dried, the residue weighed into precombusted (5 hr @ 500°C) silver cups, acidified with 30% HCl to remove carbonates, and analyzed for $\delta^{13}C_{DOC}$, $\delta^{15}N_{TDN}$, and percents DOC and TDN on a Fison elemental analyzer coupled to an Optima mass spectrometer (Micromass Inc., Manchester, UK). Although freeze drying has been previously utilized to concentrate dissolved materials for isotopic analyses (e.g. Peterson et al. 1994; Guo and Santischi 1997), tests are ongoing to confirm that there was no isotopic fractionation associated with the sample processing. The DOC concentration was divided by the DOC/TDN ratio to calculate the TDN concentration of each sample. Dissolved organic nitrogen (DON) concentrations were calculated as the difference between TDN and DIN.

Water samples (100 to 200 ml) collected with the ISCO automated samplers were filtered through precombusted and preweighed 47 mm GF/F filters for total suspended solid (TSS) analysis. Filters were dried at 50°C for greater than 1 week and reweighed. Subsamples were analyzed for $\delta^{13}C$, $\delta^{15}N$, percents particulate organic carbon (POC) and particulate nitrogen (PN) on a Fison elemental analyzer coupled to an Optima mass spectrometer following acidification with 30% HCl to remove carbonates. For water column chl a, 5 ml samples were filtered through 25 mm GF/F filters and extracted in the

166

dark for 24 hours in a mixture of acetone, DMSO, deionized water, and diethylamine (45:45:10:0.1; Shoaf and Lium 1976). Chlorophyll a concentrations were measured before and after acidification with 1 N HCl using a Turner Designs Model 10-AU flourometer (Sunnyvale, CA).

A detailed examination of the ^{13}C and ^{15}N data revealed that, for many of the dissolved and suspended particulate samples, the masses of carbon and nitrogen analyzed in the mass spectrometer were near the detection limits of the instrument (~10 μg C and 5 μg N). Therefore, the isotopic data for these small samples (those with < 10 μg C or 5 μg N) were considered suspect and not included in this section of the dissertation. Furthermore, all δ^{13}C values for particulate samples from November 1999 were discarded due to the probability of contamination because several samples had δ^{13}C signatures of -60 to -40‰. A compilation of all isotopic data collected during the diurnal samplings is provided in appendices 1 and 2 (for particulate and dissolved samples, respectively). For samples where the sample size for duplicates was greater than 10 μg C, the average reproducibility of δ^{13}C values for dissolved and particulate water column samples was ±1.1‰ (± 1 standard deviation; n = 15 pairs of duplicate samples). When the mass of nitrogen was greater than 5 μg, isotopic precision for δ^{15}N was ±0.5‰ (± 1 standard deviation; n = 2 pairs of duplicates).

Isotopic Characterization of Marsh Primary Producers: Macrophyte samples were collected as described in Neubauer et al. (2000). Briefly, samples were collected in a stratified random design along a 30 m transect extending roughly perpendicular to the

167

tidal creek. In June, September and November 1996, all vegetation rooted within a 0.11 m^2 ring was clipped. In July 1999, the dominant species at each randomly selected location were sampled. Samples were sorted by species into living (50-100% green), dying (0-50% green) and dead fractions. All plants were washed with deionized water to remove sediments and dried at 50°C for 3 to 4 weeks. For each analysis, approximately 20 to 40 live plants (or 5 to 10 dead plants) were ground in a Wiley Mill (#40 screen), a subsample weighed into ashed (5 hr @ 500°C) silver cups, and analyzed for $\delta^{13}C$ and $\delta^{15}N$ on a Fison elemental analyzer coupled to an Optima mass spectrometer. The isotopic reproducibility for macrophyte samples averaged ±0.3‰ (±1 standard deviation) for both $\delta^{13}C$ and $\delta^{15}N$.

Benthic microalgae were collected in February, March and July 1999 as described by Currin et al. (1995) with the following modifications. In the field, surface sediments (0 to ~2 cm) were placed into metal trays (~750 cm^2) for transport to the lab. Two to 4 trays were collected during each sampling period. In the lab, the sediments were covered with two alternating layers of acid-washed and combusted beach sand (~1 to 2 mm thick), and 63 μm nitex mesh. After misting with 0.7 μm filtered creek water, the trays were placed in a lighted (400 μE m^{-2} s^{-1}) temperature controlled environmental chamber. After 24 hr, the nitex sheets were removed and algae adhering to the sheets were scraped or rinsed with filtered creek water into a beaker. The beaker was swirled to separate sand particles from algae. To further purify the microalgae samples, the algae in the beaker were pipetted into a centrifuge tube and centrifuged at 2000 rpm for 3 min. The water in the tube was carefully decanted and filtered through a precombusted 25 mm GF/F filter. The

168

filter was examined under a dissecting microscope and forceps were used to remove any contaminating sand, detrital particles or small invertebrates (primarily worms) remaining on the filter. Filters were dried at 50°C and processed for ^{13}C and ^{15}N. Additionally, in May 1999, filamentous blue-green algae were directly removed from an algal mat with forceps, rinsed of associated sediments and dried for isotopic analysis.

Statistical Analysis: The non-parametric Kruskal-Wallis ANOVA was used to test for seasonal and site-specific (creek vs. mouth. vs. porewater) differences. When the ANOVA was significant at $\alpha = 0.05$, a non-parametric multiple comparison was used to test for specific differences between seasons or sites (Zar, 1996).

RESULTS AND DISCUSSION

Water Column Description: The tidal range during the sampling dates varied between 0.55 and 0.83 m (see Fig. 2 in section III of this dissertation). Water temperatures ranged from a mean of 25.8°C (June) to 27.8°C (August) to 14.5°C (November). The temperature difference between creek and mouth sites was generally < 1°C. Short-term temporal patterns in temperature were driven by the day-night cycle rather than by tidal effects. Due to seasonal patterns in rainfall and runoff (e.g. Fig. 2), there was a wide variation in mean salinity between sampling dates (June: $\bar{x}$ = 2.9 ppt; Aug $\bar{x}$ =7.2 ppt; Nov $\bar{x}$ = 0.6 ppt). Over the tidal cycle, salinity varied by 2 to 3 ppt in both June and August, with <1 ppt variation in November. The pH range (~6.3 to 7.8) was similar during all months with lower values measured near low tide. Measured dissolved oxygen

169

concentrations were generally lower than saturation values and were < 2 mg l^{-1} for several hours during each 24 h period in both June and August.

Marsh Macrophyte and Microalgal Characterization: The $\delta^{13}C$ values of live macrophyte biomass were typical of C_3 plants (-28.9 to -23.3‰) with the exception of *Echinochloa walteri* which had a ^{13}C value of −14.7 (Table 1). Another species in this genus (*E. crus-galli*) has previously been identified as a C_4 plant on the basis of ^{13}C analysis (Bender 1971). Although *E. walteri* was locally abundant at a creekbank sampling site in September 1996, it was not a dominant member of the marsh flora and has been only sporadically observed at our study site since 1996. Other C_4 plants, notably *Spartina cynosuroides*, have been observed elsewhere at Sweet Hall marsh (Doumlele 1981; Perry 1991) but were virtually absent from our study site. Live *Pontederia cordata* was approximately 1‰ enriched in ^{13}C versus dying *P. cordata* (Sep 1996; Table 1). Similarly, Haines (1976) and Currin et al. (1995) observed little change in $\delta^{13}C$ between live and standing dead *Spartina alterniflora*. In contrast, live *Zizania aquatica* tissues in Nov 1996 ($\delta^{13}C$ = -27.6‰) were nearly 10‰ depleted in ^{13}C versus standing dead *Z. aquatica* ($\delta^{13}C$ = -17.7‰). This may represent the selective preservation of isotopically enriched structural polymers (e.g. cellulose and hemicellulose; Benner et al. 1987) during decomposition. Alternately, the dead *Z. aquatica* sample may actually have been a mixture of the morphologically similar species *Z. aquatica* and *S. cynosuroides*, causing an isotopic shift toward heavier ^{13}C values typical of C_4 plants.

170

Table 1: Isotopic characterization of marsh primary producers. Unless otherwise noted, analyses are for all aboveground biomass (leaves, petioles, and stems).

Species	Date	n	^{13}C (‰)	^{15}N (‰)
Peltandra virginica (live)	Jun 1996	2[a]	-26.3 (±0.8)	7.1 (±3.0)
	Jul 1999	3	-24.4 (±2.0)	6.1 (±1.9)
	Sep 1996	3	-24.3 (±0.1)	5.3 (±1.1)
Pontederia cordata (live)	Jun 1996	3	-25.8 (±0.5)	5.8 (±0.2)
	Jul 1999	3	-25.1 (±3.9)	7.4 (±3.1)
	Sep 1996	2	-23.3 (± 0.1)	5.7 (±0.8)
Pontederia cordata (dying)	Sep 1996	1	-24.2	6.7
Peltandra/Pontederia petioles[b]	Sep 1996	1	-25.4	5.6
	Nov 1996	4	-26.3 (±1.2)	7.2 (±2.0)
Zizania aquatica (live)	Jun 1996	2	-27.9 (±0.1)	8.3 (±0.0)
	Jul 1999	4	-28.9 (±4.0)	7.8 (±1.3)
	Sep 1996	1	-28.6	6.9
	Nov 1999	2	-27.6 (±0.1)	5.6 (±5.1)
Zizania aquatica (dead)	Nov 1999	2	-17.7 (±0.7)	7.9 (±0.4)
Echinochloa walteri (live)	Sep 1996	1	-14.7	8.7
Hibiscus moscheutos (live)	Jun 1996	1	-28.2	10.6
Hibiscus (live; leaves only)	Jul 1999	1	-37.3	11.0
benthic (sediment) microalgae	Feb 1999	4	-23.7 (±0.5)	8.7 (±2.3)
	Mar 1999	4	-25.1 (±0.3)	11.3 (±2.2)
	May 1999	2	-25.2 (±2.5)	8.4 (±1.3)
	Jul 1999	4	-27.7 (±0.1)	11.1 (±10.3)

[a] Each macrophyte replicate represents a pooled sample of approximately 20 to 40 live plants (or 5 to 10 dead stems) collected from the same 0.11 m^2 sampling area. For benthic microalgae, each replicate represents the algae collected from one "pan" of marsh sediment. Values are means ± 1 standard deviation.

[b] By late summer, most of the leaves of *Peltandra* and *Pontederia* have senesced and it is impossible to distinguish between the species on the basis of their petiole morphology.

171

The ^{15}N values for marsh plants ranged from 5.3 to 11.0‰ (Table 1). With the exception of *Hibiscus moscheutos*, which had the two heaviest ^{15}N values, there were no apparent species-specific patterns in δ^{15}N. Perhaps due to processes related to the availability and fractionation of DIN, ^{15}N values for the same species within a month were often highly variable (e.g. spatial variability in δ^{15}N along a marsh transect for *Peltandra virginica* in July 1999 was ±1.9‰). For live *P. virginica* and *Zizania aquatica*, there was a trend of lighter ^{15}N values from June through November. This may be related to the uptake of more isotopically depleted NH_4^+ from increased rates of mineralization during the late growing season. Because the isotopic enrichment factor[1] (ϵ) for remineralization is -3 to -5‰ (Benner et al. 1991; Velinsky et al. 1991; Tobias 1999), the mineralization of organic N will result in the production of isotopically depleted NH_4^+. For mixed *P. virginica* and *Pontederia cordata* petioles (i.e. leaves have already senesced but petioles are still green), the opposite trend was observed; δ^{15}N was heavier in November versus September. Similarly, ^{15}N values for dying *P. cordata* and dead *Z. aquatica* were slightly heavier (by 1 to 2‰) than live biomass collected during the same month although this difference was similar to the spatial variability in δ^{15}N. Alternately, the differences between live and dead biomass may represent the removal of isotopically light N from the plants during senescence, leaching and decomposition, causing the residual plant matter to become heavier. In contrast, Currin et al. (1995)

---

[1] The enrichment factor, ϵ, is defined as $\epsilon = (\alpha - 1) \times 10^3$, where α is the fractionation factor. If the substrate concentration is large enough that it is not significantly depleted by the reaction, α is defined as R_p/R_s where R is the isotope ratio (i.e. ^{15}N/^{14}N) of the product or substrate. Therefore, an enrichment factor $\epsilon < 0$ (or a fractionation factor $\alpha < 1$) indicates that the product is depleted in the heavy isotope.

172

observed a ^{15}N depletion from live to standing dead *Spartina alterniflora* in North

Carolina and hypothesized that epiphytic N_2 fixation or microbial colonization of the

stems followed by preferential microbial uptake of $^{14}NH_4^+$ led to lighter ^{15}N values in

dead *S. alterniflora* biomass.

Sediment microalgal ^{13}C and ^{15}N values were not substantially different from those of

marsh macrophytes (Table 1) and varied from –27.7 to -23.7‰ for δ^{13}C and 8.4 to 11.3‰

for δ^{15}N. The ^{13}C values presented here are approximately 10‰ more depleted than the

mean value for benthic microalgae from estuarine environments (–14.9 ± 3.1‰; Currin et

al. 1995). This large difference may be due to variations in DIC species availability (i.e.

CO_2 vs. HCO_3^-), utilization of ^{13}C-depleted DIC produced by respiration, DIC limitation

due to high rates of photosynthesis in other systems, or site-specific differences in species

composition (Fogel and Cifuentes 1993; Goericke et al. 1994; Laws et al. 1995; 1997).

The ^{15}N values (8.4 to 11.3; Table 1) are greater than the mean microalgal δ^{15}N of 2.2‰

reported by Currin et al. (1995). These values are also greater than the ^{15}N values for

water column and porewater TDN (median = 2.1‰, range = -6.2 to 10.7‰ across all

months). Although we have no isotopic data for NH_4^+, one explanation for the heavy

microalgal δ^{15}N values is that the microalgae were using a ^{15}N-enriched pool of NH_4^+

produced by nitrification or coupled nitrification/denitrification.

Because sediment microalgae are isolated from a potential inorganic carbon source

(i.e. DIC in tidal waters) during the collection process, there is the potential for a shift in

^{13}C isotope ratios between natural microalgal populations and the collected algae

analyzed in this study. In the natural marsh, which is subject to diurnal tidal flooding, the ^{13}C isotopic composition of sediment microalgae (δ_{algae}) will depend on carbon uptake rates at both high and low tides, the isotopic composition of the carbon sources used at each tidal stage, and the discrimination between the carbon source and algal biomass during uptake and fixation. Using a simple model. expected δ_{algae} values can be calculated:

$$\delta_{algae} = \frac{R_{low}}{R_{daily}} \times \left(\delta_{algae,low}\right) + \frac{R_{high}}{R_{daily}} \times \left(\delta_{algae,high}\right) \tag{1}$$

where R_{low} is the microalgal photosynthetic rate (units C area^{-1} time^{-1}) at low tide, R_{high} is the photosynthetic rate when the marsh is flooded (units C area^{-1} time^{-1}), and R_{daily} is the daily algal carbon fixation rate ($R_{low} + R_{high}$; units C area^{-1} time^{-1}). Because microalgal photosynthesis rates at high tide are 25 to 49% of low tide rates (Holmes and Mahall 1982; Pinckney and Zingmark 1993) and the marsh is typically flooded for ~12 h per day, $R_{high} = (0.25 \text{ to } 0.49) \times R_{low}$. The ^{13}C isotopic composition of algae growing at low tide ($\delta_{algae,low}$) and high tide ($\delta_{algae,high}$) depends on the $\delta^{13}C$ value of the inorganic carbon source available during each stage of the tidal cycle (i.e. atmospheric CO_2 or water column DIC) and the isotopic discrimination ($\Delta = \delta_{product} - \delta_{substrate}$) between carbon source and algal biomass:

$$\delta_{algae,low} = \delta_{CO_2} + \Delta_{CO_2} \text{ and } \delta_{algae,high} = \delta_{DIC} + \Delta_{DIC}. \tag{2}$$

Values of Δ for inorganic carbon utilization by algae range from -29 to -5‰ (a more typical range is -20 to -10‰) and depend on the species and availability of DIC, rates of DIC diffusion and uptake, and other factors (see discussion in Cifuentes and Fogel 1993; Goericke et al. 1994). A value of -7.8‰ was used for δ_{CO_2} (Levin et al. 1987) while δ_{DIC}

174

was -13.4‰ (average of all water column DIC measurements presented in this dissertation, section III; n = 27). Using these values and equation 1, calculated sediment microalgal $\delta^{13}C$ values (δ_{algae}) for Sweet Hall marsh ranged from -29.6 to -18.9‰ (Table 2; the range is primarily due to the 10‰ variation in Δ). During the microalgal isolation procedure in the laboratory, the marsh sediments were not flooded so the only inorganic carbon source was atmospheric CO_2 (i.e. $\delta_{algae} = \delta_{CO_2} + \Delta_{CO_2}$). Calculated algal $\delta^{13}C$ values for this case ranged from -27.8 to -17.8‰ (Table 2). This simple model did not include the possible utilization of porewater DIC which may have occurred in the marsh (regardless of tidal stage) and in the laboratory. When Δ_{CO_2} was -20‰, there was a slight (~1 to 2‰) difference between δ_{algae} values under field and laboratory conditions (Table 2). Furthermore, these calculated algal ^{13}C signatures (-29.6 to -26.4‰) were similar to those measured on actual samples of benthic microalgae (-27.7 to -23.7‰; Table 1), suggesting that the microalgal isolation procedure did not significantly alter $\delta^{13}C$ values of the marsh sediment microalgae.

Particulate Organic Carbon and Nitrogen

<u>Total Suspended Solid Concentrations</u>: Total suspended solid (TSS) concentrations varied on temporal (tidal cycle, seasonal) and spatial (creek versus mouth) scales (Fig. 3). "Baseline" TSS loads in August were lower than during other months, most likely due to the deeper water column during August (Fig. 3) which would reduce resuspension of bottom sediments. At the creek site, spikes in TSS concentration were typically observed on the ebb and flood tides, approximately mid-way between slack highs and lows, when

175

Table 2: Calculation of sediment microalgal ^{13}C composition (δ_{algae}). Field conditions assume uptake of atmospheric CO_2 ($\delta^{13}C = -7.8\%o$) during low tide and water column DIC ($\delta^{13}C = -13.4\%o$) when the marsh is flooded. In the laboratory, algae are not exposed to tidal flooding; thus their only carbon source is atmospheric CO2. Both cases ignore potential porewater DIC uptake which can occur in the field (regardless of tidal stage) and in the laboratory.

Field Growing Conditions			Laboratory Isolation	
(‰)	(‰)	(‰)	(‰)	(‰)
Δ_{CO_2}[a]	Δ_{DIC}	δ_{algae}[b]	Δ_{CO_2}	δ_{algae}
-20	-20	-29.6 to -28.9	-20	-27.8
-20	-10	-26.9 to -26.4	-10	-17.8
-10	-20	-22.9 to -20.9		
-10	-10	-19.6 to -18.9		

[a] The isotopic discrimination for each inorganic carbon source ($\Delta_{substrate}$) is defined as $\delta^{13}C_{product} - \delta^{13}C_{substrate}$ where the product is microalgae and the substrate is either CO_2 or DIC.

[b] The range in δ_{algae} is caused by variations in the rate of photosynthesis at high tide relative to that at low tide; $R_{high} = (0.25 \text{ to } 0.49) \times R_{low}$ (see equation 1).

176
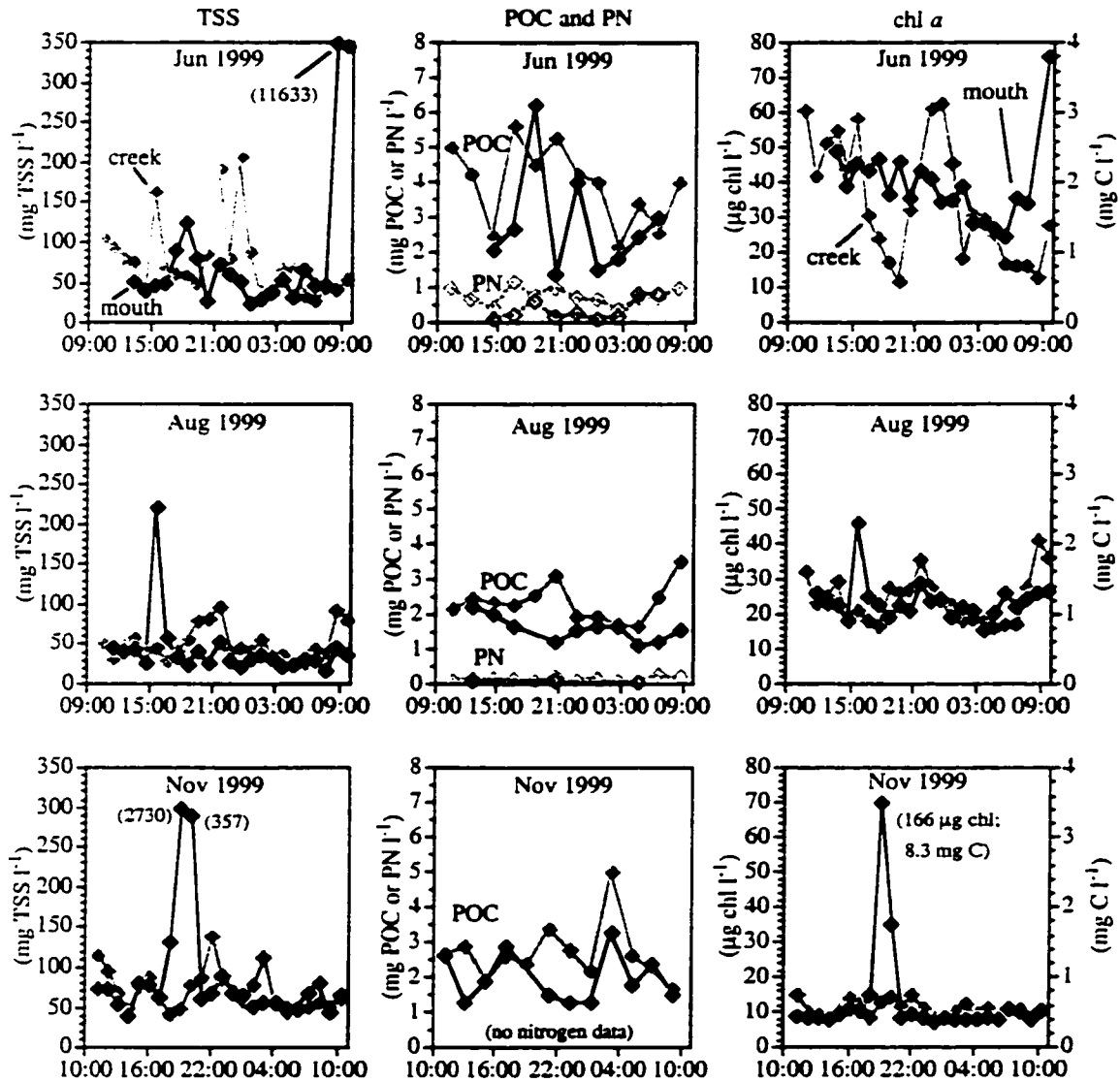
Figure 3: Diurnal patterns of suspended particulate and chl *a* concentrations. Chl *a* concentrations were converted to carbon using a C:chl ratio of 50:1. Gray symbols indicate the creek site; black symbols indicate the mouth site. Shading in each panel indicates water depth; in all months water depth is depicted on the same scale (1.5 m depth at top of panel). All times are in eastern standard time (EST).

177

maximum current velocities are expected (Fig. 3). On 29 June, the large TSS pulses in the creek at 15:30, 21:30 and 23:30 EST were likely due to a combination of flood/ebb tide sediment resuspension as well as a series of thunderstorms which occurred at those times and further agitated creek bottom sediments. Because the water intake at the mouth site was suspended from a floating platform, rather than set at a fixed height above the sediment surface, the temporal patterns in TSS at the mouth site were slightly different. Instead of occurring on flood and ebb tides, the maximum TSS loads at the mouth site occurred near low water when the water intake was the minimum distance above the sediment (Fig. 3).

POC/PN Ratios: Across all sites and months, there was a general trend of increasing carbon and nitrogen with decreasing TSS load, suggesting that the source of high TSS concentrations was low quality organic material (i.e. high mineral content). Percent carbon at the creek station decreased from a median of 6.2% in June to 4.7% in August to 3.8% in November, while nitrogen similarly decreased from 1.2% in June to 0.33% in August (no %N data from November due to small sample sizes). The same general trend was observed at the mouth site. Simultaneous with the decreases in carbon and nitrogen, there was an increase in the median POC/PN ratio from June (median = 6.5) to August (17.5; Fig. 4). Although the samples analyzed in November were too small to detect nitrogen, we estimated POC/PN ratios in November. Based on minimum nitrogen amounts measured in other months (<1 μg N), we assumed that the samples in November contained less than 1 μg N and therefore estimated a median POC/PN ratio of 31.2 (Fig. 4). The steady increase in POC/PN from June to August to November suggests an

178
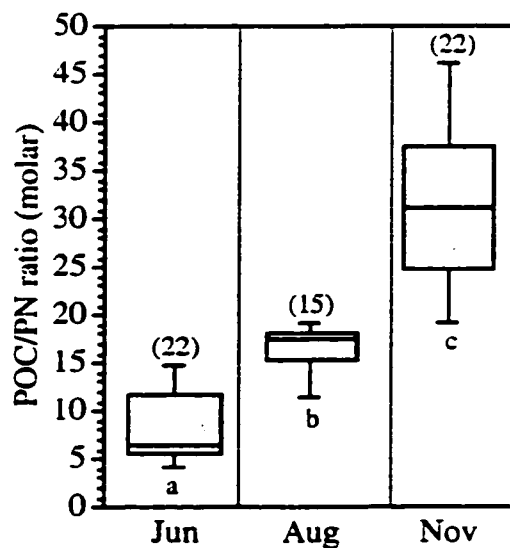
Figure 4: Seasonal changes in the molar POC/PN ratio of suspended particulates. The top and bottoms of the shaded box indicate the 75th and 25th percentiles of each data set, the line in the center of each box is the seasonal median; the ends of the bars denote the 10th and 90th percentiles. Numbers in parentheses above each bar show the number of samples. Letters below each bar denote statistical similarity at $\alpha = 0.05$ as determined with the non parametric Kruskal-Wallis ANOVA followed by a non parametric multiple comparison test. Bars with the same letter are not statistically different.

179

increasing contribution of terrestrial or marsh-derived organic matter to the water column (e.g. molar POC/PN for Sweet Hall macrophytes = 13 to 30; Neubauer et al. 2000).

Chlorophyll Concentrations: In both June and August, chl a concentrations at the creek site generally followed the tidal cycle, with higher chl a at high tide than low tide (Fig. 3). This pattern was not observed at the mouth site, or at either site in November. These results were somewhat surprising as previous studies in the same tidal creek during 1996 and 1997 documented higher chl a concentrations near low tide – these peaks were hypothesized to result from detrital or microalgal chlorophyll export from the marsh or enhanced water column primary production due to inputs of inorganic nutrients from the marsh (Anderson et al. 1998). The highest peaks in chl a at the mouth site were associated with high TSS concentrations and were caused by the water intake being located near the bottom sediments (within 5 cm) at low tide. Although the range of chl a concentrations were similar between sites within a month, there was a steady decrease in median chl a concentration from June (36 µg l^{-1}) to August (24 µg l^{-1}) to November (10 µg l^{-1}). In the York River estuary, mid-summer blooms are typically observed in the upper estuary while the chlorophyll maximum in the lower estuary occurs in the spring. This difference in the timing of the peak in chlorophyll biomass is primarily related to river discharge and water residence time (Filardo and Dunstan 1985; Malone et al. 1988; Sin et al. 1999). By converting chl a concentrations to carbon units assuming C:chl ratios of 35:1 (Cloern et al. 1995, calculated for San Francisco Bay) and 50:1 (DiToro et al. 1971; Wienke and Cloern 1987), we estimated that phytoplankton C made up a median of 41 to 59% of total POC in June and August (compare POC and chl a concentrations in

Fig. 3), while the importance of phytoplankton to the POC pool in November was considerably lower at 17 to 24%.

The ratio of chl a flourescence before and after acidification with 1 N HCl is indicative of the degree of chlorophyll degradation to phaeopigments. A higher ratio (before/after = chl/phaeo) indicates a relatively fresh or healthy chlorophyll source, while lower ratios indicate a stressed (e.g. grazed) phytoplankton community or dilution by a detrital chlorophyll source (Welschmeyer and Lorenzen 1985; Sin 1998). The median chl/phaeo ratios in June (1.58) and August (1.64; Fig. 5) were not significantly different, indicating little change in the relative health of the phytoplankton community or the contribution of detrital chlorophyll. These ratios were, however, lower than those reported by Sin (1998) who reported chl/phaeo ratios greater than 2.0 at several sites throughout the York River estuary. Therefore, the marsh phytoplankton communities were stressed relative to those measured in Sin's study, or there was a larger detrital component associated with our samples. This was not unexpected as Sin (1998) worked in the main channel of the river while this study took place in a marsh tidal creek with likely inputs of benthic microalgae and detritus from the marsh. By November, the chl/phaeo ratio decreased significantly to a median value of 1.29 (Fig. 5), indicating an increased degree of detrital input. This interpretation is consistent with the POC/PN data which suggested the increasing dominance of a terrestrial or macrophyte-derived organic matter source in November.

181
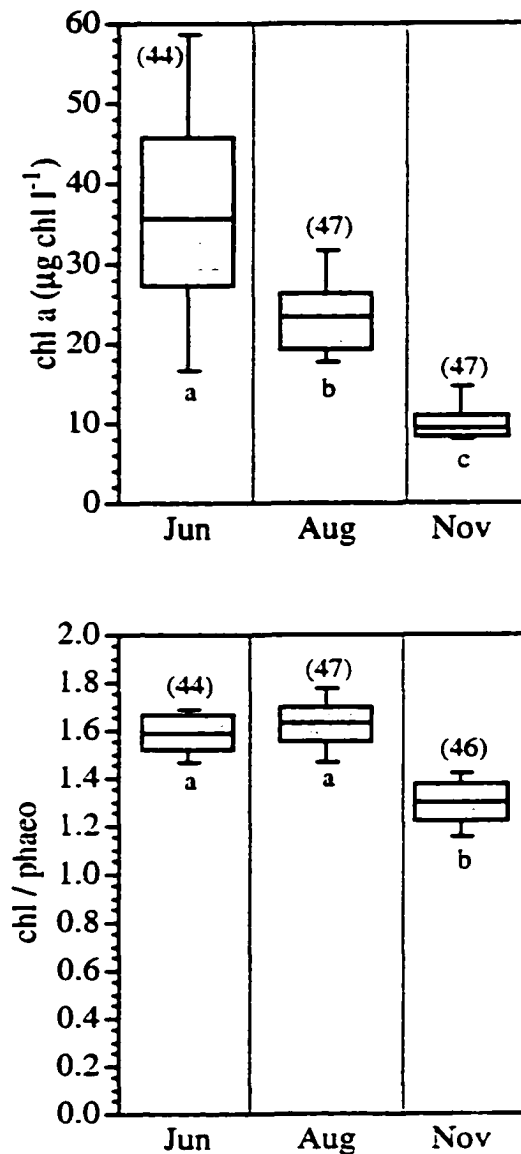
Figure 5: Seasonal changes in water column chl *a* and chl / phaeo ratios. There were no significant differences between sites within a month for either parameter ($\alpha = 0.05$). See Fig. 4 caption for description of figure layout.

182

POC Isotopic Composition: Overall, $^{13}C_{POC}$ distributions were homogenous, with

statistically similar $\delta^{13}C_{POC}$ signatures between all months (excluding November mouth

site; Fig. 6A). The ^{13}C values for POC (-29 to -22‰; Fig. 6A) were similar to the range

in ^{13}C for both macrophytes and microalgae (-29 to -23‰; Table 1). However, as

previously discussed, there was a substantial contribution of phytoplankton to the total

POC pool (median of 41 to 59% in June and August) so the $^{13}C_{POC}$ data can not be

explained as an exclusive mixture of macrophyte and microalgal detritus. Water column

$\delta^{13}C_{POC}$ values can be calculated using a simple ^{13}C mass balance:

$$\delta^{13}C_{POC} = (f_{phyto\ POC} \times \delta^{13}C_{phyto\ POC}) + (f_{other\ POC} \times \delta^{13}C_{other\ POC}), \quad (3)$$

where f is the fraction of carbon derived from phytoplankton or other sources with known

or estimated $\delta^{13}C$ signatures. If the measured and calculated isotope ratios are similar, it

implies a certain level of understanding of the relative importance and isotopic

compositions of different organic carbon sources to the water column. Admittedly, the

non-phytoplankton fraction encompasses macrophyte and microalgal carbon (as well as

possible terrestrial inputs from watershed runoff); it is difficult to differentiate these

sources on the basis of their ^{13}C signatures. The contribution of phytoplankton carbon to

the total POC pool has been previously discussed. The ^{13}C composition of phytoplankton

POC was estimated using previously measured $\delta^{13}C_{DIC}$ values (this dissertation, section

III) and an isotopic discrimination (Δ) of -20 to -10‰ between phytoplankton and DIC

(Cifuentes and Fogel 1993; Goericke et al. 1994). Similarly, the isotopic signature of

"other" POC inputs was estimated from measured $\delta^{13}C$ values for marsh microalgae and

the biomass dominant macrophytes (Table 1).

183
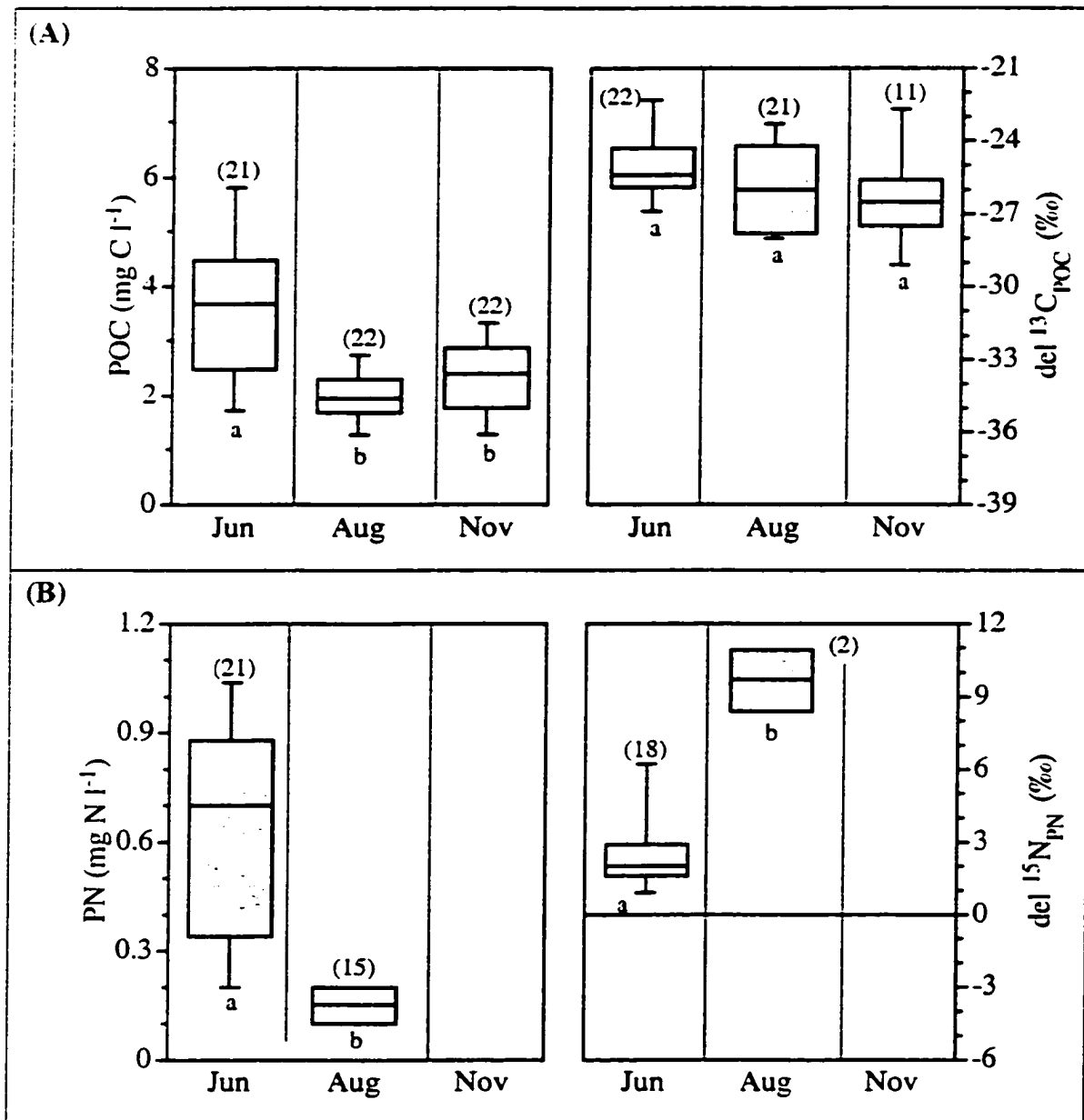
Figure 6: Water column POC and PN characterization for pooled creek and mouth data. There were no significant differences between sites within a month ($\alpha = 0.05$) (A) Seasonal concentrations and ^{13}C isotopic composition of suspended POC. (B) Seasonal concentrations and ^{15}N signatures of suspended PN. See Fig. 4 caption for description of figure layout.

Using this mass balance approach, calculated $\delta^{13}C_{POC}$ values in June (-32.5 to -22.8‰: Table 3) were in the same range as measured values ($\delta^{13}C_{POC}$ = -27.8 to -21.7; Fig. 6A). A similar overlap between measured and calculated values was observed in both August and November (compare Table 3 and Figure 6A). This suggests that the biomass dominant marsh macrophytes and microalgae were significant contributors to the non-phytoplankton portion of the POC pool whereas plants with more extreme ^{13}C signatures (e.g. *Hibiscus moscheutos* leaves, $\delta^{13}C$ = -37.3‰; dead *Zizania aquatica*, $\delta^{13}C$ = -17.7‰; Table 1) were quantitatively less important.

PN Isotopic Composition: Isotopic signatures of particulate nitrogen will reflect the isotopic composition of DIN and fractionation associated with DIN uptake, as well as changes in the particulate matter during degradation and microbial reworking. In June, the median water column $\delta^{15}N_{PN}$ signature was 2.0‰ (Fig. 6B). The median value in August ($\delta^{15}N$ = 9.7‰) was significantly ^{15}N enriched versus June and may have been due to high rates of organic matter mineralization in late summer. As isotopically light NH_4^+ was produced, the ^{15}N of the residual particulate N increased (e.g. Altabet and McCarthy 1985; Altabet 1988). However, due to the small size of many of the August particulate samples (Appendix 1), this median is based on only 2 data points and may not be representative of all August particulates.

Table 3: Calculation of $\delta^{13}C_{POC}$ signatures based on estimated phytoplankton $\delta^{13}C$ values and measured $\delta^{13}C$ values for macrophytes and algae.

	(‰)			(‰)	(‰)
	$f_{phyto\ POC}$[a]	$\delta^{13}C_{phyto\ DOC}$[b]	$f_{other\ POC}$	$\delta^{13}C_{other\ POC}$[c]	$\delta^{13}C_{POC.\ calc}$
Jun	0.41 to 0.58	-35.1 to -21.1	0.42 to 0.59	-28.9 to -25.2	-32.5 to -22.8
Aug	0.41 to 0.59	-35.4 to -23.7	0.41 to 0.59	-28.9 to -23.3	-32.7 to -23.5
Nov	0.17 to 0.24	-35.9 to -21.9	0.76 to 0.83	-27.7 to -26.2	-29.7 to -25.2

[a] Values of $f_{phyto\ POC}$ were calculated from chl a concentrations (converted to C using C:chl ratios of 35:1 and 50:1) and water column POC concentrations (Fig. 3).

[b] The ^{13}C composition of phytoplankton-derived POC was estimated by applying an isotopic discrimination (Δ) of -20 to -10‰ between water column $\delta^{13}C_{DIC}$ values (see dissertation section III) and phytoplankton.

[c] "Other POC" includes inputs from marsh macrophytes and sediment microalgae. Range in ^{13}C values encompasses range in ^{13}C values for the biomass dominant marsh plants (live *Peltandra virginica*, *Pontederia cordata*, and *Zizania aquatica*; see Table 1). Although not measured, terrestrial plants may also produce POC with a similar $\delta^{13}C_{POC}$ signature.

186

Dissolved Organic Carbon

DOC Concentrations: Water column DOC concentrations ranged from 400 to >1000 μM-C and were variable across tidal cycles, between creek and mouth sites, and from month to month (Fig. 7). Although the median water column DOC concentration was greater in August (781 μM) than June (543 μM) and November (670 μM), there were no significant differences between months (Fig. 8A). Similarly, there were no significant differences between water column and porewater samples within a month (Fig. 8A). There was a general, but non-significant trend of increasing porewater DOC concentrations from June (median = 426 μM) to August (532 μM) to November (703 μM; Fig. 8A). Within a marsh–estuary system, DOC concentrations are affected by a variety of biotic and abiotic factors including autotrophic and heterotrophic DOC production via exudation or feeding, microbial DOC consumption, photodegradation, DOC sorption to particles, inputs of DOC from marsh, groundwater and upland sources, and advective DOC losses (e.g. Cole et al. 1982; Peterson and Howarth 1987; Burdige and Homestead 1994; Amon and Benner 1996; Roy et al. 1996; Moran et al. 1999). The general trend of increasing DOC concentration from June to August to November coincided with increased rates of sediment mineralization in the autumn as well as the senescence and decomposition of marsh biomass which begins in mid summer (late June to July) and continues through the end of the growing season (Neubauer et al. 2000).

DOC Isotopic Composition: In the York River estuary, Raymond (1999) measured $\delta^{13}C$ values for DOC between -28.8 to -24.0‰ at mid-channel sites and suggested that the DOC was primarily of terrestrial origin with only a small contribution from riverine
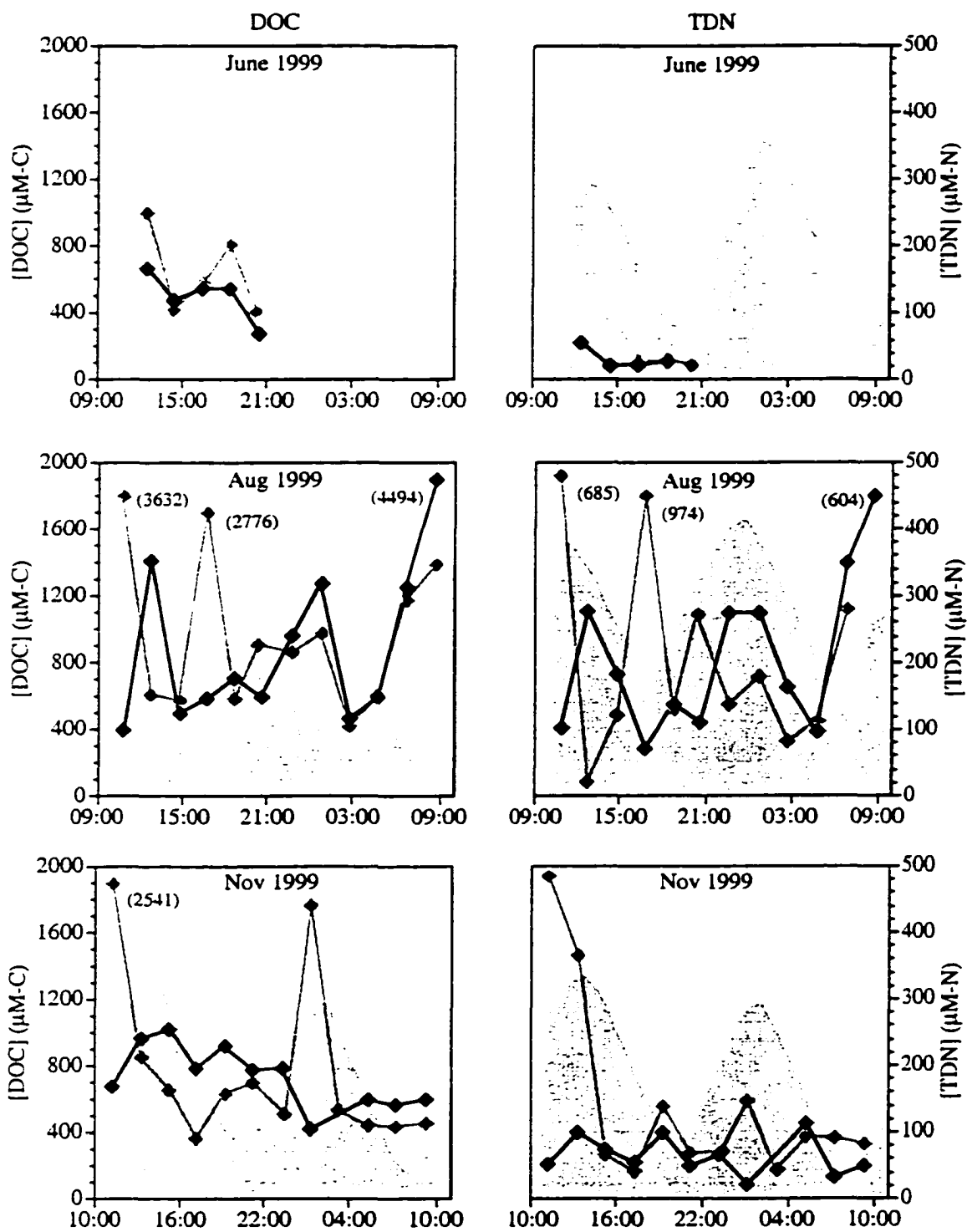
Figure 7: Diurnal patterns of DOC (μM C) and TDN (μM N) concentration at the creek

(gray symbols) and mouth (black symbols) sampling sites. Shading in each panel

indicates water depth; in all months water depth is depicted on the same scale (1.5 m

depth at top of panel). All times are in eastern standard time (EST).

188

(A)

Jun Aug Nov   Jun Aug Nov

DOC (µM)

3000
2800
2800
1500
1000
500
0

(24)
(9)
(23)
(10)
(9)
(8)
b
a, b
a
b
a, b
b
a, b

del $^{13}C_{DOC}$ (‰)

-21
-24
-27
-30
-33
-36
-39

(23)
(9)
(19)
(8)
(10)
(9)
b
a, b
b
b
a
a

Water Pore Water Pore Water Pore   Water Pore Water Pore Water Pore

(B)

Jun Aug Nov   Jun Aug Nov

TDN (µM)

700
650
300
200
100
0

(23)
(21)
(8)
(9)
(9)
(8)
a, c
a, c
b
a, b
a, b
a, c

del $^{15}N_{TDN}$ (‰)

12
9
6
3
0
-3
-6

(14)
(2)
(7)
a
a
a

Water Pore Water Pore Water Pore   Water Pore Water Pore Water Pore
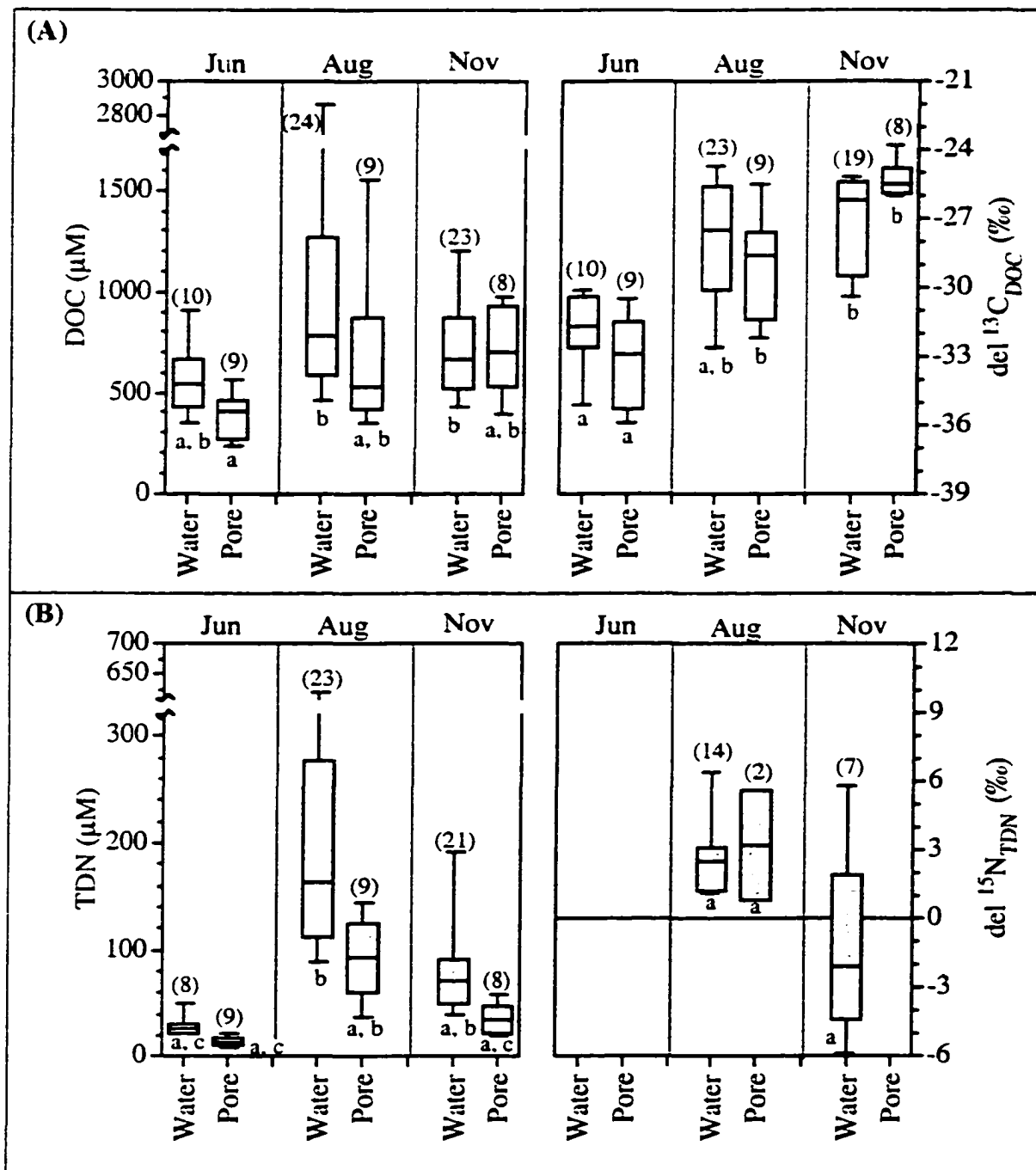
Figure 8: Seasonal characterization of DOC and TDN samples from water column and porewater. There were no significant differences between creek and mouth sites within a month ($\alpha = 0.05$) (A) Seasonal concentrations and ^{13}C isotopic composition of DOC. (B) Seasonal concentrations and ^{15}N signatures of TDN. See Fig. 4 caption for description of figure layout.

189

phytoplankton. In June, the $\delta^{13}C_{DOC}$ values measured at the creek and mouth sites were similar but slightly more negative than those reported by Raymond, with values ranging from -37.6 to -29.9‰ (median = -31.7‰); these values were significantly ^{13}C depleted relative to August and November values (Fig. 8A). In both August and November, water column $\delta^{13}C_{DOC}$ values at Sweet Hall marsh were within the range reported by Raymond (median $\delta^{13}C$ = -27.3 and -26.5‰, respectively; Fig. 8A). In all months, there were no significant differences between water column and porewater $\delta^{13}C_{DOC}$ signatures (Fig. 8A).

Using an isotopic mixing model similar to equation 3, $\delta^{13}C_{DOC}$ values were calculated for each month and used to assess the contributions of phytoplankton, macrophyte, and microalgal-derived DOC to the water column DOC pool. Phytoplankton production was estimated using measured water column chlorophyll concentrations and seasonal assimilation ratios (i.e. primary production / chl a) measured in the tidal freshwater Pamunkey River (Table 4; CBP 2000). Reported phytoplankton exudation rates range from 5 to >35% of primary production (Lancelot 1979; Wolter 1982; Baines and Pace 1991; Malone et al. 1991). The ratio of phytoplankton exudation to the standing stock of DOC was used as an estimate of the fractional contribution of phytoplankton DOC to the total DOC pool. The $\delta^{13}C$ values for phytoplankton and other inputs (macrophytes and microalgae) were estimated as previously described, see Table 3). Using the mass balance model, calculated $\delta^{13}C_{DOC}$ values in June ranged from -29.5 to -24.8‰ (Table 5), this was slightly ^{13}C enriched relative to measured values of -37.6 to -29.9‰ (Fig. 8A), suggesting that there was an additional source of ^{13}C-depleted DOC to the water column. In both August and November, measured and calculated $\delta^{13}C_{DOC}$ values were similar.

190

Table 4: Calculation of phytoplankton primary production and exudation rates using median water column chlorophyll concentrations and assimilation ratios (ASR) for EPA monitoring station TF4.2 in the tidal freshwater Pamunkey River (CBP 2000).

	(μg chl l^{-1})	$\left(\dfrac{\mu g\ C\ l^{-1}\ h^{-1}}{\mu g\ chl\ l^{-1}}\right)$	(μmol C l^{-1} d^{-1})	(μmol C l^{-1} d^{-1})
	chl a	ASR	GPP[a]	Exudation[a]
Jun	35.6	3.57	156	8 to 55
Aug	23.5	2.11	55	3 to 19
Nov	9.7	4.01	33	2 to 12

[a] Gross phytoplankton production (GPP) was calculated from chl a concentrations, assimilation ratios, and seasonally varying day lengths (10.4 to 14.7 hr light d^{-1}). The exudation of DOC is typically 5 to 35% of primary production (e.g. Lancelot 1979; Wolter 1982; Baines and Pace 1991; Malone et al. 1991)

191

Table 5: Calculation of $\delta^{13}C_{DOC}$ signatures from estimated rates of phytoplankton DOC exudation (Table 4), calculated phytoplankton $\delta^{13}C$ values and measured $\delta^{13}C$ values for macrophytes and algae. A mixing model similar to equation 3 was used. See Table 3 for values of $\delta^{13}C_{phyto}$ and $\delta^{13}C_{other}$.

	$f_{phyto\,DOC}$[a]	$f_{other\,DOC}$	(‰) $\delta_{DOC,\,calc}$
Jun	0.01 to 0.10	0.90 to 0.99	-28.6 to -24.8
Aug	0.00 to 0.02	0.98 to 1.00	-29.1 to -23.3
Nov	0.00 to 0.02	0.98 to 1.00	-27.7 to -26.2

[a] $f_{phyto\,DOC}$ = DOC exudation / DOC concentration; $f_{other\,DOC}$ = 1 - $f_{phyto\,DOC}$. See Table 4 for calculated DOC exudation rates.

192

One explanation for the difference between measured and calculated $\delta^{13}C_{DOC}$ values in June is that calculated exudation rates underestimated the actual contribution of phytoplankton DOC by failing to account for DOC released at night, due to feeding, or from the decomposition of dead phytoplankton (Cole et al. 1982; Fuhrman et al. 1985; Baines and Pace 1991). Alternately, DOC leached from marsh plants (e.g. *Spartina alterniflora*) may be 1 to 2‰ depleted in ^{13}C relative to bulk tissues (e.g. Coffin et al. 1990; Hullar et al. 1996) although the magnitude (and direction) of this shift can vary by species. A third input of isotopically depleted carbon is from the leaves of *Hibiscus moscheutos* ($\delta^{13}C = -37.3$‰, Table 1). However, the low biomass of *H. moscheutos* at the study site (S. C. Neubauer, unpublished) and the recalcitrant nature of *H. moscheutos* suggest that contributions of *H. moscheutos* to the water column DOC pool will be insignificant relative to inputs from the abundant and fleshy *Peltandra virginica* and *Pontederia cordata*.

Total Dissolved Nitrogen

TDN Concentrations: Water column TDN concentrations were significantly higher in August (median = 163 μM) than June (26 μM; Fig. 8B). Values in November (72 μM) were intermediate between June and August concentrations and not significantly different from either month. In all months, there were no significant differences between water column and porewater TDN concentrations (Fig. 8B). Creek, mouth, and porewater DIN and DON concentrations were similarly variable and controlled by seasonal patterns in nitrogen demand by autotrophs, leaching of DON from marsh plants, and rates of organic nitrogen remineralization. Water column DIN concentrations ranged from a median of

193

7.1 μM (Aug creek) to 28.0 μM (Jun creek). Concentrations were similar in both June and November, and slightly (but not significantly) lower in August. In contrast, median porewater DIN concentrations were slightly higher in August (10.6 μM) than either June (8.2 μM) or November (3.4 μM). Calculated water column DON concentrations showed a much larger seasonal variation – concentrations at the creek and mouth sites ranged from <20 μM in June and were significantly higher at >100 μM in August.

TDN Isotopic Composition: While exudates and leachates from phytoplankton and macrophytes within the marsh-tidal creek system exerted a seasonal control on $^{13}C_{DOC}$, dissolved ^{15}N values are more complex because sources and cycling of both DON and DIN must be considered. Due to high variability within a month, there were no significant differences in water column $\delta^{15}N_{TDN}$ between August (median = 2.6‰) and November (-2.1‰; Fig. 8B). These values were not statistically different from porewater $\delta^{15}N_{TDN}$ values in August (3.2‰) although this value was based on only 2 porewater samples (Fig. 8B). Due to low flow conditions during the summer of 1999 (Fig. 2), watershed contributions of TDN to the marsh-tidal creek system were most likely minimal throughout the summer. Thus, processes within the marsh/creek system (rather than those in the watershed) likely exerted the strongest controls on water column $\delta^{15}N_{TDN}$ signatures.

194

SUMMARY

Seasonal patterns in stable carbon isotope ratios of DOC and POC in the tidal freshwater marsh creek system were used to characterize organic carbon sources within the system. In the suspended particulate pool, there was a significant increase in the POC/PN ratio from June to August to November. Simultaneously, there was a decrease in the stsnding stock of water column chl a which resulted in a decreasing contribution of chl a to the POC pool from mid summer (June) through the late growing season (November). This decrease in the importance of phytoplankton suggests a steadily increasing input of macrophyte and microalgal-derived particulate carbon through the growing season that is coincident with seasonal patterns of macrophyte growth and senescence. A stable isotope mixing model was used to confirm the seasonal shift in the importance of marsh-derived versus phytoplankton carbon.

Interpretation of the ^{15}N data for both particulate and dissolved samples was compromised because the small size of many of the samples resulted in low confidence in some of the $\delta^{15}N$ data. In the particulate pool, there was an approximately 7‰ enrichment in $\delta^{15}N_{PN}$ in August versus June. One interpretation of these data is that there was selective mineralization of isotopically light NH_4^+ from suspended particles that resulted in ^{15}N-enriched particles.

There were seasonal shifts in the contributions of phytoplankton and marsh autotrophs to DOC in the tidal creek. Due to decreasing chl a concentrations and a

195

coupling between primary production and exudation rates, there was a steady decrease in the significance of phytoplankton exudates to the DOC pool from June to November. A comparison of $\delta^{13}C_{DOC}$ values predicted by a mixing model with measured $\delta^{13}C_{DOC}$ signatures suggested the presence of a ^{13}C depleted DOC source in mid summer. In late summer and at the end of the growing season, there was close agreement between measured and calculated DOC isotope ratios.

The data presented herein have suggested seasonal changes in the importance of marsh-derived (i.e. macrophyte and microalgal) and phytoplankton carbon to the particulate and dissolved pools. Due to the broad expanses of tidal marshes in the lower Pamunkey River and the similarity of ^{13}C isotopic signatures for marsh-derived and terrestrially-derived POC and DOC, rates of import or export of these materials from the marsh could not be quantified. Other important issues that have yet to be resolved include the fates and turnover times of phytoplankton, macrophyte and microalgal derived POC and DOC. Because the summer of this study was characterized by record low water discharge, we caution that these results (especially with respect to the importance of terrestrial POC and DOC sources) may not be representative of years with greater river flow.

196

LITERATURE CITED

Altabet, M. A., McCarthy, J. J. 1985. Temporal and spatial variations in the natural abundance of ^{15}N in PON from a warm-core ring. Deep-Sea Res. 32(7): 755-772.

Altabet, M. A. 1988. Variations in nitrogen isotopic composition between sinking and suspended particles: implications for nitrogen cycling and particle transformation in the open ocean. Deep-Sea Res. 35(4): 535-554.

Amon, R. M., Benner, R. 1996. Photochemical and microbial consumption of dissolved organic carbon and dissolved oxygen in the Amazon River system. Geochim. Cosmochim. Acta. 60: 1783-1792.

Anderson, I. C., Tobias, C. R., Neikirk, B. B., Wetzel, R. L. 1997 Development of a process-based nitrogen mass balance model for a Virginia (USA) *Spartina alterniflora* salt marsh: implications for net DIN flux. Mar Ecol Prog Ser 159: 13-27.

Anderson, I. C., Neubauer, S. C., Neikirk, B. B., Wetzel, R. L. 1998. Exchanges of carbon and nitrogen between tidal freshwater wetlands and adjacent tributaries. Final report submitted to the Virginia Coastal Resources Management Program, Virginia Department of Environmental Quality.

Baines, S. B., Pace, M. L. 1991. The production of dissolved organic matter by phytoplankton and its importance to bacteria: patterns across marine and freshwater systems. Limnol. Oceanogr. 36: 1078-1090.

Bender, M. M. 1971. Variations in the ^{13}C/^{12}C ratios of plants on relation to the pathway of photosynthetic carbon dioxide fixation. Phytochemistry. 10: 1239-1244.

Benner, R., Fogel M. L., Sprague E. K. 1991. Diagenesis of belowground biomass of *Spartina alterniflora* in salt-marsh sediment. Limnol. Oceanogr. 36: 1358-1374.

Benner R., Fogel M. L., Sprague E. K., Hodson, R. E. 1987. Depletion of ^{13}C in lignin and its implications for stable carbon isotope studies. Nature. 329: 708-710.

Bilby, R. E., Fransen, B. R., Bisson, P. A. 1996. Incorporation of nitrogen and carbon from spawning coho salmon into the trophic system of small streams: evidence from stable isotopes. Can. J. Fish. Aquat. Sci. 53: 164-173.

197

Bowden W. B. 1984. A nitrogen-15 isotope dilution study of ammonium production and consumption in a marsh sediment. Limnol. Oceanogr. 29: 1004-1015.

Brooks T. J. 1983 *Pamunkey River slack water data report: Temperature, salinity, dissolved oxygen 1970-1980* Virginia Institute of Marine Science Data Report 20.

Burdige. D. J., Homestead. J. 1994. Fluxes of dissolved organic carbon from Chesapeake Bay sediments. Geochim. Cosmochim. Acta. 58: 3407-3424.

CBP. 2000. Chesapeake Bay Program 1999 phytoplankton monitoring database for the Pamunkey River. (accessed 27 Jul 2000); available at http://www.chesapeakebay.net.

Cifuentes. L. A., Fogel. M. L., Pennock. J. R., Sharp, J. H. 1989. Biogeochemical factors that influence the stable nitrogen isotope ratio of dissolved ammonium in the Delaware Estuary. Geochim. Cosmochim. Acta. 53: 2713-2721.

Cifuentes, L. A., Sharp, J. H., Fogel, M. L. 1988. Stable carbon and nitrogen isotope biogeochemistry in the Delaware estuary. Limnol. Oceanogr. 33(5): 1102-1115.

Cloem, J. E., Grenz, C., Viderger-Lucas, L. 1995. An empirical model of the phytoplankton chlorophyll:carbon ratio – the conversion factor between productivity and growth rate. Limnol. Oceanogr. 40(7): 1313-1321.

Coffin, R. B., Velinsky, D. J., Devereux, R., Price, W. A., Cifuentes, L. A. 1990. Stable carbon isotope analysis of nucleic acids to trace sources of dissolved substrates used by estuarine bacteria. Appl. Env. Microb. 56(7): 2012-2020.

Cole, J. J., Likens, G. E., Strayer, D. L. 1982. Photosynthetically produced dissolved organic carbon: an important source for planktonic bacteria. Limnol. Oceanogr. 34: 1305-1310.

Currin C. A., Newell S. Y., Paerl H. W. 1995. The role of standing dead *Spartina alterniflora* and benthic microalgae in salt marsh food webs: considerations based on multiple stable isotope analysis. Mar Ecol Prog Ser 121:99-116.

Deegan, L. A., Garritt, R. H. 1997. Evidence for spatial variability in estuarine food webs. Mar. Ecol. Prog. Ser. 147: 31-47.

DiToro, D. M., O'Connor, D. J., Thomann, R. V. 1971. A dynamic model of phytoplankton populations in the Sacramento-San Joaquin delta. Advan. Chem. Ser. 106: 131-180.

198

Doumlele, D. G. 1981. Primary production and seasonal aspects of emergent plants in a tidal freshwater marsh. Estuaries 4(2):139-142

EPA. 1996 *Region III Land Cover Data Set* United States Environmental Protection Agency, Washington DC.

Filardo, M. J., Dunstan, W. M. 1985. Hydrodynamic control of phytoplankton in low salinity waters of the James River estuary, Virginia. Est. Coast. Shelf. Sci. 21: 653-667.

Fogel, M. L., Cifuentes, L. A. 1993. Isotope fractionation during primary production. In: Engel, M. H., Macko, S. A. (eds). Organic Geochemistry. Plenum: New York. 73-98.

Fogel, M. L., Sprague, E. K., Gize, A. P., Frey. R. W. 1989. Diagenesis of organic matter in Georgia salt marshes. Est. Coast. Shelf Sci. 28: 211-230.

Fuhrman, J. A., Eppley, R. W., Hagstrom, Å, Azam, F. 1985. Diel variations in bacterioplankton, phytoplankton, and related parameters in the Southern California Bight. Mar. Ecol. Prog. Ser. 27: 9-20.

Garman, G. C., Macko, S. A. 1998. Contribution of marine-derived organic matter to an Atlantic coast, freshwater, tidal stream by anadromous clupeid-fishes. J. N. Am. Benthol. Soc. 17(3): 277-285.

Goericke, R., Montoya, J. P., Fry, B. 1994. Physiology of isotope fractionation in algae and cyanobacteria. In: Lajtha, K., Michener, B. (eds). Stable isotopes in ecology. Blackwell Scientific: Cambridge. 187-221.

Guo, L., Santischi, P. H. 1997. Isotopic and elemental characterization of colloidal organic matter from the Chesapeake Bay and Galveston Bay. Mar. Chem. 59: 1-15.

Haines, E. B. 1976. Stable carbon isotope ratios in the biota, soils and tidal water of a Georgia salt marsh. Est. Coast. Mar. Sci. 4: 609-616.

Holmes RW, Mahall BE 1982. Preliminary observations on the effects of flooding and dessication upon the net photosynthetic rates of high intertidal estuarine sediments. *Limnol. Oceanogr.* 27(5):954-958.

Hughes, J. E., Deegan, L. A., Peterson, B. J., Holmes, R. M., Fry, B. 2000. Nitrogen flow through the food web in the oligohaline zone of a New England estuary. Ecology. 81(2): 433-452.

199

Hullar, M. A. J., Fry, B., Peterson, B. J., Wright, R. T. 1996. Microbial utilization of estuarine dissolved organic carbon: a stable isotope tracer approach tested by mass balance. Appl. Env. Microb. 62(7): 2489-2493.

Kline, T. C., Goering, J. J., Mathisen, O. A., Poe, P. H., Parker, P. L. 1990. Recycling of elements transported upstream by runs of Pacific salmon. I. $\delta^{15}N$ and $\delta^{13}C$ evidence in Sashin Creek, southeastern Alaska. Can. J. Fish. Aquat. Sci. 47: 136-144.

Lajtha K. Marshall JD 1994. Sources of variation in the stable isotopic composition of plants. in Lajtha K, Michener RH (eds). *Stable isotopes in ecology and environmental science*. Blackwell: Oxford. pp. 222-240.

Lancelot, C. 1979. Gross excretion rates of natural marine phytoplankton and heterotrophic uptake of excreted products in the Southern North Sea, as determined by short-term kinetics. Mar. Ecol. Prog. Ser. 1: 179-186.

Laws, E. A., Bidigare, R. R., Popp, B. N. 1997. Effect of growth rate and CO2 concentration on carbon isotopic fractionation by the marine diatom *Phaeodactylum tricornutum*. Limnol. Oceanogr. 42(7) 1552-1560.

Laws, E. A., Popp, B. N., Bidigare, R. R., Kennicutt, M. C., Macko, S. A. 1995. Dependence of phytoplankton carbon isotopic composition on growth rate and $[CO_2]_{aq}$: Theoretical considerations and experimental results. Geochim. Cosmochim. Acta. 59: 1131-1138.

Levin, I., Kromer, B., Wagenback, D., Munnich, K. O. 1987. Carbon isotope measurements of atmospheric CO_2 at a coastal station in Antarctica. *Tellus*. 39B: 89-95.

MacAvoy, S. E., Macko, S. A., Garman, G. C. 1998. Tracing marine biomass into tidal freshwater ecosystems using stable sulfur isotopes. Naturwissenschaften. 54: 544-546.

MacAvoy, S. E., Macko, S. A., McIninch, S. P., Garman, G. C. 2000. Marine nutrient contributions to freshwater apex predators. Oecologia. 122: 568-573.

Macko, S. A. 1983. Sources of organic nitrogen in Mid-Atlantic coastal bays and continental shelf sediment of the United States. Carnegie Inst. of Wash. Yearb. 82: 390-394.

200

Malone, T. C., Crocker, L. H., Pike, S. E., Wendler, B. W. 1988. Influences of river flow on the dynamics of phytoplankton production in a partially stratified estuary. Mar. Ecol. Prog. Ser. 48: 235-249.

Malone, T. C., Ducklow, H. W., Peele, E. R., Pike, S. E. 1991. Picoplankton carbon flux in Chesapeake Bay. 78: 11-22.

Mariotti, A., Lancelot, C. Billen, G. 1984. Natural isotopic composition of nitrogen as a tracer of origin for suspended organic matter in the Scheldt estuary. Geochim. Cosmochim. Acta. 48: 549-555.

Moran, M. A., Sheldon, W. M., Sheldon, J. E. 1999. Biodegradation of riverine dissolved organic carbon in five estuaries of the southeastern United States. Estuaries. 22: 55-64.

Morris, J. T., Bowden, W. B. 1986. A mechanistic, numerical model of sedimentation, mineralization, and decomposition for marsh sediments. Soil Sci. Soc. Am. J. 50: 96-105.

Neubauer. S. C., Miller, W. D. and Anderson, I. C. 2000. Carbon cycling in a tidal freshwater marsh ecosystem: A carbon gas flux study. Mar. Ecol. Prog. Ser. 199:13-30.

Odum W. E., Heywood M. A. 1978 Decomposition of intertidal freshwater marsh plants. In: Good R. E., Whigham D. F., Simpson R. L. (eds) Freshwater wetlands: ecological processes and management potential. Academic Press, New York, p 89-98

Perry III, J. E. 1991. Analysis of vegetation patterns in a tidal freshwater marsh. PhD dissertation, College of William and Mary, Virginia Institute of Marine Science, Gloucester Point.

Peterson, B. J., Fry, B., Hullar, M., Saupe, S., Wright, R. 1994. The distribution and stable carbon isotopic composition of dissolved organic carbon in estuaries. Estuaries. 17(1B): 111-121.

Peterson, B. J., Howarth. R. W. 1987. Sulfur, carbon, and nitrogen isotopes used to trace organic matter flow in the salt-marsh estuary of Sapelo Island, Georgia. Limnol. Oceanogr. 32: 1195-1213.

Pinckney JL, Zingmark RG 1993. Modeling the annual production of intertidal benthic microalgae in estuarine ecosystems. *J. Phycol.* 29:396-407.

Raymond, P. A. 1999. Carbon cycling in the York River estuary: An isotopic and mass balance approach using natural ^{14}C and ^{13}C isotopes. PhD dissertation, College of William and Mary, Virginia Institute of Marine Science, Gloucester Point

Roy, S., Chanut, J.-P., Gosselin, M., Sime-Ngando, T. 1996. Characterization of phytoplankton communities in the lower St. Lawrence estuary using HPLC-detected pigments and cell microscopy. Mar. Ecol. Prog. Ser. 142: 55-73.

Schubauer JP, Hopkinson CS 1984. Above- and belowground emergent macrophyte production and turnover in a coastal marsh ecosystem, Georgia. *Limnol. Oceanogr.* 29(5):1052-1065.

Shoaf, W. T., Lium, B. W. 1976. Improved extraction of chlorophyll a and b from algae using dimethyl sulfoxide. Limnol. Oceanogr. 21: 926-928.

Sin, Y 1998. Ecosystem analysis of water column processes in the York River estuary, Virginia: historical records, field studies and modeling analysis. PhD dissertation, College of William and Mary, Virginia Institute of Marine Science, Gloucester Point

Sin, Y., Wetzel, R. L., Anderson, I. C. 1999. Spatial and temporal characteristics of nutrient and phytoplankton dynamics in the York River estuary, Virginia: Analyses of long-term data. Estuaries. 22(2A): 260-275.

Solorzano, L. 1969. Determination of ammonium in natural waters by the phenolhypochlorite method. Limnol. Oceanogr. 14: 799-801.

Sullivan, M. J., Moncreiff, C. A. 1990. Edaphic algae are an important component of salt marsh food-webs: evidence from multiple stable isotope analyses. Mar. Ecol. Prog. Ser. 62: 149-159.

Sweeney, R. E., Kaplan, I. R. 1980. Natural Abundances of ^{15}N as a Source Indicator for Near-Shore Marine Sedimentary and Dissolved Nitrogen. Mar. Chem. 9(2): 81-94.

Tobias, C. R., Anderson, I. C., Canuel, E. A., Macko, S. A. in press. Nitrogen cycling through a fringing marsh-aquifer ecotone. Mar. Ecol. Prog. Ser.

Tobias, C. R. 1999. Nitrate reduction at the groundwater-salt marsh interface. PhD dissertation, College of William and Mary, Virginia Institute of Marine Science, Gloucester Point.

USGS 2000. Water resources for the United States; discharge data for the Pamunkey River near Hanover VA; station no. 01673000. United States Geological Survey, Washington D.C. (accessed 14 Jun 2000); available at http://water.usgs.gov.

Velinsky, D. J., Burdige, D. J., Fogel, M. L. 1991. Nitrogen diagenesis in anoxic marine sediments: isotope effects. Carnegie Inst. Washington Annu. Rep. Director. 151-162.

Wienke, S. M., Cloern, J. E. 1987. The phytoplankton component of seston in San Francisco Bay. *Neth. J. Sea Res.* 21(1): 25-33.

Welschmeyer, N. A., Lorenzen, C. J. 1985. Chlorophyll budgets: Zooplankton grazing and phytoplankton growth in a temperate fjord and the Central Pacific Gyres. Limnol. Oceanogr. 31(1): 1-21.

Whigham DF, McCormick J, Good RE, Simpson RL 1978. Biomass and primary production in freshwater tidal wetlands of the middle Atlantic Coast. In: Good RE, Whigham DF, Simpson RL (eds) *Freshwater wetlands: ecological processes and management potential*. Academic Press, New York, p 3-20.

Wolter, K. 1982. Bacterial incorporation of organic substances released by natural phytoplankton populations. Mar. Ecol. Prog. Ser. 7: 287-295.

Zar, J. H. 1996. Biostatistical analysis, 3rd edition. Prentice-Hall, Upper Saddle River, New Jersey.

Appendix 1: Compilation of POC and PN concentration and isotope data by date, time, and location. The shaded $\delta^{13}C_{POC}$ and $\delta^{15}N_{PN}$ values are discussed in the report; isotope values for samples that had less than 10 µg C or 5 µg N were not included in the text of this report because these sample masses are near the detection limit of the mass spectrometer. Values outlined with a gray dotted line are analytical duplicates for $\delta^{13}C_{POC}$ and $\delta^{15}N_{PN}$.

Site	Date	(EST) Time	(mg l⁻¹) POC	(mg l⁻¹) PN	(molar) POC/PN	(‰) $\delta^{13}C_{POC}$	(‰) $\delta^{15}N_{PN}$	(µg C) mass analyzed	(µg N)	Comments
creek	06/29/99	10:30	5.0	1.0	5.7	-25.1	3.4	84.2	17.2	normal
creek	06/29/99	12:30	4.2	0.7	7.1	-25.4	1.8	70.9	11.7	normal
creek	06/29/99	14:30	2.5	0.5	6.1	-25.9	2.9	68.9	13.1	normal
creek	06/29/99	16:30	5.6	1.2	5.6	-24.3	2.7	63.0	13.1	normal
creek	06/29/99	18:30	4.5	0.8	6.5	-25.0	0.9	75.2	13.5	normal
creek	06/29/99	20:30	5.3	1.0	6.0	-25.5	2.1	88.6	17.2	normal
creek	06/29/99	22:30	4.2	0.8	6.5	-25.5	0.9	71.0	12.8	normal
creek	06/30/99	00:30	4.0	0.7	6.8	-25.5	1.8	66.9	11.4	normal
creek	06/30/99	02:30	2.3	0.5	5.8	-24.6	1.0	75.9	15.2	normal
creek	06/30/99	02:30	2.1	0.4	6.3	-25.5	2.4	71.7	13.2	normal
creek	06/30/99	04:30	3.4	0.8	5.2	-25.2	1.6	94.4	21.3	normal
creek	06/30/99	06:30	2.6	0.7	4.2	-26.7	2.2	71.2	19.9	normal
creek	06/30/99	08:30	4.0	1.0	4.6	-25.9	1.9	89.5	22.7	normal
mouth	06/29/99	14:30	2.1	0.2	16.5	-24.3	11.9	46.6	3.3	low mass N
mouth	06/29/99	16:30	2.7	0.2	13.2	-22.7	6.9	59.5	5.3	normal
mouth	06/29/99	18:30	6.3	0.6	11.6	-23.0	4.3	104.8	10.6	normal

mouth	06/29/99	20:30	1.4	0.2	8.8	-22.4	7.8	47.3	6.2	normal
mouth	06/29/99	22:30	4.0	0.3	16.8	-25.5	3.5	67.5	4.7	low mass N
mouth	06/29/99	00:30	1.6	0.1	13.7	-21.8	5.2	35.8	3.0	low mass N
mouth	06/29/99	00:30	1.4	0.1	14.8	-109.5	11.1	32.0	2.5	questionable C, low mass N
mouth	06/29/99	02:30	1.8	0.2	12.3	-21.7	7.2	51.2	4.9	low mass N
mouth	06/29/99	04:30	2.5	0.8	3.5	-26.2	1.3	55.4	18.4	normal
mouth	06/29/99	06:30	2.9	0.9	3.6	-27.9	0.3	48.6	15.6	normal
mouth	06/29/99	06:30	3.1	0.8	4.6	-27.6	0.4	52.5	13.5	normal
mouth	06/29/99	08:30	403.6	49.2	9.6	-26.6	2.8	225.5	27.5	normal
creek	08/24/99	10:45	2.2	0.1	17.9	-25.2	7.0	36.3	2.4	low mass N
creek	08/24/99	12:45	2.5	0.1	19.3	-24.2	9.1	41.5	2.5	low mass N
creek	08/24/99	14:45	2.3	0.2	15.1	-28.1	6.0	38.9	3.0	low mass N
creek	08/24/99	16:45	2.3	0.2	17.5	-27.7	5.8	51.0	3.4	low mass N
creek	08/24/99	18:45	2.7	0.1	18.9	-25.6	6.6	59.7	3.7	low mass N
creek	08/24/99	18:45	2.5	0.2	15.2	-27.8	7.0	55.6	4.3	low mass N
creek	08/24/99	20:45	3.1	0.2	18.5	-26.1	8.7	69.2	4.4	low mass N
creek	08/24/99	22:45	1.9	0.1	16.4	-24.1	10.0	43.5	3.1	low mass N
creek	08/25/99	00:45	2.0	0.2	13.8	-25.3	7.6	43.7	3.7	low mass N
creek	08/25/99	02:45	1.7	0.1	16.7	-22.8	6.1	58.5	4.1	low mass N
creek	08/25/99	04:45	1.7	0.1	21.0	-22.2	9.6	37.4	2.1	low mass N
creek	08/25/99	06:45	2.5	0.3	11.4	-25.5	10.9	56.3	5.8	normal
creek	08/25/99	08:45	3.5	0.2	17.5	-24.3	8.4	77.9	5.2	normal

mouth	08/24/99	12:45	2.2	0.2	14.4	-26.0	11.1	49.3	4.0	low mass N
mouth	08/24/99	12:45	2.2	0.1	24.5	-28.6	16.6	49.2	2.3	low mass N
mouth	08/24/99	14:45	2.2	–	–	-26.7	14.7	48.6	0	mass N = 0
mouth	08/24/99	14:45	1.9	–	–	-26.7	–	41.3	–	undetectable N
mouth	08/24/99	16:45	1.7	–	–	-24.2	–	37.2	–	undetectable N
mouth	08/24/99	20:45	1.3	0.1	11.1	-28.0	–	28.0	2.9	low mass N
mouth	08/24/99	22:45	1.5	–	–	-28.0	–	34.5	–	undetectable N
mouth	08/25/99	00:45	1.7	–	–	-26.0	-942.7	37.2	0	mass N = 0
mouth	08/25/99	02:45	1.7	–	–	-28.2	–	37.3	–	undetectable N
mouth	08/25/99	04:45	1.1	0.1	18.1	–	16.4	25.1	1.6	no ^{13}C data, low mass N
mouth	08/25/99	06:45	1.2	–	–	-28.0	–	33.9	–	undetectable N
mouth	08/25/99	08:45	1.6	–	–	-23.6	–	35.1	–	undetectable N
creek	11/09/99	11:15	2.7	–	–	-23.5	–	29.7	–	undetectable N
creek	11/09/99	13:15	2.9	–	–	-25.8	–	32.8	–	undetectable N
creek	11/09/99	15:15	1.9	–	–	-28.5	–	21.3	–	undetectable N
creek	11/09/99	17:15	3.0	–	–	-27.8	–	33.2	–	undetectable N
creek	11/09/99	17:15	2.2	–	–	-23.4	–	25.0	–	undetectable N
creek	11/09/99	19:15	2.4	–	–	-21.6	–	26.9	–	undetectable N
creek	11/09/99	21:15	3.4	–	–	-27.5	–	37.9	–	undetectable N
creek	11/09/99	23:15	2.8	–	–	-27.2	–	31.3	–	undetectable N
creek	11/10/99	01:15	2.2	–	–	-30.1	–	24.2	–	undetectable N
creek	11/10/99	03:15	5.0	–	–	-25.6	–	55.8	–	undetectable N

creek	11/10/99	05:15	2.6	–	–	-27.4	–	28.5	–	undetectable N
creek	11/10/99	09:15	2.0	–	–	-29.8	–	22.6	–	undetectable N
creek	11/10/99	09:15	1.5	–	–	-23.1	–	16.4	–	undetectable N
mouth	11/09/99	11:15	2.6	–	–	-36.9	–	43.7	–	questionable C,
mouth	11/09/99	13:15	1.3	–	–	-59.1	–	21.2	–	undetectable N
mouth	11/09/99	15:15	1.9	–	–	-39.7	–	21.5	–	for all samples
mouth	11/09/99	17:15	2.9	–	–	-53.2	–	32.2	–	at November
mouth	11/09/99	21:15	1.5	–	–	-31.2	–	16.6	–	mouth site
mouth	11/09/99	23:15	1.3	–	–	-35.7	–	14.7	–	
mouth	11/09/99	23:15	1.3	–	–	-44.3	–	14.6	–	
mouth	11/10/99	01:15	1.3	–	–	-20.6	–	21.7	–	
mouth	11/10/99	03:15	3.3	–	–	-33.2	–	36.5	–	
mouth	11/10/99	05:15	1.8	–	–	-21.0	–	19.7	–	
mouth	11/10/99	07:15	2.4	–	–	-23.3	–	26.5	–	
mouth	11/10/99	09:15	1.5	–	–	-28.8	–	16.2	–	

Appendix 2: Compilation of DOC and TDN concentration and isotope databy date, time, and location. Concentrations of DOC and DOC/TDN ratios were measured; TDN concentrations were subsequently calculated. The shaded $\delta^{13}C_{DOC}$ and $\delta^{15}N_{TDN}$ values were discussed in the report; isotope values for samples that had less than 10 μg C or 5 μg N were not included in the text of this report because these sample masses are near the detection limit of the mass spectrometer. Values outlined with a gray dotted line are analytical duplicates for $\delta^{13}C_{DOC}$ and $\delta^{15}N_{TDN}$.

Site	Date	(EST) Time	(μM-C) DOC	(μM-N) TDN	(molar) DOC/TDN	(‰) $\delta^{13}C_{DOC}$	(‰) $\delta^{15}N_{TDN}$	(μg C) mass analyzed	(μg N)	Comments
creek	06/29/99	12:30	994.1	–	–	-32.1	91.5	19.6	0	mass N = 0
creek	06/29/99	14:30	424.8	21.5	19.8	-29.9	-7.3	13.6	0.8	low mass N
creek	06/29/99	16:30	579.8	29.3	19.8	-30.3	11.0	27.3	1.6	low mass N
creek	06/29/99	18:30	813.0	30.9	26.3	-31.9	14.8	39.6	1.8	low mass N
creek	06/29/99	20:30	409.0	21.9	18.7	-31.4	17.2	37.7	2.4	low mass N
mouth	06/29/99	12:30	664.5	56.8	11.7	-32.6	12.3	17.7	1.8	low mass N
mouth	06/29/99	14:30	482.3	24.4	19.8	-32.1	18.8	14.0	0.8	low mass N
mouth	06/29/99	14:30	482.3	24.4	19.8	-33.2	14.6	16.5	1.0	low mass N
mouth	06/29/99	16:30	546.3	22.3	24.5	-31.6	18.5	18.5	0.9	low mass N
mouth	06/29/99	18:30	540.3	27.3	19.8	-30.4	17.5	26.5	1.6	low mass N
mouth	06/29/99	20:30	278.8	–	–	-37.6	339.7	24.4	0	mass N = 0
pore 1-5	06/29/99	low tide	409.0	12.5	32.7	-35.7	15.5	22.6	0.8	low mass N
pore 1-15	06/29/99	low tide	232.3	9.0	25.7	-31.7	19.8	35.5	1.6	low mass N
pore 1-25	06/29/99	low tide	340.2	20.8	16.3	-33.8	15.5	26.6	1.9	low mass N

	Date	Tide/Time							
pore 15-5	06/29/99	low tide	635.0	21.8	29.2	-31.8	12.6	18.3	0.7	low mass N
pore 15-5	06/29/99	low tide	635.0	21.8	29.2	-34.0	17.1	18.5	0.7	low mass N
pore 15-15	06/29/99	low tide	461.9	14.1	32.7	-35.2	12.2	22.2	0.8	low mass N
pore 15-25	06/29/99	low tide	457.7	14.0	32.7	-32.4	14.0	47.0	1.7	low mass N
pore 30-5	06/29/99	low tide	443.7	17.3	25.7	-36.1	12.7	17.1	0.8	low mass N
pore 30-15	06/29/99	low tide	245.8	9.6	25.7	-30.2	14.6	18.3	0.8	low mass N
pore 30-25	06/29/99	low tide	281.0	10.5	26.8	-31.1	14.8	34.3	1.5	low mass N
creek	08/24/99	10:45	3631.5	684.8	5.3	-25.7	10.7	40.5	8.9	normal
creek	08/24/99	12:45	608.6	21.7	28.0	-31.2	32.7	35.8	1.5	low mass N
creek	08/24/99	12:45	608.6	21.7	28.0	-32.7	21.9	18.6	0.8	low mass N
creek	08/24/99	14:45	569.8	122.1	4.7	-22.6	2.3	6.3	1.6	low mass C, N
creek	08/24/99	16:45	2775.9	973.4	2.9	-24.1	1.1	15.5	6.3	normal
creek	08/24/99	18:45	583.1	131.5	4.4	-24.9	7.4	15.4	4.1	low mass N
creek	08/24/99	20:45	909.5	271.2	3.4	-25.2	1.8	18.5	6.4	normal
creek	08/24/99	22:45	858.4	140.2	6.1	-22.3	2.0	17.7	3.4	low mass N
creek	08/25/99	00:45	972.9	181.3	5.4	-27.1	0.3	18.5	4.0	low mass N
creek	08/25/99	02:45	414.5	88.8	4.7	-26.2	11.8	19.4	4.8	low mass N
creek	08/25/99	02:45	414.5	78.2	5.3	-26.3	3.1	30.3	6.7	normal
creek	08/25/99	04:45	603.2	114.9	5.3	-25.6	2.7	33.5	7.4	normal
creek	08/25/99	06:45	1173.7	281.7	4.2	-27.5	2.6	19.0	5.3	normal
creek	08/25/99	08:45	1382.8	-	-	-30.3	-16.7	12.4	0	mass N = 0
mouth	08/24/99	10:45	398.5	103.9	3.8	-27.3	2.5	17.2	5.2	normal

	Date	Time								
mouth	08/24/99	12:45	1402.4	277.4	5.1	-29.3	4.9	20.3	4.7	low mass N
mouth	08/24/99	14:45	499.6	183.5	2.1	-36.2	1.2	15.6	6.7	normal
mouth	08/24/99	16:45	585.6	48.4	12.1	-26.2	5.9	65.8	6.3	normal
mouth	08/24/99	16:45	585.6	132.1	4.4	-25.5	1.9	15.6	4.1	low mass N
mouth	08/24/99	18:45	703.0	137.7	5.1	-27.7	2.1	25.9	5.9	normal
mouth	08/24/99	20:45	600.9	112.0	5.4	-27.8	1.2	17.7	3.9	low mass N
mouth	08/24/99	22:45	958.7	273.9	3.5	-29.3	2.6	13.7	4.6	low mass N
mouth	08/25/99	00:45	1277.7	273.8	4.7	-29.8	3.3	20.7	5.2	normal
mouth	08/25/99	02:45	462.0	163.1	2.8	-25.5	2.9	13.2	5.4	normal
mouth	08/25/99	04:45	599.5	97.9	6.1	-32.5	0.9	30.6	5.8	normal
mouth	08/25/99	06:45	1251.3	469.2	2.7	-31.0	3.4	11.3	4.9	low mass N
mouth	08/25/99	06:45	1251.3	279.8	4.5	-30.9	2.0	16.4	4.3	low mass N
mouth	08/25/99	08:45	4494.4	604.3	7.4	-33.3	1.1	41.3	6.5	normal
pore 1-5	08/24/99	low tide	1934.4	146.3	13.2	-24.1	-66.7	52.6	4.6	low mass N
pore 1-15	08/24/99	low tide	416.5	119.0	3.5	-30.9	5.6	25.6	8.5	normal
pore 1-25	08/24/99	low tide	834.0	73.6	11.3	-31.6	2.4	45.8	4.7	low mass N
pore 15-5	08/24/99	low tide	983.2	140.5	7.0	-27.7	2.4	28.6	4.8	low mass N
pore 15-15	08/24/99	low tide	298.7	23.3	12.8	-31.4	2.5	39.2	3.6	low mass N
pore 15-25	08/24/99	low tide	712.0	60.0	11.9	-28.9	3.3	42.1	4.1	low mass N
pore 15-25	08/24/99	low tide	712.0	60.0	11.9	-28.2	3.6	46.1	4.5	low mass N
pore 30-5	08/24/99	low tide	532.4	114.1	4.7	-27.6	0.8	20.6	5.1	normal
pore 30-15	08/24/99	low tide	431.5	92.5	4.7	-32.6	3.8	12.7	3.2	low mass N
pore 30-25	08/24/99	low tide	421.7	57.8	7.3	-28.6	-0.4	20.4	3.3	low mass N

Site	Date	Time								Category
creek	11/09/99	11:15	2541.1	487.2	5.2	-31.0	-2.2	20.3	4.5	low mass N
creek	11/09/99	13:15	852.1	365.2	2.3	-29.9	3.2	7.5	3.8	low mass C, N
creek	11/09/99	15:15	647.5	65.3	9.9	-29.6	-0.5	13.5	1.6	low mass N
creek	11/09/99	17:15	363.9	41.3	8.8	-30.1	2.1	27.1	3.6	low mass N
creek	11/09/99	19:15	624.0	138.7	4.5	-30.9	-0.1	1.1	0.3	low mass C, N
creek	11/09/99	21:15	697.4	70.3	9.9	-30.6	3.8	19.1	2.2	low mass N
creek	11/09/99	23:15	511.3	73.0	7.0	-31.3	4.3	3.6	0.6	low mass C, N
creek	11/10/99	01:15	1760.2	148.4	11.9	-26.5	1.8	10.4	1.0	low mass N
creek	11/10/99	03:15	530.1	44.7	11.9	-29.0	5.8	11.1	1.1	low mass N
creek	11/10/99	05:15	436.1	93.4	4.7	-29.0	1.1	5.9	1.5	low mass C, N
creek	11/10/99	07:15	429.7	92.1	4.7	-31.6	1.1	4.1	1.0	low mass C, N
creek	11/10/99	09:15	446.1	83.3	5.4	-30.1	2.5	34.6	7.5	normal
mouth	11/09/99	11:15	670.3	53.5	12.5	-29.3	6.7	53.7	5.0	normal
mouth	11/09/99	13:15	670.3	68.8	9.7	-25.7	-4.1	44.1	5.3	normal
mouth	11/09/99	15:15	900.7	52.0	17.3	-24.7	3.1	56.0	3.8	low mass N
mouth	11/09/99	15:15	1137.3	114.4	9.9	-25.5	-2.1	45.7	5.4	normal
mouth	11/09/99	17:15	1019.0	70.3	14.5	-25.9	3.9	55.1	4.4	low mass N
mouth	11/09/99	19:15	784.7	86.4	9.1	-25.2	-4.4	79.8	10.2	normal
mouth	11/09/99	21:15	918.8	58.7	15.7	-25.3	2.5	51.4	3.8	low mass N
mouth	11/09/99	23:15	778.4	65.5	11.9	-25.3	-3.5	47.6	4.7	low mass N
mouth	11/10/99	01:15	782.7	43.4	18.0	-25.4	1.3	51.9	3.4	low mass N
mouth	11/10/99	03:15	412.5	34.9	11.8	-25.4	0.1	58.8	5.8	normal
mouth	11/10/99	05:15	sample lost		5.2	-26.2	-6.2	31.5	7.0	normal

mouth	11/10/99	07:15	593.9	34.5	17.2	-26.0	1.6	40.5	2.7	low mass N
mouth	11/10/99	09:15	567.0	49.1	11.5	-26.5	-5.0	38.0	3.8	low mass N
pore 1-15	11/09/99	low tide	797.5	51.5	15.5	-26.0	-1.4	54.9	4.1	low mass N
pore 1-25	11/09/99	low tide	972.1	24.8	39.2	-25.6	-0.2	58.1	1.7	low mass N
pore 15-5	11/09/99	low tide	965.2	60.5	15.9	-24.5	5.6	44.1	3.2	low mass N
pore 15-15	11/09/99	low tide	471.5	19.2	24.5	-25.9	-0.7	37.4	1.8	low mass N
pore 15-25	11/09/99	low tide	357.2	18.6	19.3	-25.2	-3.9	23.6	1.4	low mass N
pore 30-5	11/09/99	low tide	607.5	41.8	14.5	-26.1	2.0	51.2	4.1	low mass N
pore 30-15	11/09/99	low tide	885.7	32.6	27.2	-25.5	4.0	52.9	2.3	low mass N
pore 30-25	11/09/99	low tide	587.7	36.9	15.9	-23.6	-3.6	24.3	1.8	low mass N

PROJECT SUMMARY AND SYNTHESIS

A Process-Based Carbon Mass Balance for a Mid-Atlantic Tidal Freshwater Marsh

-

This research project was guided by 2 questions that are of fundamental importance in determining the role that tidal freshwater marshes play with respect to estuarine carbon cycling: 1) What are the sources of carbon to these marshes? and 2) What are the ultimate fates of this carbon? Measured carbon sources included macrophyte and benthic microalgal photosynthesis as well as sedimentation during tidal flooding. Carbon losses included CO_2 and CH_4 gas fluxes due to belowground, macrophyte, and microalgal respiration and decomposition, tidally driven dissolved inorganic (DIC) and organic carbon (DOC) export, and sediment burial.

CARBON INPUTS ("SOURCES")

On an annual scale, gross macrophyte photosynthesis (996 g C m^{-2} y^{-1}; Table 1) was the dominant carbon input to the marsh, accounting for >60% of all carbon sources. However, a model of macrophyte influenced carbon cycling indicated that photosynthetic rates were insufficient to explain the mid-summer peak in aboveground biomass accumulation without a large (405 g C m^{-2}) translocation of carbon from belowground rhizomes during spring and early summer. This spring translocation was followed by autumn retranslocation of a similar amount of carbon (460 g C m^{-2}). Because large amounts of carbon are recycled between aboveground and belowground tissues, harvest techniques alone may provide an inaccurate representation of the total amount of "new" carbon fixed by the macrophytes. Gross photosynthesis by the other marsh primary producers, benthic microalgae, was significantly lower at 66 g C m^{-2} y^{-1} (Table 1) and

214

Table 1: A process-based carbon mass balance for Sweet Hall marsh

Sources	(g C m^{-2} y^{-1})	Citation
Gross macrophyte photosynthesis	996	Section I
Net Sedimentation	517	Section II
Benthic microalgal photosynthesis	66	Section I
Total sources	1579	

Sinks	(g C m^{-2} y^{-1})	Citation
Belowground respiration	620[a]	Section I
Macrophyte respiration	370[a]	Section I
Macrophyte decomposition	273[a]	Section I
Sediment burial (decadal)	229	Section II
Microalgal respiration	7[a]	Section I
DOC export	???[b]	Section IV
Total sinks	1499	

[a] The DIC export of 282 g C m^{-2} y^{-1} (Section III) is implicitly included in the sediment respiration, macrophyte and microalgal respiration, and macrophyte decomposition terms. See text for discussion.

[b] There were no systematic variations in DOC concentration or $\delta^{13}C_{DOC}$ over tidal cycles so DOC export from the marsh could not be quantified.

215

accounted for only ~6% of total community photosynthesis (~4% of total marsh carbon inputs). While rates of algal production were low relatively to those of marsh macrophytes. benthic microalgae may be significant as a food source in marsh and estuarine food webs due to lower algal C/N ratios and fiber (e.g. lignin, cellulose) content.

The flooding of the marsh surface by semi-diurnal tides provides a mechanism for the delivery of sediment-associated organic carbon to the marsh. Sedimentation rates ranged from 1268 g C m^{-2} y^{-1} adjacent to a tidal creek to 199 g C m^{-2} y^{-1} in the marsh interior. This large spatial variation is primarily due to the distance from the sediment source (i.e. the creek) and less related to the duration and depth of tidal flooding. When averaged across the entire transect, the annual sedimentation rate was 517 ± 353 g C m^{-2} y^{-1} and accounted for over 30% of the total organic carbon inputs to the marsh (Table 1). Seasonal sediment inventories of the radioisotope ^{7}Be ($t_{1/2}$ = 53.3 d) were greater than atmospherically supported ^{7}Be inventories, indicating that the spatial patterns of sedimentation were not due to sediment erosion and redistribution from one part of the marsh to another.

CARBON LOSSES ("SINKS")

The dominant mechanism for loss of carbon from the marsh was belowground respiration (620 g C m^{-2} y^{-1}; Table 1) which includes the decomposition of sediment associated carbon, detritus, and DOC within the marsh sediments. Of this flux, ~85%

216

was as CO_2 and DIC while the remainder was as CH_4. Because of the high porosity of the marsh plants, about 80% of the CO_2 and CH_4 produced via belowground respiration was actually transported through plant tissues rather than diffusing directly across the sediment-atmosphere interface. Carbon losses associated with the normal metabolic costs of plant growth (i.e. growth and maintenance respiration) were 371 g C m^{-2} y^{-1} or about 37% of gross macrophyte photosynthesis (Table 1). An additional 273 g C m^{-2} y^{-1} were lost late in the growing season as a result of the decomposition of standing macrophyte stems. These 3 carbon loss routes were closely linked to the cycle of macrophyte growth and senescence with the greatest rates of both belowground respiration and macrophyte decomposition in the late growing season (~late July to September). Macrophyte growth and maintenance respiration losses were highest in June, coincident with the peak in aboveground macrophyte biomass.

Export of DIC from the marsh occurred during high tides from the decomposition of plants and detritus on the marsh surface as well as from the diffusion of DIC rich porewaters into overlying tidal waters. Low tide inputs of DIC from the marsh to tidal creek include the drainage of marsh porewater and fluxes from subtidal sediments. Based on late summer data (August and September), approximately 58% of the total exported DIC was added to tidal waters when the marsh was flooded. Thus, while marsh tidal creeks accounted for only ~5% of the total marsh area, DIC inputs to these creeks at low tide accounted for over 40% of the total DIC flux from the marsh. Because the carbon gas flux model described in Section I included the production and losses of inorganic carbon losses (CO_2, DIC, CH_4) from the marsh, regardless of tidal stage, the total DIC

217

export of 282 g C m^{-2} y^{-1} is implicitly included in the previously discussed belowground respiration, growth and maintenance respiration, and macrophyte decomposition terms. Similar to gaseous carbon losses from the marsh, DIC export was greatest in the late summer when rates of decomposition and senescence were greatest.

In contrast to the DIC data, there were no distinct changes in the concentration or isotopic composition of water column DOC. This could be interpreted as no exchange of marsh-derived DOC between the marsh, tidal creek and river. Alternately, the lack of significant concentration and isotopic differences between marsh porewater and water column DOC could disguise any export (or import) of DOC. Marsh macrophyte leaching rates can be high and enhanced rates of bacterial and fish production have been reported in waters adjacent to tidal freshwater marshes. Therefore, there may be significant DOC export from these marshes and additional research in this area is warranted.

When constructing a marsh carbon budget, burial can represent a significant loss term. The magnitude of the burial term will, however, depend strongly on the time scale of interest and depth in the sediment over which the budget is being constructed. Based on ^{137}Cs activity over the last 35 to 40 years (equivalent to ~30 cm), burial can remove 229 g C m^{-2} y^{-1} (Table 1). This represents the "loss" of 15% of the total carbon sources to the marsh (photosynthesis + sedimentation) and 44% of net marsh sedimentation. The fate of the remaining 57% of sediment carbon deposited on the marsh was likely exported from the marsh as DIC or lost as gaseous CO_2 or CH_4. Over longer time scales (e.g. centuries to millennia) burial rates are typically much lower, reflecting periodic storm

218

induced erosion. historical changes in the supply and deposition of sediments, and the metabolism of a "labile" fraction of sediment carbon.

MARSH CARBON BALANCE

Over short time scales (<40 y), the carbon sources and sinks in the marsh were closely balanced (1579 versus 1499 g C m^{-2} y^{-1}: Table 1). The similarity between sources and sinks suggests that carbon flux terms that were not quantified (notably consumption and subsequent export of marsh-produced carbon by biota) are not significant with respect to the total marsh carbon budget. However, the input of 80 g C per m^2 marsh area per year (i.e. the difference between sources and sinks) may be important in the food web dynamics or biogeochemical processes in adjacent riverine and estuarine habitats, especially in the upper estuary where the ratio of marsh to open water is large. From year to year, the net carbon balance for the marsh will vary with changes in photosynthesis, respiration, and sedimentation which are influenced by variability in temperature, tidal range, salinity, plant species composition and other factors. Thus, in some years the marsh may be significant carbon sink and increase its elevation relative to sea level, while in other years it may experience an accretion deficit due to increased carbon losses from the marsh or reduced inputs.

While the marsh is closely balanced on short time scales, on a larger time scale (centuries to millennia) the marsh must be sequestering carbon as evidenced by the nearly 7 m layer of organic substrate underlying the marsh. Using measured percent carbon data

for these deposits and assuming a homogenous bulk density (0.35 g sed cm^{-3}; 0 to 2 cm average) throughout the sediment profile (i.e. no compaction), the marsh has sequestered 2.6 x 10^5 g C m^{-2} since 3640 BP (deepest ^{14}C date from this site: 6.5 m). Over this time period the marsh has been a carbon sink for 72 g C m^{-2} y^{-1}. It is interesting to note that this rate is nearly identical to the difference between sources and sinks (80 g C m^{-2} y^{-1}) reported in Table 1. Thus, a slight annual imbalance between marsh carbon sources and sinks can result in significant carbon sequestration over long time periods.

220

VITA

Scott Christopher Neubauer

Born in Silver Spring, Maryland in October 1973. Raised in Frederick, Maryland and West Chester, Pennsylvania. Graduated from B. Reed Henderson High School, West Chester, Pennsylvania in May 1991. Received a B.S. degree in Marine Science and Biology from the University of Miami, Coral Gables, Florida in May 1994. Entered the Ph.D. program at the Virginia Institute of Marine Science, Gloucester Point, Virginia in August 1994.